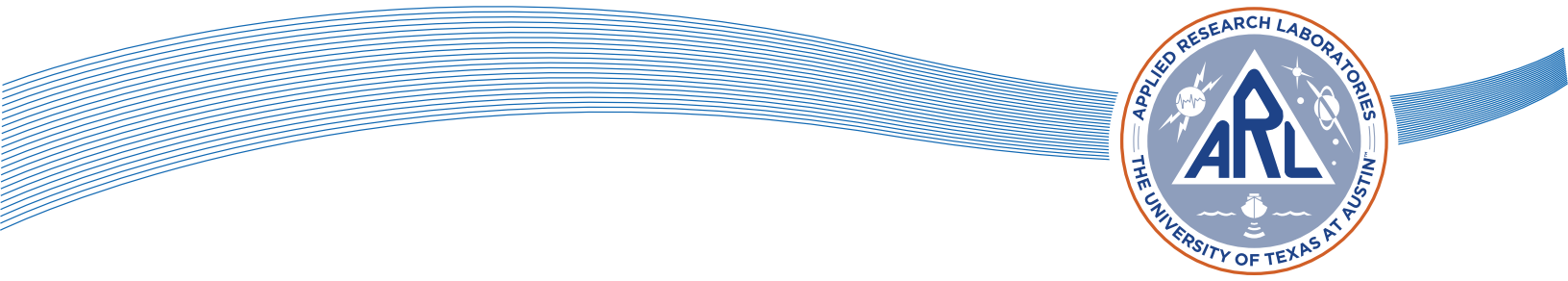

An Analysis of Global Positioning System Standard Positioning Service Performance for 2023

Space and Geophysics Laboratory
Applied Research Laboratories
The University of Texas at Austin

Miquela Stein, Austin Finn, Emery B. Reed, Brent A. Renfro

August 4, 2025

Contract: NAVSEA Contract N00024-17-D-6421
Task Order: 5101070
Technical Report: TR-SGL-24-02

This Page Added for Document Spacing

Executive Summary

Applied Research Laboratories, The University of Texas at Austin (ARL:UT) examined the performance of the Global Positioning System (GPS) throughout 2023 for the U.S. Space Force (USSF) Space Systems Command (SSC), Military Communications & Positioning, Navigation, and Timing (PNT) Program Executive Office (PEO).

This report is based upon work supported by SSC through U.S. Navy Naval Sea Systems Command (NAVSEA) Contract N00024-17-D-6421, Task Order 5101070, "GNSS Signal Performance and Anomaly Analysis."

Performance is defined by the 2020 Standard Positioning Service (SPS) Performance Standard (SPS PS) [1]. The performance standard provides the U.S. government's assertions regarding the expected performance of GPS. This report covers those assertions which can be verified by anyone with knowledge of standard GPS data analysis practices, familiarity with the relevant signal specification, and access to a GPS data archive. The few assertions that are not covered are noted in the summary and the reasons are discussed in the text.

The assertions evaluated include those of coverage, accuracy, integrity, continuity, and availability of the GPS signal-in-space (SIS) along with the assertions on accuracy of positioning and time transfer. Chapter 1 is an introduction to the report. Chapter 2 contains a tabular summary of performance stated in terms of the metrics provided in the SPS PS. Chapter 3 presents a more detailed explanation of the analysis conducted in evaluating each assertion. The assertions are presented in order of appearance in the SPS PS.

All but one of the SPS PS assertions examined in this report were met in 2023. The exception was the P_{sat} assertion. For more information see Section 3.3.3.

Contents

1 Introduction **1**

2 Summary of SPS PS Results **6**

3 Discussion of SPS PS Metrics and Results **9**

3.1 SIS Coverage . . . 12

3.1.1 Per-Satellite Coverage . . . 12

3.1.2 Constellation Coverage . . . 12

3.2 SIS Accuracy . . . 13

3.2.1 URE Over All AOD . . . 14

3.2.1.1 Constellation URE . . . 23

3.2.2 URE at Any AOD . . . 24

3.2.3 URE at Zero AOD . . . 25

3.2.4 URE Bounding . . . 28

3.2.5 URE After 14 Days Without Upload . . . 28

3.2.6 URRE Over All AOD . . . 29

3.2.7 URAE Over All AOD . . . 33

3.2.8 UTC Offset Error . . . 36

3.3 SIS Integrity . . . 38

3.3.1 URE Integrity . . . 38

3.3.2 UTCOE Integrity . . . 39

3.3.3 Instantaneous P_{sat} and P_{const} . . . 40

3.4 SIS Continuity . . . 41

3.4.1 Unscheduled Failure Interruptions . . . 41

3.4.2 Status and Problem Reporting Standards . . . 45

3.4.2.1 Scheduled Events . . . 45
3.4.2.2 Unscheduled Outages . . . 47
3.5 SIS Availability . . . 48
3.5.1 Per-Slot Availability . . . 48
3.5.2 Constellation Availability . . . 50
3.5.3 Operational Satellite Counts . . . 51
3.6 Position/Velocity/Time Domain Standards . . . 52
3.6.1 Evaluation of DOP Assertions . . . 52
3.6.1.1 PDOP Availability . . . 52
3.6.2 Position Service Availability . . . 55
3.6.3 Position/Velocity Accuracy . . . 55
3.6.3.1 Results for Daily Average . . . 56
3.6.3.2 Results for Worst Site 95th Percentile . . . 60
3.6.4 Time Transfer Accuracy . . . 63

A Additional Results of Interest **65**
A.1 Health Values . . . 67
A.2 Age of Data . . . 69
A.3 User Range Accuracy Index Values . . . 71
A.4 Extended Mode Operations . . . 74
A.5 URE as a Function of AOD . . . 76
A.5.1 SPS Results . . . 76
A.5.1.1 Block IIR SVs . . . 77
A.5.1.2 Block IIR-M SVs . . . 79
A.5.1.3 Block IIF SVs . . . 81
A.5.1.4 GPS III SVs . . . 84
A.6 SVN 63/PRN 1 Integrity Fault Events . . . 86
A.7 Additional DOP Analysis . . . 88

B Supporting Data **90**
B.1 PRN to SVN Mapping for 2023 . . . 92
B.2 NANU Activity in 2023 . . . 92
B.3 SVN to Plane-Slot Mapping for 2023 . . . 95

C Analysis Details **97**

C.1 Signals Used 99

C.2 URE Methodology 100

C.2.1 Clock and Position Values for Broadcast and Truth 101

C.2.2 ISCs and DCBs 102

C.2.3 Definition of 95^{th} Percentile Global Statistic 105

C.2.4 Definition of 95^{th} Percentile Global Average 107

C.2.5 Limitations of URE Analysis 108

C.2.6 Challenges of Comparing UREs Between Signal Combinations 109

C.3 Selection of Broadcast Navigation Message Data 110

C.4 AOD Methodology 111

C.5 Position Methodology 112

C.6 Plane/Slot Methodology 115

D Acronyms and Abbreviations **116**

Bibliography **120**

List of Figures

1.1 Maps of the Networks of Stations Used in this Report 5

3.1 Range of the L1 C/A Monthly 95th Percentile Values for All SVs 17
3.2 Range of the L1 C/A + L2C Monthly 95th Percentile Values for All SVs . . 19
3.3 Range of the L1 C/A + L5Q Monthly 95th Percentile Values for All SVs . . 21
3.4 Range of Differences in Monthly Values between Dual-Frequency and L1 C/A UREs for All SVs 22
3.5 Best Performing Block IIR SV by URE Over Any AOD 26
3.6 Worst Performing Block IIR SV by URE Over Any AOD 26
3.7 Best Performing Block IIR-M SV by URE Over Any AOD 26
3.8 Worst Performing Block IIR-M SV by URE Over Any AOD 26
3.9 Best Performing Block IIF SV by URE Over Any AOD 27
3.10 Worst Performing Block IIF SV by URE Over Any AOD 27
3.11 Best Performing GPS III SV by URE Over Any AOD 27
3.12 Worst Performing GPS III SV by URE Over Any AOD 27
3.13 Range of the Monthly URRE 95th Percentile Values for All SVs 32
3.14 Range of the Monthly URAE 95th Percentile Values for All SVs 35
3.15 UTCOE LNAV Time Series for 2023 37
3.16 UTCOE CNAV Time Series for 2023 37
3.17 Daily Average Number of Occupied Slots 50
3.18 Count of Operational SVs by Day for 2023 51
3.19 Daily PDOP Metrics Using All SVs for 2023 54
3.20 Daily Averaged Position Residuals Computed Using a RAIM Solution 58
3.21 Daily Averaged Position Residuals Computed Using No Data Editing 58
3.22 Daily Averaged Position Residuals Computed Using a RAIM Solution (enlarged) 59
3.23 Daily Averaged Position Residuals Computed Using No Data Editing (enlarged) 59

3.24 Worst Site 95th Daily Averaged Position Residuals Computed Using a RAIM Solution 61
3.25 Worst Site 95th Daily Averaged Position Residuals Computed Using No Data Editing 61
3.26 Worst Site 95th Daily Averaged Position Residuals Computed Using a RAIM Solution (enlarged) 62
3.27 Worst Site 95th Daily Averaged Position Residuals Computed Using No Data Editing (enlarged) 62
3.28 10° Grid for UUTCE Calculation 64
3.29 UUTCE 95th Percentile Values 64

A.1 Constellation Age of Data for 2023 70
A.2 Stacked Bar Plot of SV LNAV URA Index Values for 2023 72
A.3 Stacked Bar Plot of Binned SV CNAV URA Index Values for 2023 73
A.4 Integrity Fault Event on 25 January 2023, SVN 63/PRN 1 87
A.5 Integrity Fault Event on 10 July 2023, SVN 63/PRN 1 87

B.1 PRN to SVN Mapping for 2023 93
B.2 Plot of NANU Activity for 2023 94
B.3 Time History of Satellite Plane-Slots for 2023 96

C.1 Illustration of the 577 Point Grid 106
C.2 Global Average URE as defined in 2008 SPS PS 107

List of Tables

1.1 SPS SIS Signal Combinations Covered by SPSPS20 2
1.2 SPS SIS Signals Present by Block in 2023 2

2.1 Summary of SPSPS20 Metrics Examined for 2023 7
2.2 References of SPSPS20 Metrics Examined for 2023 8

3.1 Monthly 95th Percentile Values of L1 C/A SIS Instantaneous URE for All SVs 16
3.2 Monthly 95th Percentile Values of L1 C/A + L2C SIS Instantaneous URE for All SVs 18
3.3 Monthly 95th Percentile Values of L1 C/A + L5Q SIS Instantaneous URE for All SVs 20
3.4 Monthly 95th Percentile Values of Constellation SIS Instantaneous URE for All Signals 23
3.5 Monthly 95th Percentile Values of L1 C/A + L2C SIS Instantaneous URRE for All SVs 31
3.6 Monthly 95th Percentile Values of L1 C/A + L2C SIS Instantaneous URAE for All SVs 34
3.7 95th Percentile Global Statistic UTCOE for 2023 37
3.8 Probability Over Any Hour of Not Losing L1 C/A Availability Due to Unscheduled Interruption for 2023 43
3.9 Scheduled Events Covered in NANUs for 2023 46
3.10 Decommissioning Events Covered in NANUs for 2023 46
3.11 Usable Events Covered in NANUs for 2023 46
3.12 Unscheduled Events Covered in NANUs for 2023 47
3.13 Per-Slot L1 C/A Availability for 2023 49
3.14 Summary of PDOP Availability 53
3.15 Daily Average Position Errors for 2023 57
3.16 Daily Worst Site 95th Percentile Position Errors for 2023 60

A.1 Distribution of SV Health Values 68
A.2 Age of Data of the Navigation Message by SV Type 69
A.3 Summary of Occurrences of Extended Mode Operations 75
A.4 Additional DOP Annually-Averaged Visibility Statistics for 2020 – 2023 . . . 89
A.5 Additional PDOP Statistics 89

C.1 SPS SIS Signal Combinations Covered by SPSPS20 99
C.2 Rationale for Selection of Signal Combinations 99
C.3 Characteristics of SIS URE Methods 101
C.4 GPS Signal Combinations of Interest and Orbit Adjustments 103

D.1 List of Acronyms and Abbreviations 116

Chapter 1

Introduction

Applied Research Laboratories, The University of Texas at Austin (ARL:UT) examined the performance of the Global Positioning System (GPS) throughout 2023 for the U.S. Space Force (USSF) Space Systems Command (SSC), Military Communications & Positioning, Navigation, and Timing (PNT) Program Executive Office (PEO). This report is based upon work supported by SSC through U.S. Navy Naval Sea Systems Command (NAVSEA) Contract N00024-17-D-6421, Task Order 5101070, "GNSS Signal Performance and Anomaly Analysis."

Performance is assessed relative to selected assertions in the 2020 Standard Positioning Service (SPS) Performance Standard (SPS PS or SPSPS20) [1]. The SPS PS presents assertions that are supported by USSF 2nd Space Operations Squadron (2 SOPS) operational procedures, tempered with technical and operational margin.

Chapter 2 of this report contains a tabular summary of performance evaluated against the metrics provided in the SPS PS. Chapter 3 presents a more detailed explanation of the analysis conducted in evaluating each assertion. The assertions are presented in order of appearance in the SPSPS20. Appendix A contains additional results of interest that are, in some cases, beyond the assertions. Appendix B contains supporting data used to interpret the results. Appendix C contains notes on how the analysis was conducted. Appendix D contains acronyms and abbreviations.

The SPS PS defines services delivered through multiple signals. The signals and signal combinations defined are listed in Table 1.1. For the SPSPS20, the signals and signal combinations duplicate SPS PS Table 2.2-2. LNAV refers to the GPS Legacy Navigation Message [2] and CNAV refers to the GPS Civil Navigation Message [2], [3].

Table 1.1: SPS SIS Signal Combinations Covered by SPSPS20

One Carrier Single Frequency (SF)	**Two Carriers Dual Frequency (DF)**	**Three Carriers Triple Frequency (TF)**
C/A-code + LNAV Data	(C/A + CM)-codes + CNAV Data	(C/A + CM + I5)-codes + CNAV Data
CM-code + CNAV Data	(C/A + CL)-codes + CNAV Data	(C/A + CL + I5)-codes + CNAV Data
CL-code + CNAV Data	(C/A + CM+CL)-codes + CNAV Data	(C/A + CM+CL + I5)-codes + CNAV Data
(CM+CL)-codes + CNAV Data	(C/A + I5)-codes + CNAV Data	(C/A + CM + Q5)-codes + CNAV Data
I5-code + CNAV Data	(C/A + Q5)-codes + CNAV Data	(C/A + CL + Q5)-codes + CNAV Data
Q5-code + CNAV Data	(C/A + I5+Q5)-codes + CNAV Data	(C/A + CM+CL + Q5)-codes + CNAV Data
(I5+Q5)-codes + CNAV Data		(C/A + CM+CL + I5+Q5)-codes + CNAV Data

Table 1.1 contains a large number of signal combinations; however, it is possible to evaluate the performance of all these combinations by focusing on a subset that examines each unique signal and each unique message. The signal combinations directly examined in this report are listed below and are described in further detail in Appendix C.1.

- Single-frequency L1 C/A with LNAV messages
- Dual-frequency L1 C/A + L2C with CNAV messages
- Dual-frequency L1 C/A + L5Q with CNAV messages

Four different GPS space vehicle (SV) types were operational during 2023. Not all types are capable of broadcasting all signals. The signals broadcast by each type and the navigation message data on each signal are shown in Table 1.2.

Table 1.2: SPS SIS Signals Present by Block in 2023

Block	**SVNs**	**# SVs**	**L1 C/A (LNAV)**	**L2C (CNAV)**	**L5Q (CNAV**
IIR	41, 43, 44, 45, 51, 56, 59, 61	8	✔	–	–
IIR-M	48, 50, 52, 53, 55, 57, 58	7	✔	✔	–
IIF	62, 63, 64, 65, 66, 67, 68, 69, 70, 71, 72, 73	12	✔	✔	✔
III	74, 75, 76, 77, 78, 79	6	✔	✔	✔

The assertions examined include those related to coverage, accuracy, continuity, availability, and position/time domain. These metrics, with the exception of position/time domain, are limited to the signal-in-space (SIS) and do not address atmospheric errors, receiver errors, or errors due to the user environment (e.g., multipath errors, terrain masking, and foliage).

This report addresses assertions in the SPSPS20 that can be verified by anyone with knowledge of standard GPS data analysis practices, familiarity with the relevant signal specification [2] [3], and access to a GPS data archive (such as that available via the International Global Navigation Satellite System (GNSS) Service (IGS)) [4].

The majority of the assertions related to user range error (URE) values are evaluated by comparison of the SV clock and position broadcast and truth representations. Broadcast clock and position data (BCP) are provided by the GPS LNAV and CNAV message data. Truth clock and position data (TCP) are provided by a precise orbit calculated after the time of interest. The URE calculation process requires both BCP and TCP and is detailed in Appendix C.2.

Many of the analyses are conducted at a 30 s cadence due to the fact that the GPS LNAV clock, ephemeris, and integrity (CEI) data repeats every 30 s and that is the highest frequency with which quantities such as satellite health can change. This 30 s cadence was selected prior to CNAV data processing and has been retained for consistency, even though the CEI data repetition rate for CNAV is different.

Observation data from tracking stations were used to cross-check the URE values and to evaluate non-URE assertions, such as those found in Section 3.4 (Continuity), Section 3.5 (Availability), and Section 3.6 (Position/Time Domain). In these cases, data from two networks are used. The two networks considered were the National Geospatial-Intelligence Agency (NGA) Monitor Station Network (MSN) [5] and a subset of the tracking stations that contribute to the IGS. A subset of the IGS network was selected to cover a wide geographic distribution, prioritizing receivers with high quality clocks and long term data availability. The geographic distribution of these stations is shown in Figure 1.1. The selection of these sets of stations ensures continuous, simultaneous observation of all space vehicles by multiple stations. The assertions focus on SIS performance, which is not directly observable from ground tracking locations. To mitigate this issue, this performance review uses ionospherically-corrected dual-frequency observation data.

Navigation message data used in this report were collected from the NGA MSN. The collection and selection of navigation message data are described in general terms in Appendix C.3.

The majority of the metrics in this report are evaluated on either a per SV basis or for the full constellation. The metrics associated with continuity and availability are defined with respect to the slot definitions in SPSPS20. The slot definitions are stated in terms of either the Baseline 24 constellation, which consists of six orbital planes with four slots per plane, or the Expandable 24 constellation, in which six of the 24 slots may be occupied by two SVs. Of the operational SVs, 31 were located in the Expandable 24 constellation throughout 2023. The SVs in excess of those located in defined slots are assigned to locations in planes in accordance with operational considerations. Depending on the time of year, there were 1 or 2 such satellites during 2023. For additional information on slot definitions, see Appendix B.3.

Each GPS SV is identified by pseudo-random noise ID (PRN) and by space vehicle number (SVN). PRNs are assigned to SVs for periods of time. A given SV may be assigned different PRNs at different times during its operational life. The SVN represents the permanent unique identifier for each SV. As the number of active SVs has increased to the total number of PRNs available, thirty-two [1], PRNs are now being used by multiple SVs within a given year (but by no more than one SV at a time). In general, we list the SVN first and the PRN second because the SVN is the unique identifier of the two. The SVN-to-PRN relationships were provided by the GPS Master Control Station (MCS). Other useful summaries

of this information may be found on the U.S. Coast Guard Navigation Center website [6]. See Appendix B.1 for a summary of the SVN-to-PRN mapping for 2023.

For the operational signals addressed in this report, only results obtained when a signal was trackable and transmitting a healthy indication are included in the analysis.

L5 was pre-operational during the period covered by this report and although L5 signals indicate an unhealthy status, that does not imply inaccuracy. In order to derive results for signal combinations that include L5, the L5 signal was treated as if it were healthy whenever the corresponding L1 C/A signal indicated a healthy condition. In some cases when L1 C/A transitions between health states, the corresponding L5 navigation message transition may lag by a few minutes. As a result, the L5 signal is regarded as unavailable after a L1 C/A transition from unhealthy-to-healthy until the next L5 navigation message is received. For assertions related to L5, the navigation message was obtained from L5I while the observation data was obtained from L5Q.

The authors acknowledge and appreciate the effort of several individuals who reviewed these results. For 2023, this included ARL:UT staff members Scott Sellers, Sydney A. Holdampf, and Benjamin Brutocao. Albert Hayden and James Pace of The Aerospace Corporation have long been interested in GPS performance metrics and have provided valuable comments on the final draft. Karl Kovach of The Aerospace Corporation provided valuable assistance in interpreting the SPSPS20 assertions. However, the results presented in this report are derived by ARL:UT, and any errors in this report are the responsibility of ARL:UT.

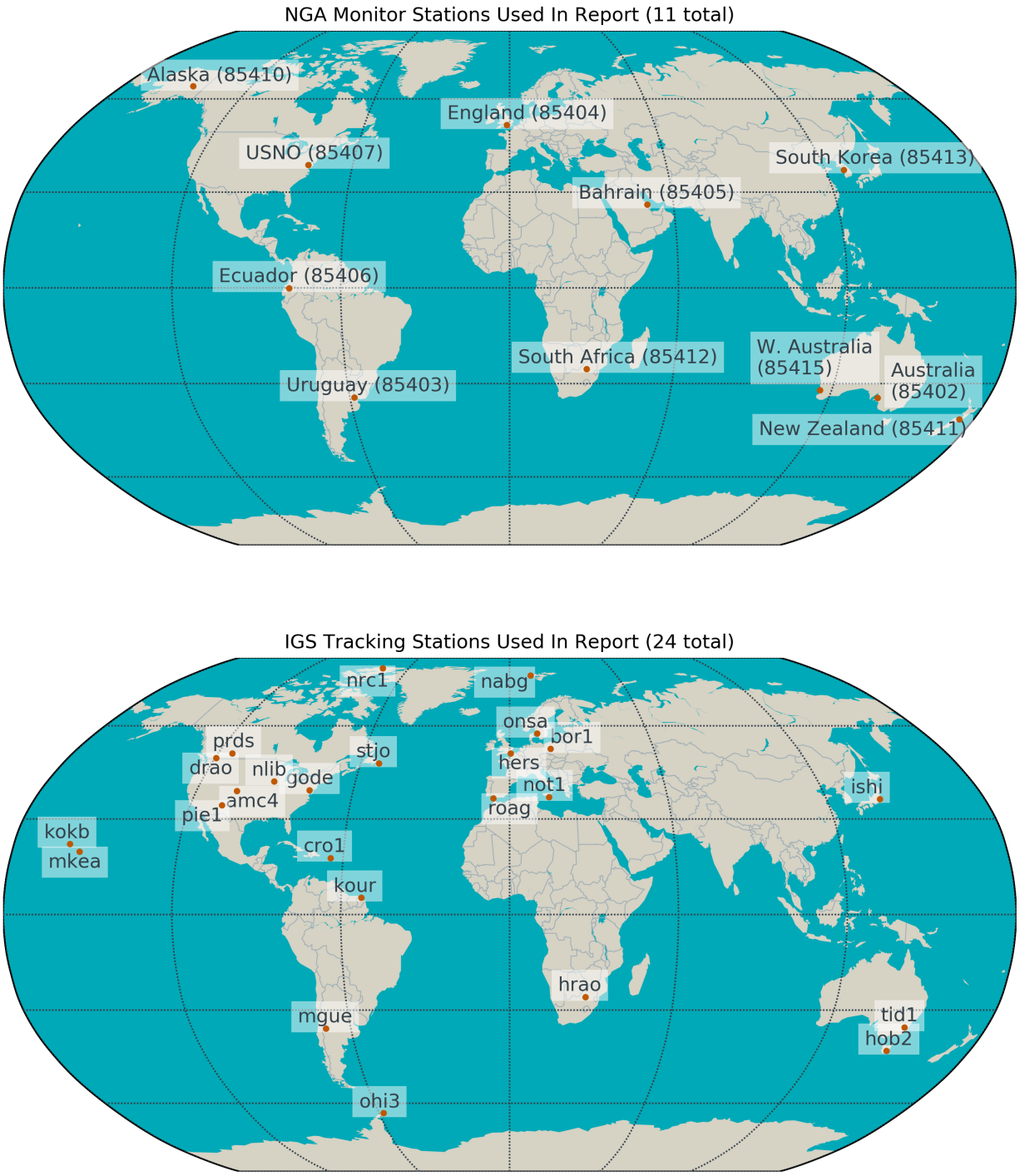

Figure 1.1: Maps of the Networks of Stations Used in this Report

Chapter 2

Summary of SPS PS Results

Table 2.1 provides a summary of the assertions defined in SPSPS20. The table is annotated to show which assertions are evaluated in this report and the status of each assertion.

Of the assertions evaluated, all but one were met in 2023. The exception was the P_{sat} assertion. For more information see Section 3.3.3.

Details regarding each result may be found in Chapter 3. All abbreviations used in Table 2.1 may be found in Appendix D. The reasons some assertions were not evaluated are provided in the text.

Table 2.1: Summary of SPSPS20 Metrics Examined for 2023

SPSPS20 Section	SPS PS Assertion	Signal Status			System Status
		L1 C/A	L1 C/A + L2C	L1 C/A + L5Q	
3.3.1 SIS Per-Satellite Coverage	100% Coverage of terrestrial service volume	–	–	–	**NE**
3.3.2 SIS Constellation Coverage	100% Coverage of terrestrial service volume	–	–	–	✔
3.4.1 SIS URE Accuracy	$\leq$ 7.0 m 95% Global statistic URE during normal operations over all AODs	✔	✔	✔	–
	$\leq$ 9.7 m 95% Global statistic URE during normal operations at any AOD	✔	✔	✔	–
	$\leq$ 3.8 m 95% Global statistic URE during normal operations at zero AOD	✔	✔	✔	–
	$\leq$ 30 m 99.94% Global statistic URE during normal operations	✔	✔	✔	–
	$\leq$ 30 m 99.79% Worst case single point statistic URE during normal operations	✔	✔	✔	–
	$\leq$ 388 m 95% Global statistic URE during extended operations after 14 days without upload	**NE**	–	–	–
	$\leq$ 2.0 m 95% Global statistic URE during normal operations over all AODs for the ensemble of constellation slots	✔	✔	✔	–
3.4.2 SIS URRE Accuracy	$\leq$ 0.006 m/s 95% Global statistic URRE over any 3-second interval during normal operations at any AOD	✔	✔	✔	–
3.4.3 SIS URAE Accuracy	$\leq$ 0.002 m/s^2 95% Global statistic URAE over any 3-second interval during normal operations at any AOD	✔	✔	✔	–
3.4.4 SIS UTCOE Accuracy	$\leq$ 30 nsec 95% Global statistic UTCOE during normal operations at any AOD	✔	✔	✔	–
3.5.1 SIS Instantaneous URE Integrity	$\leq 1 \times 10^{-5}$ Probability over any hour of exceeding the NTE tolerance without a timely alert	✔	✔	✗	–
3.5.4 SIS Instantaneous UTCOE Integrity	$\leq 1 \times 10^{-5}$ Probability over any hour of exceeding the NTE tolerance without a timely alert during normal operations	✔	✔	✔	–
3.5.5 SIS Instantaneous P_{sat} and P_{const}	$\leq 1 \times 10^{-5}$ Fraction of time when the SPS SIS instantaneous URE exceeds the NTE tolerance without a timely alert (P_{sat})	✗	✗	✗	–
	$\leq 1 \times 10^{-8}$ Fraction of time when the SPS SIS instantaneous URE from two or more satellites exceeds the NTE tolerance due to a common cause without a timely alert (P_{const})	✔	✔	✔	–
3.6.1 SIS Continuity - Unscheduled Failure Interruptions	$\geq$ 0.9998 Probability over any hour of not losing the SPS SIS availability from the slot due to unscheduled interruption	✔	–	–	–
3.6.3 Status and Problem Reporting	Appropriate NANU issued at least 48 hours prior to a scheduled event for 95% of the events	✔	✔	✔	–
3.7.1 SIS Per-Slot Availability	$\geq$ 0.957 Probability that (a) a slot in the baseline 24-slot will be occupied by a satellite broadcasting a healthy SF C/A-Code SPS SIS, or (b) a slot in the expanded configuration will be occupied by a pair of satellites each broadcasting a healthy SF C/A-Code SPS SIS	✔	–	–	–
3.7.2 SIS Constellation Availability	$\geq$ 0.98 Probability that at least 21 slots out of the 24 slots will be occupied by a satellite (or pair of satellites for expanded slots) broadcasting a healthy SF C/A-Code SPS SIS	✔	–	–	–
	$\geq$ 0.99999 Probability that at least 20 slots out of the 24 slots will be occupied by a satellite (or pair of satellites for expanded slots) broadcasting a healthy SF C/A-Code SPS SIS	✔	–	–	–
3.7.3 Operational Satellite Counts	$\geq$ 0.95 Probability that the constellation will have at least 24 operational satellites regardless of whether those operational satellites are located in slots or not	–	–	–	✔
3.8.1 PDOP Availability	$\geq$ 98% Global PDOP of 6 or less	✔	–	–	–
	$\geq$ 88% Worst site PDOP of 6 or less	✔	–	–	–
3.8.2 Position Service Availability	$\geq$ 99% Horizontal service availability, average location	✔	–	–	–
	$\geq$ 99% Vertical service availability, average location	✔	–	–	–
	$\geq$ 90% Horizontal service availability, worst-case location	✔	–	–	–
	$\geq$ 90% Vertical service availability, worst-case location	✔	–	–	–
3.8.3 Position/Velocity/Time Service Accuracy	$\leq$ 8 m 95% Horizontal error, global average position accuracy	✔	–	–	–
	$\leq$ 13 m 95% Vertical error, global average position accuracy	✔	–	–	–
	$\leq$ 15 m 95% Horizontal error, worst site position accuracy	✔	–	–	–
	$\leq$ 33 m 95% Vertical error, worst site position accuracy	✔	–	–	–
	$\leq$ 0.2 m/s 95% Velocity error, any axis	✔	–	–	–
	$\leq$ 30 nsec Time transfer error 95% of the time	✔	–	–	–

✔ Assertion met ✗ Assertion not met **NE** Assertion not evaluated – No assertion

L5 is pre-operational and set unhealthy. See Section 1 for more information.

Table 2.2: References of SPSPS20 Metrics Examined for 2023

SPSPS20 Section	**SPS PS Assertion**	**Report Section**
3.3.1 SIS Per-Satellite Coverage	100% Coverage of terrestrial service volume	3.1.1
3.3.2 SIS Constellation Coverage	100% Coverage of terrestrial service volume	3.1.2
3.4.1 SIS URE Accuracy	$\leq$ 7.0 m 95% Global statistic URE during normal operations over all AODs	3.2.1
	$\leq$ 9.7 m 95% Global statistic URE during normal operations at any AOD	3.2.2
	$\leq$ 3.8 m 95% Global statistic URE during normal operations at zero AOD	3.2.3
	$\leq$ 30 m 99.94% Global statistic URE during normal operations	3.2.4
	$\leq$ 30 m 99.79% Worst case single point statistic URE during normal operations	
	$\leq$ 388 m 95% Global statistic URE during extended operations after 14 days without upload	3.2.5
	$\leq$ 2.0 m 95% Global statistic URE during normal operations over all AODs for the ensemble of constellation slots	3.2.1.1
3.4.2 SIS URRE Accuracy	$\leq$ 0.006 m/s 95% Global statistic URRE over any 3-second interval during normal operations at any AOD	3.2.6
3.4.3 SIS URAE Accuracy	$\leq$ 0.002 m/s^2 95% Global statistic URAE over any 3-second interval during normal operations at any AOD	3.2.7
3.4.4 SIS UTCOE Accuracy	$\leq$ 30 nsec 95% Global statistic UTCOE during normal operations at any AOD	3.2.8
3.5.1 SIS Instantaneous URE Integrity	$\leq 1 \times 10^{-5}$ Probability over any hour of exceeding the NTE tolerance without a timely alert	3.3.1
3.5.4 SIS Instantaneous UTCOE Integrity	$\leq 1 \times 10^{-5}$ Probability over any hour of exceeding the NTE tolerance without a timely alert during normal operations	3.3.2
3.5.5 SIS Instantaneous P_{sat} and P_{const}	$\leq 1 \times 10^{-5}$ Fraction of time when the SPS SIS instantaneous URE exceeds the NTE tolerance without a timely alert (P_{sat})	3.3.3
	$\leq 1 \times 10^{-8}$ Fraction of time when the SPS SIS instantaneous URE from two or more satellites exceeds the NTE tolerance due to a common cause without a timely alert (P_{const})	
3.6.1 SIS Continuity - Unscheduled Failure Interruptions	$\geq$ 0.9998 Probability over any hour of not losing the SPS SIS availability from the slot due to unscheduled interruption	3.4.1
3.6.3 Status and Problem Reporting	Appropriate NANU issued at least 48 hours prior to a scheduled event for 95% of the events	3.4.2.1
3.7.1 SIS Per-Slot Availability	$\geq$ 0.957 Probability that (a) a slot in the baseline 24-slot will be occupied by a satellite broadcasting a healthy SPS SIS, or (b) a slot in the expanded configuration will be occupied by a pair of satellites each broadcasting a healthy SF C/A-Code SPS SIS	3.5.1
3.7.2 SIS Constellation Availability	$\geq$ 0.98 Probability that at least 21 slots out of the 24 slots will be occupied by a satellite (or pair of satellites for expanded slots) broadcasting a healthy SF C/A-Code SPS SIS	3.5.2
	$\geq$ 0.99999 Probability that at least 20 slots out of the 24 slots will be occupied by a satellite (or pair of satellites for expanded slots) broadcasting a healthy SF C/A-Code SPS SIS	
3.7.3 Operational Satellite Counts	$\geq$ 0.95 Probability that the constellation will have at least 24 operational satellites regardless of whether those operational satellites are located in slots or not	3.5.3
3.8.1 PDOP Availability	$\geq$ 98% Global PDOP of 6 or less	3.6.1.1
	$\geq$ 88% Worst site PDOP of 6 or less	
3.8.2 Position Service Availability	$\geq$ 99% Horizontal service availability, average location	3.6.2
	$\geq$ 99% Vertical service availability, average location	
	$\geq$ 90% Horizontal service availability, worst-case location	
	$\geq$ 90% Vertical service availability, worst-case location	
3.8.3 Position/Velocity/Time Service Accuracy	$\leq$ 8 m 95% Horizontal error, global average position accuracy	3.6.3
	$\leq$ 13 m 95% Vertical error, global average position accuracy	
	$\leq$ 15 m 95% Horizontal error, worst site position accuracy	
	$\leq$ 33 m 95% Vertical error, worst site position accuracy	
	$\leq$ 0.2 m/s 95% Velocity error, any axis	
	$\leq$ 30 nsec Time transfer error 95% of the time	3.6.4

Chapter 3

Discussion of SPS PS Metrics and Results

While Chapter 2 summarizes the status of the SPSPS20 metrics for 2023, the statistics and trends reported in this chapter provide both additional information and support for those conclusions.

Contents

3.1 SIS Coverage 12
3.1.1 Per-Satellite Coverage 12
3.1.2 Constellation Coverage 12
3.2 SIS Accuracy 13
3.2.1 URE Over All AOD 14
3.2.1.1 Constellation URE 23
3.2.2 URE at Any AOD 24
3.2.3 URE at Zero AOD 25
3.2.4 URE Bounding 28
3.2.5 URE After 14 Days Without Upload 28
3.2.6 URRE Over All AOD 29
3.2.7 URAE Over All AOD 33
3.2.8 UTC Offset Error 36
3.3 SIS Integrity 38
3.3.1 URE Integrity 38
3.3.2 UTCOE Integrity 39
3.3.3 Instantaneous P_{sat} and P_{const} 40
3.4 SIS Continuity 41
3.4.1 Unscheduled Failure Interruptions 41
3.4.2 Status and Problem Reporting Standards 45
3.4.2.1 Scheduled Events 45
3.4.2.2 Unscheduled Outages 47
3.5 SIS Availability 48
3.5.1 Per-Slot Availability 48
3.5.2 Constellation Availability 50

3.5.3 Operational Satellite Counts 51
3.6 Position/Velocity/Time Domain Standards 52
3.6.1 Evaluation of DOP Assertions 52
3.6.1.1 PDOP Availability 52
3.6.2 Position Service Availability 55
3.6.3 Position/Velocity Accuracy 55
3.6.3.1 Results for Daily Average 56
3.6.3.2 Results for Worst Site 95^{th} Percentile 60
3.6.4 Time Transfer Accuracy 63

3.1 SIS Coverage

3.1.1 Per-Satellite Coverage

SIS per-satellite coverage is asserted in Section 3.3.1 of the SPSPS20. The following standard is provided (from Table 3.3-1):

- *"100% Coverage of Terrestrial Service Volume"*

This means that the direction of the Earth coverage beam of each GPS SV will be managed such that the beam will cover the terrestrial service volume visible to that SV, providing at least the minimum required received power at every point in its terrestrial footprint. This assertion is not evaluated at this time. Within the GPS Control Segment, the operators have various tools which enable them to monitor and control SV pointing. Monitoring this assertion external to the control segment will require both SV-specific antenna gain pattern information and calibrated power observations. The potential for evaluation may be examined in future reports.

3.1.2 Constellation Coverage

SIS constellation coverage is asserted in Section 3.3.2 of the SPSPS20. The following standard is provided (from Table 3.3-2):

- *"100% Coverage of Terrestrial Service Volume"*

This assertion is interpreted to mean that a user will have at least four SVs transmitting a healthy or marginal signal visible at any moment. This is evaluated as part of the examination of DOP (see Section 3.6). The condition was true throughout the year, thus the assertion is met for 2023.

3.2 SIS Accuracy

SIS URE accuracy is asserted in Section 3.4 of the SPSPS20. The following standards (from Tables 3.4-1 through 3.4-4 in the SPS PS) are considered in this report for each SPS SIS signal combination, per SPSPS20 Table 2.2-2:

- *"≤ 7.0 m 95% Global Statistic URE during Normal Operations over all AODs"*
- *"≤ 9.7 m 95% Global Statistic URE during Normal Operations at Any AOD"*
- *"≤ 3.8 m 95% Global Statistic URE during Normal Operations at Zero AOD"*
- *"≤ 30 m 99.94% Global Statistic URE during Normal Operations"*
- *"≤ 30 m 99.79% Worst Case Single Point Statistic URE during Normal Operations"*
- *"≤ 388 m 95% Global Statistic URE during Extended Operations after 14 Days without Upload (C/A only)"*
- *"≤ 2.0 m 95% Global Statistic URE during Normal Operations over all AODs for the ensemble of constellation slots"*
- *"≤ 0.006 m/s 95% Global Statistic URRE over any 3-second interval during Normal Operations at Any AOD"*
- *"≤ 0.002 m/s^2 95% Global Statistic URAE over any 3-second interval during Normal Operations at Any AOD"*
- *"≤ 30 nsec 95% Global Statistic UTCOE during Normal Operations at Any AOD"*

SIS accuracy values are included in the statistics only when the SV is healthy (except for L5, as described in the Introduction). Throughout this report, an SV is considered healthy based on the definition in SPS PS Section 2.3.2.

The URE statistics presented in this report are based on a comparison of the BCP against the TCP (see Appendix C).

3.2.1 URE Over All AOD

The 95th percentile Global Statistic URE over all ages of data (AODs) is the performance standard URE metric that is most closely related to a user's observations. This is associated with the SPSPS20 Section 3.4 metric:

- *"Each SPS SIS Component Combination per Table 2.2-2:*
  ≤ 7.0 m 95% Global Statistic URE during Normal Operations over all AODs"

This metric can be decomposed into several pieces to better understand the process, as follows:

- *Each SPS SIS Component Combination per Table 2.2-2* - This applies to all signal combinations.
- *7.0 m* - This is the limit against which to test.
- *95%* - This is the statistical measure applied to the data. In this case, there is a sufficiently large number of samples to allow direct sorting of the results across time and selection of the 95th percentile.
- *Global Statistic URE* - This refers to examining the URE across the field-of-view and across time. The brute force methods described in SPSPS20 A.4.11 are applicable to computing statistics over field-of-view and over time.
- *during Normal Operations* - This is a constraint related to normal vs. extended mode operations. See IS-GPS-200 20.3.4.4 [2] and Appendix A.4 of this report.
- *over all AODs* - This constraint means that the Global Statistic URE is considered at each evaluation time regardless of the AOD at the evaluation time. A more detailed explanation of the AOD and how this quantity is computed can be found in Appendix A.2.

In addition, the following general statements in Section 3.4 of SPSPS20 have a bearing on this calculation:

- These statistics are "per SV" - that is, they apply to the signal from each satellite, not for averages across the constellation.
- *"The ergodic period contains the minimum number of samples such that the sample statistic is representative of the population statistic. Under a one-upload-per-day scenario, for example, the traditional approximation of the URE ergodic period is 30 days."* (SPSPS20 Section 3.4, Note 2)

In order to evaluate this assertion, it is practical to compute a sufficiently dense spatial grid of Instantaneous SIS URE values across the period of interest separated by uniform timesteps (see Appendix C.2.3 for details), and then select the 95th percentile values from this set.

In this case, the time steps are 5 minutes and the period of interest is monthly. The monthly period approximates the suggested 30 day period while conforming to a familiar time scale. We have computed the monthly statistic regardless of the number of available days in each month, but have identified SV-months with fewer than 25 days of availability to note any SV-month with significantly less data than expected.

The results are organized as follows: Table 3.1 and Figure 3.1 contain L1 C/A single-frequency results, Table 3.2 and Figure 3.2 contain L1 C/A + L2C dual-frequency results, and Table 3.3 and Figure 3.3 contain L1 C/A + L5Q dual-frequency results.

Tables 3.1, 3.2, and 3.3 contain the monthly 95th percentile values of the Instantaneous SIS URE values based on the assumptions and constraints described above. For each SV, the worst value across the year is marked in red. In all cases, no values exceed the stated threshold of 7.0 m, and so this assertion is met for 2023.

Figures 3.1, 3.2, and 3.3 provide a summary of these results for the entire constellation.

A number of points are evident from this set of tables and figures:

1. All SVs meet the performance assertion of the SPSPS20, even when only the worst performing month is considered. Even the worst value for each SV (indicated by the upper extent of the range bars) is more than a factor of 2 smaller than the threshold.
2. For most of the SVs, the value of the 95th percentile SIS URE metric is relatively stable over the course of the year, as indicated by relatively small range bars.
3. The "best" SVs are those which cluster at the 1.0 m level and whose range variation is small.
4. SVN 72/PRN 8 (Block IIF) and SVN 73/PRN 10 (Block IIF) were the two SVs operating on a Cesium frequency standard, resulting in higher URE values for the year.
5. SVN 79/PRN 28 (GPS III), which was set operational February 2023, had larger URE values February through May than in the remainder of the year. These were likely related to early estimates of group delay (T_{GD}) and inter-signal correction (ISC) values as these were updated in May 2023.

Table 3.1: Monthly 95th Percentile Values of L1 C/A SIS Instantaneous URE for All SVs in Meters

SVN	PRN	Block	Jan	Feb	Mar	Apr	May	Jun	Jul	Aug	Sep	Oct	Nov	Dec	2023
41	22	IIR	0.71	–	–	–	–	–	–	–	–	–	–	–	0.71
43	13	IIR	0.85	1.01	0.86	0.98	1.02	0.97	0.93	0.92	1.10	0.89	0.97	0.95	0.96
44	22	IIR	–	–	–	–	–	–	–	1.19	0.96	0.82	0.80	0.92	0.92
45	21	IIR	1.32	1.75	1.46	1.36	1.29	1.41	1.68	1.33	1.30	1.37	1.09	1.21	1.39
48	7	IIR-M	1.04	0.97	1.05	0.98	1.19	1.19	0.92	1.10	1.05	1.15	1.21	1.25	1.09
50	5	IIR-M	0.69	0.53	0.56	0.62	0.90	0.60	0.91	0.99	0.71	0.86	0.75	0.64	0.76
51	20	IIR	1.31	1.52	1.21	1.04	1.00	1.17	1.12	1.21	1.06	1.02	1.19	0.89	1.18
52	31	IIR-M	0.94	0.95	0.99	1.03	0.88	0.97	1.02	0.91	0.70	0.86	0.81	0.85	0.92
53	17	IIR-M	1.86	1.18	1.59	1.62	1.75	1.68	1.36	1.55	1.60	1.57	1.38	1.52	1.54
55	15	IIR-M	0.47	0.76	0.48	0.48	0.50	0.52	0.65	0.60	0.67	0.71	0.81	0.93	0.70
56	16	IIR	0.62	0.58	0.63	0.56	0.69	0.76	0.73	0.83	0.88	0.86	0.91	0.89	0.79
57	29	IIR-M	0.91	1.17	1.62	1.35	1.15	1.23	1.38	1.48	1.10	0.89	1.26	1.17	1.21
58	12	IIR-M	1.01	1.16	0.88	0.85	1.50	0.96	0.78	0.76	0.65	0.64	0.63	0.71	0.95
59	19	IIR	1.42	1.30	1.25	1.39	1.28	1.13	1.21	1.08	1.09	1.30	1.31	1.17	1.27
61	2	IIR	1.13	1.16	1.15	1.11	1.28	1.19	1.13	1.26	1.18	1.34	1.31	1.29	1.23
62	25	IIF	0.84	1.10	1.11	1.19	0.98	1.02	0.90	0.83	0.73	0.69	0.99	0.76	1.00
63	1	IIF	0.58	0.66	0.68	0.85	0.92	0.67	0.64	–	–	–	–	–	0.75
64	30	IIF	0.58	0.63	0.73	0.70	0.82	0.66	0.89	0.99	1.08	1.08	1.10	0.91	0.92
65	24	IIF	0.64	0.82	1.09	0.70	0.55	0.75	0.59	0.73	0.64	0.73	0.65	0.50	0.73
66	27	IIF	0.86	0.61	1.03	0.83	0.66	0.79	1.34	0.70	0.86	0.92	0.90	0.95	0.88
67	6	IIF	0.84	0.86	1.04	1.14	0.98	1.05	1.10	1.15	0.86	0.86	0.85	0.74	1.00
68	9	IIF	0.61	0.62	0.66	0.58	0.44	0.61	0.49	0.67	0.65	0.48	0.48	0.59	0.58
69	3	IIF	1.97	1.52	1.16	2.07	1.62	1.68	1.96	2.06	1.82	1.96	1.68	2.06	1.83
70	32	IIF	0.93	0.96	0.85	0.81	0.61	0.83	0.83	1.02	0.80	0.68	0.67	0.73	0.83
71	26	IIF	0.53	0.57	0.60	0.62	0.54	0.55	0.52	0.49	0.47	0.65	0.80	0.61	0.59
72	8	IIF	2.42	2.37	1.84	1.93	2.29	2.44	2.51	2.66	2.47	2.54	2.40	2.48	2.40
73	10	IIF	2.12	2.22	1.95	1.99	2.00	2.00	1.66	2.32	1.91	2.39	2.32	2.12	2.09
74	4	III	0.71	0.81	0.76	0.81	0.77	0.74	0.77	0.80	0.80	0.74	0.76	0.59	0.76
75	18	III	0.74	0.76	0.82	0.81	0.82	0.67	0.65	0.82	0.89	1.17	1.01	0.95	0.88
76	23	III	0.82	0.87	0.86	0.79	0.73	0.85	0.76	0.83	0.97	0.91	0.88	0.95	0.86
77	14	III	0.75	0.82	0.86	0.90	0.92	0.86	0.87	0.94	1.05	1.06	1.03	1.01	0.94
78	11	III	0.74	0.70	0.77	0.96	0.84	0.81	0.91	1.07	1.04	1.09	1.11	1.17	1.00
79	28	III	–	3.39	3.31	3.43	2.79	0.69	0.89	0.98	0.66	0.72	0.75	0.90	3.11
Block IIR/IIR-M			1.16	1.21	1.16	1.15	1.19	1.13	1.14	1.12	1.06	1.12	1.12	1.08	1.14
Block IIF			1.32	1.20	1.13	1.23	1.28	1.31	1.38	1.52	1.38	1.46	1.33	1.48	1.33
GPS III			0.75	2.54	2.97	3.06	0.88	0.79	0.83	0.93	0.95	1.00	0.97	1.01	1.08
All SVs			1.15	1.25	1.46	1.51	1.18	1.12	1.15	1.20	1.12	1.15	1.13	1.14	1.19

Notes: Values not present indicate that the satellite was not healthy throughout this period. Months during which an SV was healthy for less than 25 days are shown shaded. Months with the highest SIS Instantaneous URE for a given SV are colored red. The column labeled "2023" is the 95th percentile over all the days in the year. The four rows at the bottom are the monthly 95th percentile values over various sets of SVs.

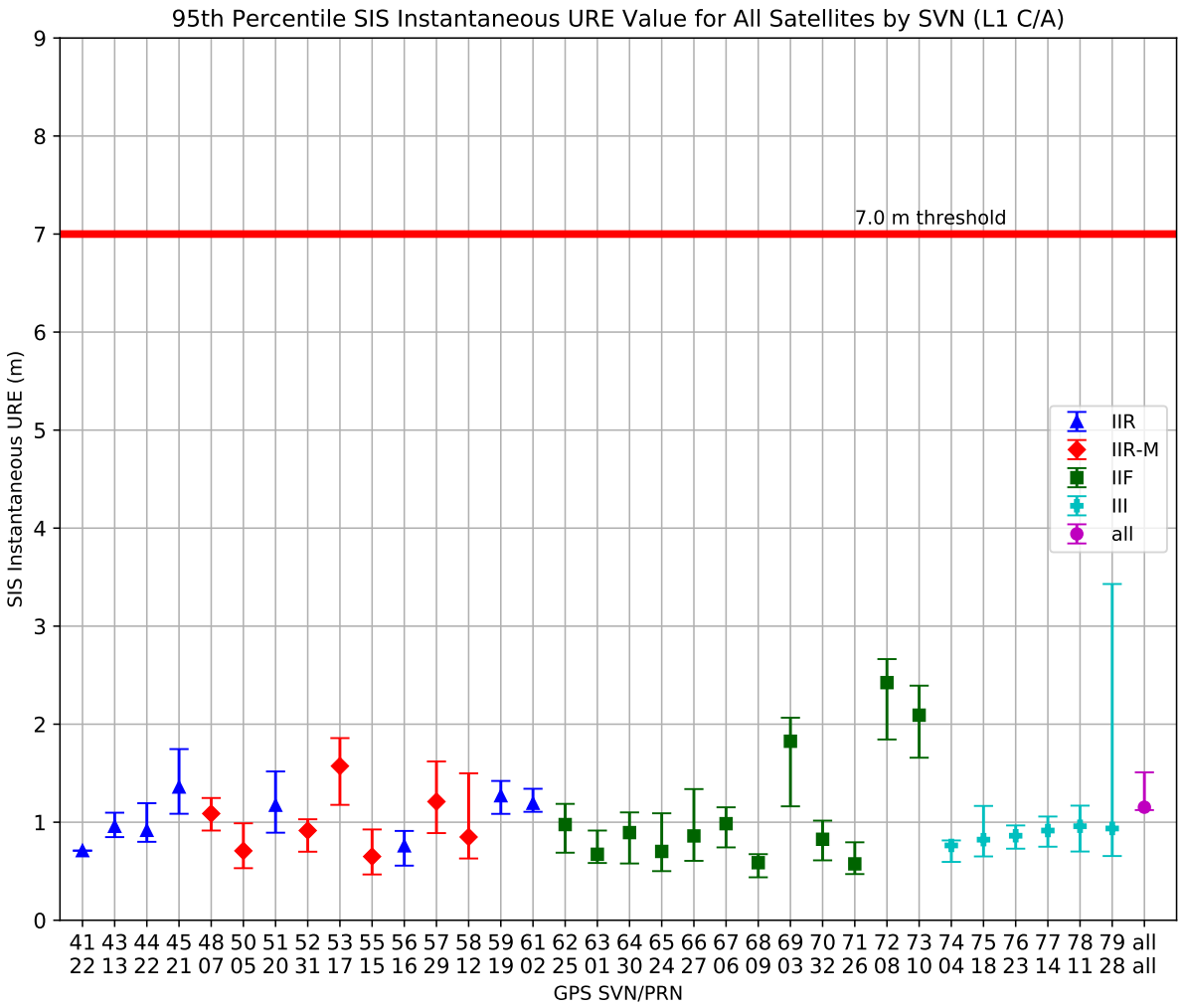

Figure 3.1: Range of the L1 C/A Monthly 95$^{\text{th}}$ Percentile Values for All SVs

Notes: Each SVN with valid data is shown sequentially along the horizontal axis. The median value of the monthly 95th percentile SIS URE is displayed as a point on each of the vertical bars. The minimum and maximum of the monthly 95th percentile SIS URE for 2023 are shown by whiskers at the top and bottom of each vertical bar. Color and shape distinguish between the Block IIR, Block IIR-M, Block IIF, and GPS III SVs. The red horizontal line at 7.0 m indicates the upper bound given by the SPSPS20 Section 3.4 performance metric. The marker for "all" represents the monthly 95th percentile values across all satellites.

Table 3.2: Monthly 95th Percentile Values of L1 C/A + L2C SIS Instantaneous URE for All SVs in Meters

SVN	PRN	Block	Jan	Feb	Mar	Apr	May	Jun	Jul	Aug	Sep	Oct	Nov	Dec	2023
48	7	IIR-M	1.01	0.95	0.99	1.02	1.15	1.06	0.93	1.20	1.02	1.13	1.16	1.32	1.08
50	5	IIR-M	0.49	0.43	0.49	0.48	0.65	0.53	0.61	0.70	0.40	0.56	0.54	0.65	0.55
52	31	IIR-M	0.91	0.83	0.94	1.15	0.87	0.95	0.98	0.91	0.72	0.81	0.78	0.90	0.90
53	17	IIR-M	1.72	1.27	1.63	1.57	1.75	1.60	1.30	1.56	1.56	1.59	1.41	1.54	1.52
55	15	IIR-M	0.39	0.63	0.40	0.46	0.50	0.47	0.57	0.52	0.53	0.61	0.51	0.46	0.51
57	29	IIR-M	0.95	1.17	1.60	1.35	1.07	1.21	1.31	1.41	1.35	0.92	1.43	1.08	1.23
58	12	IIR-M	1.02	1.16	0.92	0.81	1.49	0.85	0.75	0.77	0.65	0.67	0.59	0.63	0.93
62	25	IIF	0.66	0.76	0.76	0.75	0.72	0.66	0.53	0.52	0.59	0.51	0.64	0.65	0.67
63	1	IIF	0.57	0.59	0.60	0.73	0.80	0.58	0.60	–	–	–	–	–	0.66
64	30	IIF	0.64	0.78	0.84	0.87	0.60	0.46	0.64	0.74	0.85	0.84	0.73	0.71	0.75
65	24	IIF	0.47	0.64	0.87	0.77	0.70	0.90	0.77	0.75	0.70	0.53	0.56	0.47	0.71
66	27	IIF	0.79	0.64	0.96	0.87	0.57	0.64	1.25	0.56	0.50	0.52	0.82	1.00	0.75
67	6	IIF	0.48	0.52	0.60	0.60	0.46	0.50	0.57	0.69	0.70	0.55	0.58	0.66	0.58
68	9	IIF	0.59	0.57	0.64	0.48	0.43	0.56	0.50	0.65	0.66	0.51	0.62	0.56	0.57
69	3	IIF	1.81	1.26	1.01	1.95	1.58	1.44	1.79	1.72	1.53	1.82	1.78	1.89	1.67
70	32	IIF	0.80	0.63	0.57	0.55	0.44	0.41	0.46	0.59	0.45	0.35	0.43	0.56	0.53
71	26	IIF	0.47	0.55	0.54	0.62	0.52	0.55	0.50	0.38	0.54	0.69	0.71	0.58	0.56
72	8	IIF	2.52	2.44	1.84	1.98	2.25	2.41	2.43	2.73	2.46	2.52	2.44	2.48	2.41
73	10	IIF	2.04	2.45	2.18	2.18	2.23	2.25	1.84	2.48	2.15	2.53	2.37	2.31	2.26
74	4	III	0.41	0.55	0.46	0.53	0.43	0.38	0.44	0.49	0.38	0.33	0.36	0.40	0.44
75	18	III	0.48	0.54	0.48	0.48	0.46	0.52	0.41	0.54	0.54	0.75	0.58	0.53	0.53
76	23	III	0.57	0.60	0.61	0.51	0.48	0.58	0.51	0.63	0.73	0.58	0.54	0.62	0.58
77	14	III	0.45	0.49	0.58	0.65	0.58	0.50	0.50	0.60	0.72	0.76	0.70	0.66	0.62
78	11	III	0.47	0.49	0.53	0.67	0.50	0.46	0.55	0.62	0.52	0.58	0.64	0.68	0.58
79	28	III	–	1.12	0.67	0.73	0.62	0.56	0.75	0.81	0.62	0.56	0.53	0.64	0.67
Block IIR-M			0.97	0.99	1.01	0.98	1.15	0.94	0.92	1.02	0.93	0.89	0.97	0.97	0.98
Block IIF			1.26	1.15	1.09	1.24	1.23	1.31	1.37	1.55	1.33	1.53	1.36	1.49	1.33
GPS III			0.48	0.58	0.56	0.61	0.52	0.51	0.57	0.61	0.61	0.62	0.59	0.61	0.58
All SVs			0.99	0.97	0.94	0.99	1.05	0.98	1.02	1.15	1.02	1.08	1.02	1.08	1.02

Notes: Values not present indicate that the satellite was not healthy throughout this period. Months during which an SV was healthy for less than 25 days are shown shaded. Months with the highest SIS Instantaneous URE for a given SV are colored red. The column labeled "2023" is the 95th percentile over all the days in the year. The four rows at the bottom are the monthly 95th percentile values over various sets of SVs.

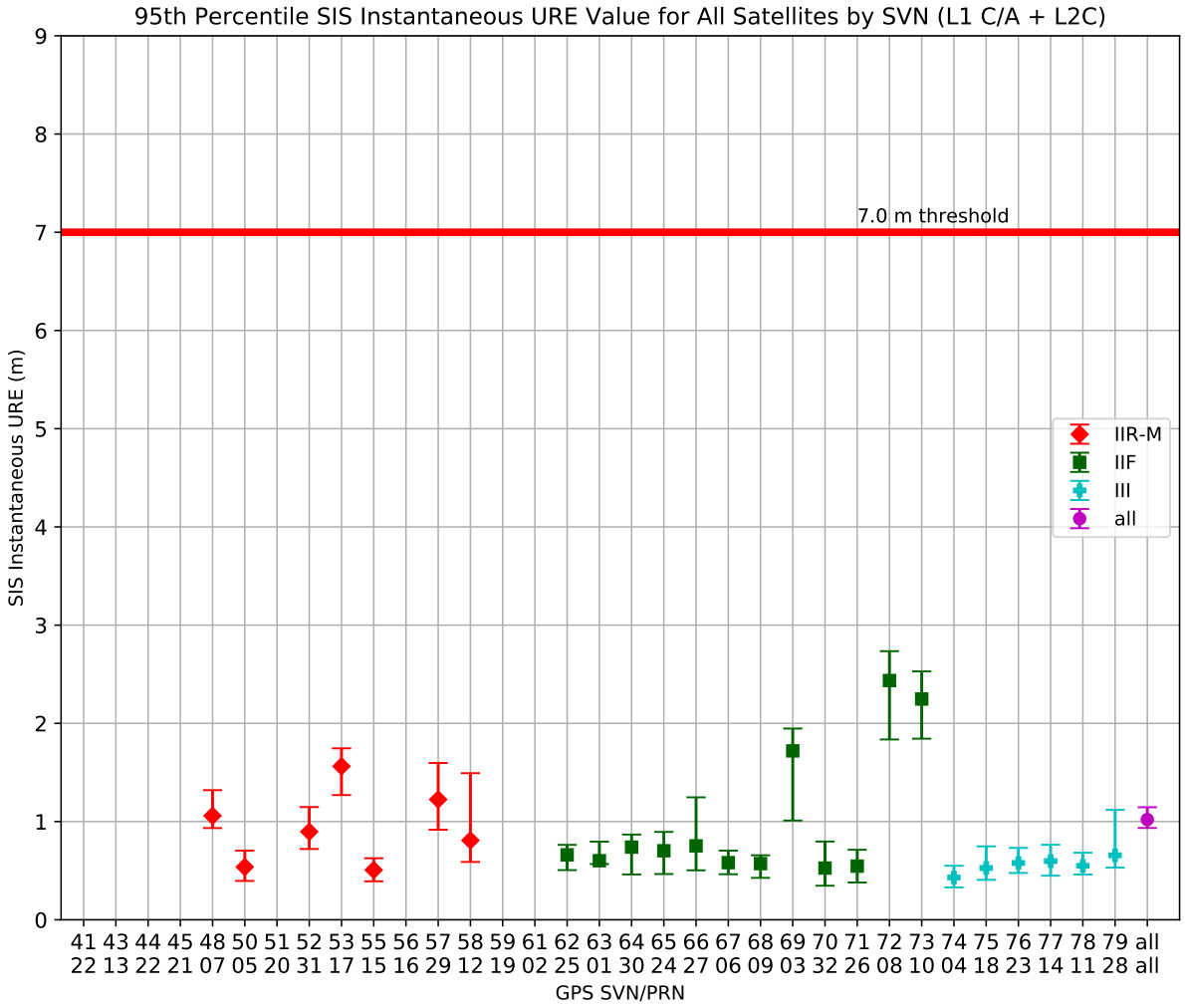

Figure 3.2: Range of the L1 C/A + L2C Monthly 95$^{\text{th}}$ Percentile Values for All SVs

Notes: Each SVN with valid data on at least one of the dual-frequency signals is shown sequentially along the horizontal axis. Satellites without valid data on both of the dual-frequency signals are not plotted. The median value of the monthly 95th percentile SIS URE is displayed as a point on each of the vertical bars. The minimum and maximum of the monthly 95th percentile SIS URE for 2023 are shown by whiskers at the top and bottom of each vertical bar. Color and shape distinguish between the Block IIR-M, Block IIF, and GPS III SVs. The red horizontal line at 7.0 m indicates the upper bound given by the SPSPS20 Section 3.4 performance metric. The marker for "all" represents the monthly 95th percentile values across all satellites.

Table 3.3: Monthly 95th Percentile Values of L1 C/A + L5Q SIS Instantaneous URE for All SVs in Meters

SVN	PRN	Block	Jan	Feb	Mar	Apr	May	Jun	Jul	Aug	Sep	Oct	Nov	Dec	2023
62	25	IIF	0.70	0.91	0.90	0.89	0.74	0.74	0.61	0.57	0.55	0.56	1.10	0.83	0.82
63	1	IIF	0.53	0.57	0.58	0.72	0.75	0.54	0.63	–	–	–	–	–	0.63
64	30	IIF	0.60	0.60	0.69	0.71	0.87	0.67	0.93	1.05	1.18	1.14	1.11	0.91	0.96
65	24	IIF	0.56	0.60	0.86	0.87	0.84	1.05	0.93	0.85	0.86	0.60	0.88	0.93	0.86
66	27	IIF	0.76	0.59	0.94	0.83	0.55	0.63	1.20	0.56	0.48	0.56	0.98	1.16	0.81
67	6	IIF	0.71	0.70	0.62	0.55	0.65	0.62	0.58	0.80	0.96	0.75	0.71	0.74	0.72
68	9	IIF	0.71	0.67	0.64	0.53	0.42	0.49	0.48	0.57	0.57	0.52	0.56	0.56	0.58
69	3	IIF	1.79	1.35	1.29	1.94	1.66	1.44	1.69	1.50	1.38	1.91	1.72	1.85	1.66
70	32	IIF	1.07	0.85	0.81	0.93	0.74	0.64	0.68	0.74	0.75	0.69	0.59	0.63	0.78
71	26	IIF	0.64	0.61	0.56	0.55	0.72	0.63	0.61	0.59	0.46	0.60	0.80	0.74	0.64
72	8	IIF	2.58	2.42	1.79	2.04	2.16	2.40	2.36	2.71	2.43	2.47	2.39	2.39	2.37
73	10	IIF	1.98	2.44	2.21	2.21	2.26	2.35	1.86	2.43	2.18	2.48	2.28	2.24	2.25
74	4	III	0.65	0.73	0.66	0.71	0.67	0.62	0.68	0.66	0.60	0.59	0.72	0.66	0.67
75	18	III	0.62	0.61	0.66	0.61	0.71	0.58	0.59	0.75	0.77	1.00	0.93	0.89	0.78
76	23	III	0.82	0.87	0.90	0.77	0.71	0.84	0.81	0.90	0.99	0.89	0.91	0.98	0.88
77	14	III	0.75	0.81	0.88	0.94	0.93	0.85	0.84	0.94	1.06	1.14	1.11	1.11	0.99
78	11	III	0.88	0.89	0.89	1.04	0.94	0.89	0.99	1.03	0.90	1.00	1.18	1.21	1.03
79	28	III	–	2.14	0.85	0.97	0.88	0.84	1.07	1.08	0.72	0.89	1.06	1.16	1.11
Block IIF			1.29	1.18	1.16	1.30	1.26	1.32	1.35	1.50	1.33	1.55	1.37	1.47	1.34
GPS III			0.78	1.26	0.83	0.91	0.84	0.81	0.91	0.93	0.89	0.97	1.04	1.08	0.94
All SVs			1.05	1.20	1.01	1.10	1.06	1.07	1.13	1.25	1.15	1.28	1.19	1.24	1.15

Notes: Values not present indicate that the satellite was not healthy throughout this period. Months during which an SV was healthy for less than 25 days are shown shaded. Months with the highest SIS Instantaneous URE for a given SV are colored red. The column labeled "2023" is the 95th percentile over all the days in the year. The three rows at the bottom are the monthly 95th percentile values over various sets of SVs.

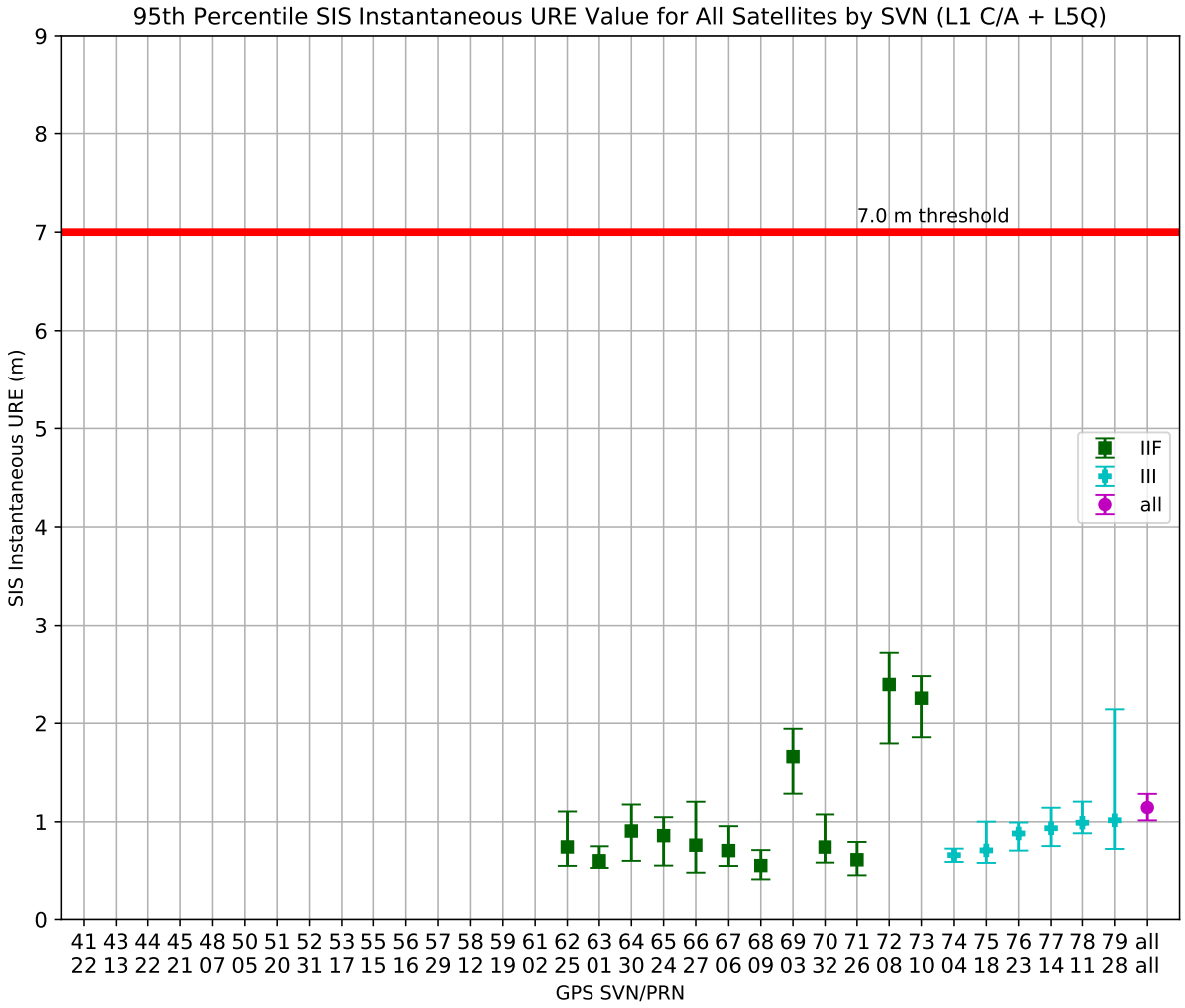

Figure 3.3: Range of the L1 C/A + L5Q Monthly 95$^{\text{th}}$ Percentile Values for All SVs

Notes: Each SVN with valid data on at least one of the dual-frequency signals is shown sequentially along the horizontal axis. Satellites without valid data on both of the dual-frequency signals are not plotted. The median value of the monthly 95th percentile SIS URE is displayed as a point on each of the vertical bars. The minimum and maximum of the monthly 95th percentile SIS URE for 2023 are shown by whiskers at the top and bottom of each vertical bar. Color and shape distinguish between the Block IIF and GPS III SVs. The red horizontal line at 7.0 m indicates the upper bound given by the SPSPS20 Section 3.4 performance metric. The marker for "all" represents the monthly 95th percentile values across all satellites.

We compute the differences between the dual-frequency (L1 C/A + L2C, L1 C/A + L5Q) and the single-frequency (L1 C/A) monthly 95$^{\text{th}}$ percentile values. This allows us to examine the relative differences between the various signal combinations. Figure 3.4 plots these differences for each SV.

It should be noted that each of the combinations starts with the same broadcast orbit and the same precise orbit.

The differences in the URE results are due to the inter-signal correction (ISC) values, the DCBs being used to evaluate the correctness of the ISCs, and the inter-signal correction process. Appendix C.2.2 describes the manner in which the ISCs, the DCBs, and the process interact. For purposes of Figure 3.4, it is sufficient to note that the L1 C/A values are assumed as "truth" and the range of the differences against the monthly values for the other signal combinations are shown.

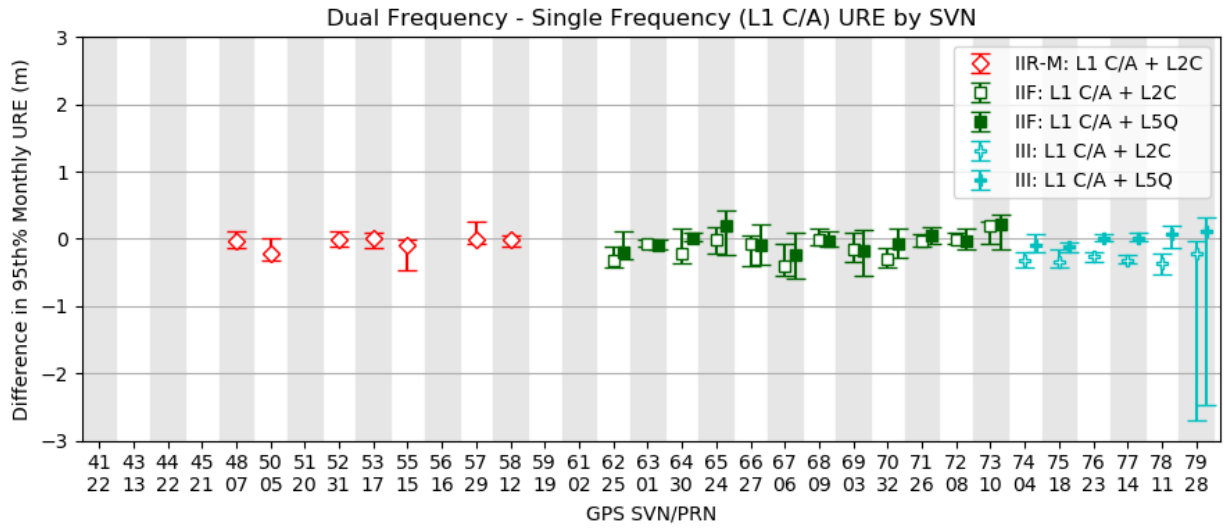

Figure 3.4: Range of Differences in Monthly Values between Dual-Frequency and L1 C/A UREs for All SVs

Notes: Each SVN with valid data is shown sequentially along the horizontal axis. The median value of the difference of monthly 95th percentile SIS URE is displayed as a point on each of the vertical bars. The minimum and maximum of the difference for 2023 are shown by whiskers at the top and bottom of each vertical bar. Color and shape distinguish between the Block IIR-M, Block IIF, and GPS III SVs.

3.2.1.1 Constellation URE

The constellation accuracy is asserted in the last row of Table 3.4-1 of Section 3.4.1 of the SPSPS20:

- *"≤ 2.0 m 95% Global Statistic URE during normal operations over all AODs for the ensemble of constellation slots"*

This assertion is unique among the SIS URE assertions in that it is across all the SVs occupying slots rather than by-SV. A similar process is used to derive a monthly statistic; however, the values for all trackable, healthy SV-epochs are included in the statistic rather than considering one SV at a time.

Figures 3.1, 3.2, and 3.3 show the constellation results as the rightmost range of values labeled "all" in the legend, shown in magenta.

Tables 3.1, 3.2, and 3.3 contain the monthly 95th percentile values for all operational SVs in the final row. These values are replicated in Table 3.4 below. As seen, these values are all below 2.0 m, thus the assertion is met.

This is a slightly larger population than the set of SVs that occupy slots. As shown in Appendix B, of the 31 or 32 operational SVs, there were 29 or 30 SVs in slots throughout the year. However, the constellation values shown have sufficient margin that the assertion is met.

This is asserted to be true for all signal combinations in SPSPS20 Table 2.2-2.

Table 3.4: Monthly 95th Percentile Values of Constellation SIS Instantaneous URE for All Signals in Meters

Signal	Jan	Feb	Mar	Apr	May	Jun	Jul	Aug	Sep	Oct	Nov	Dec	2023
L1 C/A	1.15	1.25	1.46	1.51	1.18	1.12	1.15	1.20	1.12	1.15	1.13	1.14	1.19
L1 C/A + L2C	0.99	0.97	0.94	0.99	1.05	0.98	1.02	1.15	1.02	1.08	1.02	1.08	1.02
L1 C/A + L5Q	1.05	1.20	1.01	1.10	1.06	1.07	1.13	1.25	1.15	1.28	1.19	1.24	1.15

Notes: Months with the highest SIS Instantaneous URE for a given signal or signal combination are colored red. The column labeled "2023" is the 95th percentile over all the days in the year.

3.2.2 URE at Any AOD

The next URE metric considered is the calculation of URE at any AOD. This is associated with the following SPSPS20 Section 3.4 metric:

- *"≤ 9.7 m 95% Global Statistic URE during Normal Operations at Any AOD"*

This metric may be decomposed in a manner similar to the metrics for URE over all AOD. The key differences are the term "at any AOD" and the change in the threshold value. The phrase "at any AOD" is interpreted to mean that at any AOD where sufficient data can be collected to constitute a reasonable statistical set, the value of the required statistic should be ≤ 9.7 m. See Appendix A.2 for a discussion of how the AOD is computed.

To examine this requirement, the set of 30 s Instantaneous RMS (root mean square) SIS URE values was computed as described in Appendix C.2.4, and processed as described in Appendix A.5. In summary, the RMS SIS URE values for each satellite for the entire year were divided into bins based on 15 minute intervals of AOD. The 95$^{\text{th}}$ percentile values for each bin were selected and the results were plotted as a function of the AOD in hours.

Figures 3.5 through 3.10 show up to four curves:

- 95$^{\text{th}}$ percentile URE vs. AOD for:
  - Blue: L1 C/A
  - Magenta: L1 C/A + L2C
  - Cyan: L1 C/A + L5Q
- Green: count of points in each bin vs. AOD for L1 C/A

Where multiple curves are present, the biases between the curves are a result of the influence of the ISC and DCB values on the URE calculation process. See Appendix C.2.2 for details.

The count of points is shown for L1 C/A, which is representative of the curves for other signal combinations, as the unhealthy periods for all signals for a given SV are coordinated to within a few minutes.

For satellites operating on the normal pattern (roughly one upload per day), the count of points in each bin is roughly constant from the time the upload becomes available until about 24 hours AOD. This corresponds to the plateau area of the green curve for the well-performing satellites (e.g., Figures 3.5 and 3.9). For satellites that are uploaded more frequently, the green curve will show a left-hand peak higher than the nominal count decreasing to the right. This is a result of there being fewer points at higher AOD due to the more frequent uploads. The vertical scales on Figures 3.5 through 3.10 and the figures in Appendix A.5 have been constrained to a constant value to aid in comparisons among the charts. Any satellites that were operational for only part of the year will have a lower number of points per bin than the nominal.

The representative best performers for Block IIR, Block IIR-M, Block IIF, and GPS III are shown in Figures 3.5, 3.7, 3.9, and 3.11. These are SVN 56/PRN 16, SVN 50/PRN 5, SVN 68/PRN 9, and SVN 74/PRN 4, respectively. For all blocks, several SVs have similarly good results. Best performers exhibit a low and very flat distribution of AODs, and the UREs appear to degrade roughly linearly with time, at least to the point that the distribution (represented by the green curve) shows a marked reduction in the number of points.

Figures 3.6, 3.8, 3.10, and 3.12 show the worst performing (i.e. highest URE values) Block IIR, Block IIR-M, Block IIF, and GPS III SVs. These are SVN 45/PRN 21, SVN 57/PRN 29, SVN 72/PRN 8, and SVN 78/PRN 11, respectively. Note that the distribution of AOD samples for SVN 72/PRN 8 is biased toward shorter values of AOD, which indicates that uploads are occasionally occurring more frequently than once-per-day.

The plots for all satellites are contained in Appendix A.5. A review of the full set of plots leads to the conclusion that the rate of URE growth for satellites using a Cesium frequency standard is noticeably higher. While there are differences between individual satellites, all the results are well within the assertion for this metric.

3.2.3 URE at Zero AOD

Another URE metric considered is the calculation of URE at Zero Age of Data (ZAOD). This is associated with the SPSPS20 Section 3.4 metric:

- *"$\leq$ 3.8 m 95% Global Statistic URE during Normal Operations at Zero AOD"*

This metric may be decomposed in a manner similar to the previous two metrics. The key differences are the term "at Zero AOD" and the change in the threshold value.

The broadcast ephemeris is never available to user equipment at ZAOD due to the delays inherent in preparing the broadcast ephemeris and uploading it to the SV. However, we can still make a case that this assertion is met by examining the 95^{th} percentile SIS RMS URE value at 15 minutes AOD. These values are represented by the left-most data point on the blue lines shown in Figure 3.5 through Figure 3.12. The ZAOD values should be slightly smaller than the 15 minute AOD values or, at worst, roughly comparable. Inspection of the 15 minute AOD values shows that the values for all SVs are well within the 3.8 m value associated with the assertion. Therefore, the assertion is considered fulfilled.

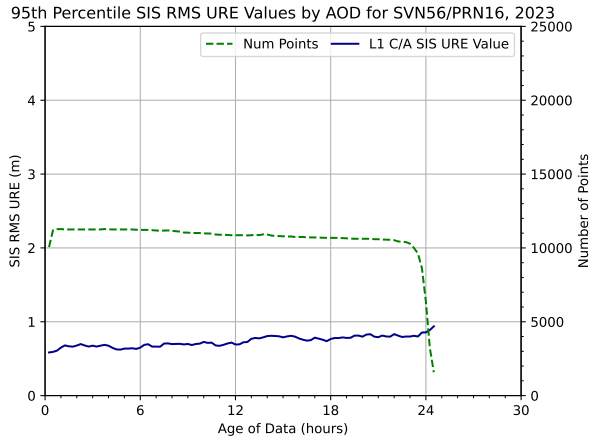

Figure 3.5: Best Performing Block IIR SV by URE Over Any AOD

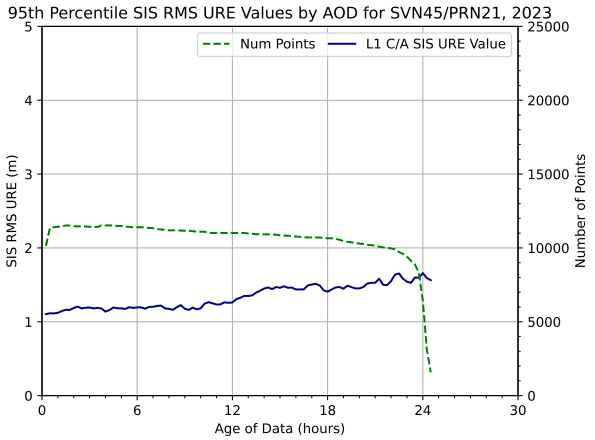

Figure 3.6: Worst Performing Block IIR SV by URE Over Any AOD

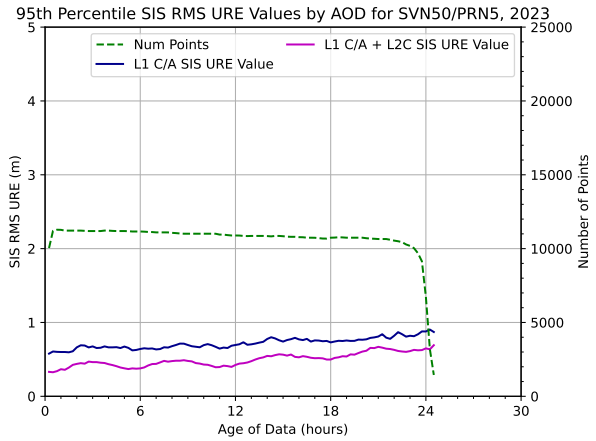

Figure 3.7: Best Performing Block IIR-M SV by URE Over Any AOD

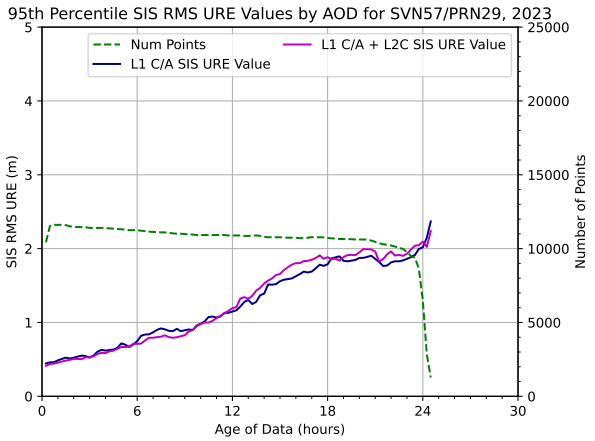

Figure 3.8: Worst Performing Block IIR-M SV by URE Over Any AOD

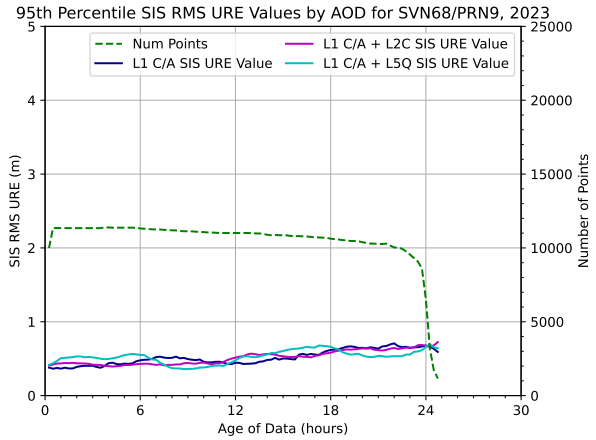

Figure 3.9: Best Performing Block IIF SV by URE Over Any AOD

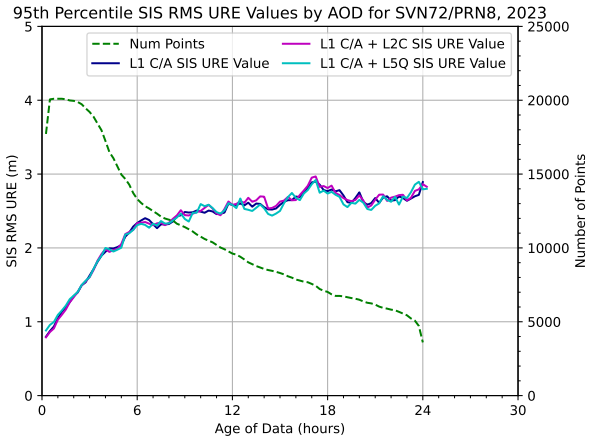

Figure 3.10: Worst Performing Block IIF SV by URE Over Any AOD

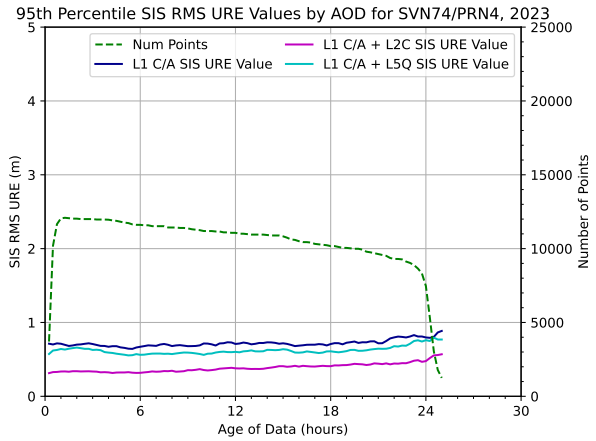

Figure 3.11: Best Performing GPS III SV by URE Over Any AOD

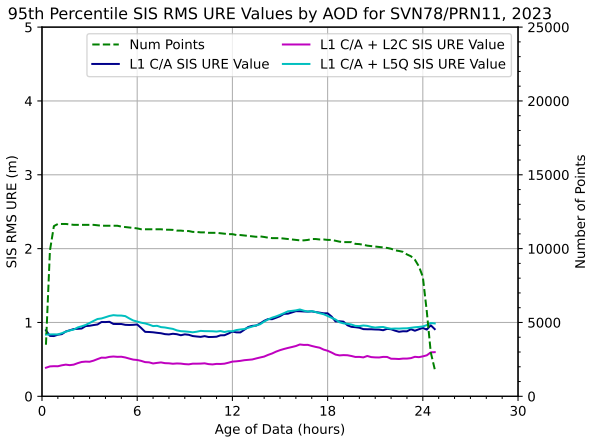

Figure 3.12: Worst Performing GPS III SV by URE Over Any AOD

3.2.4 URE Bounding

The SPSPS20 asserts the following requirements:

- *"≤ 30 m 99.94% Global Statistic URE during Normal Operations"*
- *"≤ 30 m 99.79% Worst Case Single Point Statistic URE during Normal Operations"*

The conditions and constraints do not clearly enumerate averaging periods. Therefore, the Instantaneous SIS URE values computed as part of the evaluation described in Appendix C.2.3 were checked for events exceeding the 30 m threshold. This provides a set of 577 Instantaneous SIS URE values distributed across the area visible to a given SV at each 5 min epoch, which yields a set of 60 million values per SV per year.

However, there are limitations to our technique of estimating UREs that are worth noting, such as fits across orbit/clock discontinuities, thrust events, and clock run-offs. These are discussed in Appendix C.2.5. As a result of these limitations, a set of L1 P(Y) + L2 P(Y) observed range deviations (ORDs) was also examined as a cross-check.

The ORDs were formed using the NGA observation data collected to support the position accuracy analysis described in Section 3.6.3. In the case of ORDs, the observed range is differenced from the range predicted by the geometric distance from the known station position to the SV location derived from the broadcast ephemeris. The ORDs are similar to the Instantaneous SIS URE in that both represent the error along a specific line-of-sight. However, the ORDs are not true SIS measurements due to the presence of residual atmospheric effects and receiver noise. The selected stations are geographically distributed such that at least two sets of observations are available for each SV at all times. As a result, any actual SV problems that would lead to a violation of this assertion will produce large ORDs from multiple stations.

There was one event with values that exceeded the 30 m threshold for 23 minutes on SVN 63/PRN 1. Appendix A.6 contains additional information on this event. The 99.94% Global Statistic URE for SVN 63/PRN 1 in 2023 was 1.50 m. The 99.79% Worst Case Single Point Statistic URE for SVN 63/PRN 1 in 2023 was 1.41 m. Based on these results, these assertions are considered satisfied.

3.2.5 URE After 14 Days Without Upload

The SPS PS provides the following assertion regarding URE after 14 days without an upload for single-frequency C/A-code:

- *"≤ 388 m 95% Global Statistic URE during Extended Operations after 14 Days without Upload"*

There were no periods in 2023 during which SVs were transmitting a healthy signal while operating after 14 days without an upload. As a result, this assertion was not evaluated.

3.2.6 URRE Over All AOD

The SPS PS provides the following assertion for the user range rate error (URRE):

- *"≤0.006 m/sec 95% Global Statistic URRE over any 3-second interval during Normal Operations at Any AOD"*

This is subject to the same general constraints from SPSPS20 Section 3.4 as the URE assertions.

The user range rate is the time-derivative of the range between the SV and the user; that is the rate of change of the range. For the case of a stationary user and an orbiting satellite, the actual user range rate will vary throughout a pass, but will be a smooth, continuous function. In reality, the measurement of user range, and therefore, the ability to derive the user range rate is limited by the noise of the SV frequency standard (clock) and the receiver frequency standard, along with other effects. The URRE measures the impact of the noise of the SV frequency standard on the SIS. For more information see SPSPS20 Section A.4.7.

The URRE cannot be evaluated by comparison of the BCP to the TCP. This is due to two factors:

1. as described in Note 1 to SPS PS Table 3.4-2, the primary contributing factor to the URRE is the noise from the SV frequency standards, and
2. the assertion states *"over any 3-second interval."*

In the precise orbits used for the TCP, the noise due to the SV clocks is smoothed over long periods. As a result, the comparison of BCP and TCP derivatives will not reveal short term (i.e. 3 s) changes in SV clock behavior.

To address this, a different evaluation process is used. This process uses the TCP along with the measured carrier phase observations and the known station positions to form the URRE values by differencing the range errors. The carrier phase observations have much lower noise than the pseudorange values, and because both phase and range are based on the same SV clock and the same receiver clock, the result will be a more precise measurement of the range rate error.

Dual-frequency observations are used to reduce ionospheric errors and a global tropospheric model is used to reduce tropospheric errors in order to adhere as closely as practical to the constraint that the results are to be based on SIS. The observation data available in 2023 included observations from L1 C/A and L2C at a 1 s rate. The URRE evaluation could not be conducted for Block IIR SVs due to the lack of usable dual-frequency data.

The preceding steps create a 1 s time-series of URRE values over 3 s intervals for each SV-receiver combination. This implies that the individual values are not fully independent as each 3 s interval spans three observations with the earliest/latest of each set contributing to the adjacent URRE value time periods. These results are grouped for each month for a

given SV for all healthy, trackable periods. Because the results are signed values, the 2.5% and 97.5% values are selected as the bounds of the 95^{th}%. These values are typically near-identical except for the sign. Therefore, the larger of the two is used as the 95^{th}% value. These are the results shown in Table 3.5 and Figure 3.13.

While the results are labeled as "URRE" in Table 3.5 and Figure 3.13, it should be noted that these are actually user-equivalent range rate errors (UERRE), as defined in Note 2 to SPS PS Table 3.4-2. Therefore, the results shown are the root-sum-square of the SIS-caused URRE and receiver-caused rate errors due to receiver thermal noise, local environmental issues such as multipath and room temperature, and the effect of the frequency standard that is associated with the receiver.

The values in Table 3.5 are all less than 6 mm/sec except for the values associated with SVN 72/PRN 8 for July through December. These values are at most 3% above the threshold. To explore this further, the URRE values were also computed using only data from the NGA monitor station at USNO which uses a frequency reference that is traceable to an ensemble of Hydrogen Maser frequency standards. This reduces the noise for the receiver portion of the UERRE but limits the visibility to the periods in which each SV is tracked by that station. When the data from the station at USNO are processed in isolation, the results show an improvement of 4 – 9% over the values in Table 3.5. As a result, all the values are less than 6 mm/sec. This indicates that the portion of UERRE attributable to SVN 72/PRN 8 is within the threshold.

The requirement is considered to be met in 2023 for all SVs other than Block IIR SVs. It is not possible to make a statement regarding the Block IIR SVs for 2023 due to the lack of dual-frequency observations.

Table 3.5: Monthly 95th Percentile Values of L1 C/A + L2C SIS Instantaneous URRE for All SVs in mm/s

SVN	PRN	Block	Jan	Feb	Mar	Apr	May	Jun	Jul	Aug	Sep	Oct	Nov	Dec
48	7	IIR-M	3.46	3.61	3.69	3.68	3.62	3.51	3.55	3.67	3.74	3.77	3.66	3.47
50	5	IIR-M	5.08	5.40	5.72	5.45	5.46	5.49	5.26	5.35	5.17	5.01	5.15	5.24
52	31	IIR-M	3.39	3.55	3.57	3.54	3.47	3.41	3.42	3.50	3.57	3.45	3.29	3.22
53	17	IIR-M	3.93	3.98	3.82	3.75	3.73	3.79	3.96	3.89	3.81	3.77	3.65	3.73
55	15	IIR-M	3.73	3.92	3.77	3.65	3.60	3.70	3.80	3.88	3.78	3.58	3.46	3.50
57	29	IIR-M	3.60	3.63	3.58	3.51	3.49	3.55	3.64	3.63	3.60	3.48	3.45	3.46
58	12	IIR-M	3.63	3.70	3.60	3.68	3.80	3.73	3.67	3.60	3.64	3.72	3.84	3.73
62	25	IIF	2.82	2.91	2.94	2.88	2.85	2.85	2.94	2.97	2.95	2.83	2.78	2.76
63	1	IIF	3.05	3.13	3.11	3.09	3.14	3.10	3.16	–	–	–	–	–
64	30	IIF	2.75	2.79	2.80	2.78	2.83	2.80	2.86	2.88	2.88	2.84	2.81	2.74
65	24	IIF	3.03	3.15	3.11	3.06	3.11	3.07	3.15	3.18	3.15	3.01	2.95	2.94
66	27	IIF	2.94	2.99	3.01	2.98	3.01	2.98	3.05	3.04	3.07	2.92	2.82	2.81
67	6	IIF	2.88	2.94	2.92	2.91	2.92	2.92	2.95	3.00	2.99	2.83	2.75	2.70
68	9	IIF	2.72	2.80	2.81	2.77	2.84	2.79	2.88	2.91	2.92	2.95	2.75	2.70
69	3	IIF	2.72	2.80	2.80	2.77	2.84	2.78	2.89	2.95	2.92	2.83	2.77	2.77
70	32	IIF	2.68	2.75	2.76	2.74	2.73	2.70	2.73	2.75	2.74	2.65	2.61	2.58
71	26	IIF	3.04	3.10	3.11	3.07	3.07	3.08	3.12	3.14	3.13	2.97	2.81	2.80
72	8	IIF	5.74	5.80	5.82	5.86	5.91	5.95	6.00	6.05	6.11	6.17	6.02	6.06
72*	8*	IIF	5.41	5.46	5.52	5.54	5.57	5.64	5.66	5.70	5.76	5.79	5.81	5.86
73	10	IIF	4.02	4.08	4.09	4.05	4.06	4.05	4.09	4.12	4.17	4.11	4.13	4.10
74	4	III	2.69	2.77	2.81	2.74	2.80	2.76	2.83	2.87	2.89	2.88	2.66	2.65
75	18	III	2.70	2.77	2.79	2.71	2.73	2.72	2.77	2.80	2.81	2.73	2.70	2.63
76	23	III	2.63	2.70	2.70	2.64	2.66	2.68	2.72	2.74	2.74	2.69	2.71	2.64
77	14	III	2.84	2.88	2.76	2.78	2.83	2.81	2.87	2.89	2.86	2.78	2.74	2.76
78	11	III	2.71	2.77	2.78	2.72	2.70	2.72	2.74	2.77	2.79	2.67	2.63	2.60
79	28	III	–	2.96	2.94	2.94	2.93	2.92	2.96	2.98	2.96	2.77	2.64	2.59
All SVs			3.44	3.53	3.52	3.47	3.48	3.47	3.52	3.58	3.55	3.47	3.40	3.38

*Notes: The URRE evaluation could not be conducted for Block IIR SVs due to the lack of usable dual-frequency data. Values not present otherwise indicate that the satellite was not healthy throughout this period. Months during which an SV was healthy for less than 25 days are shown shaded. Months with the highest SIS Instantaneous URRE for a given SV are colored red. The row at the bottom is the monthly 95th percentile values over all SVs. The * on the second row for SVN 72/PRN 08 indicates use of USNO data only. See Section 3.2.6 for more information.*

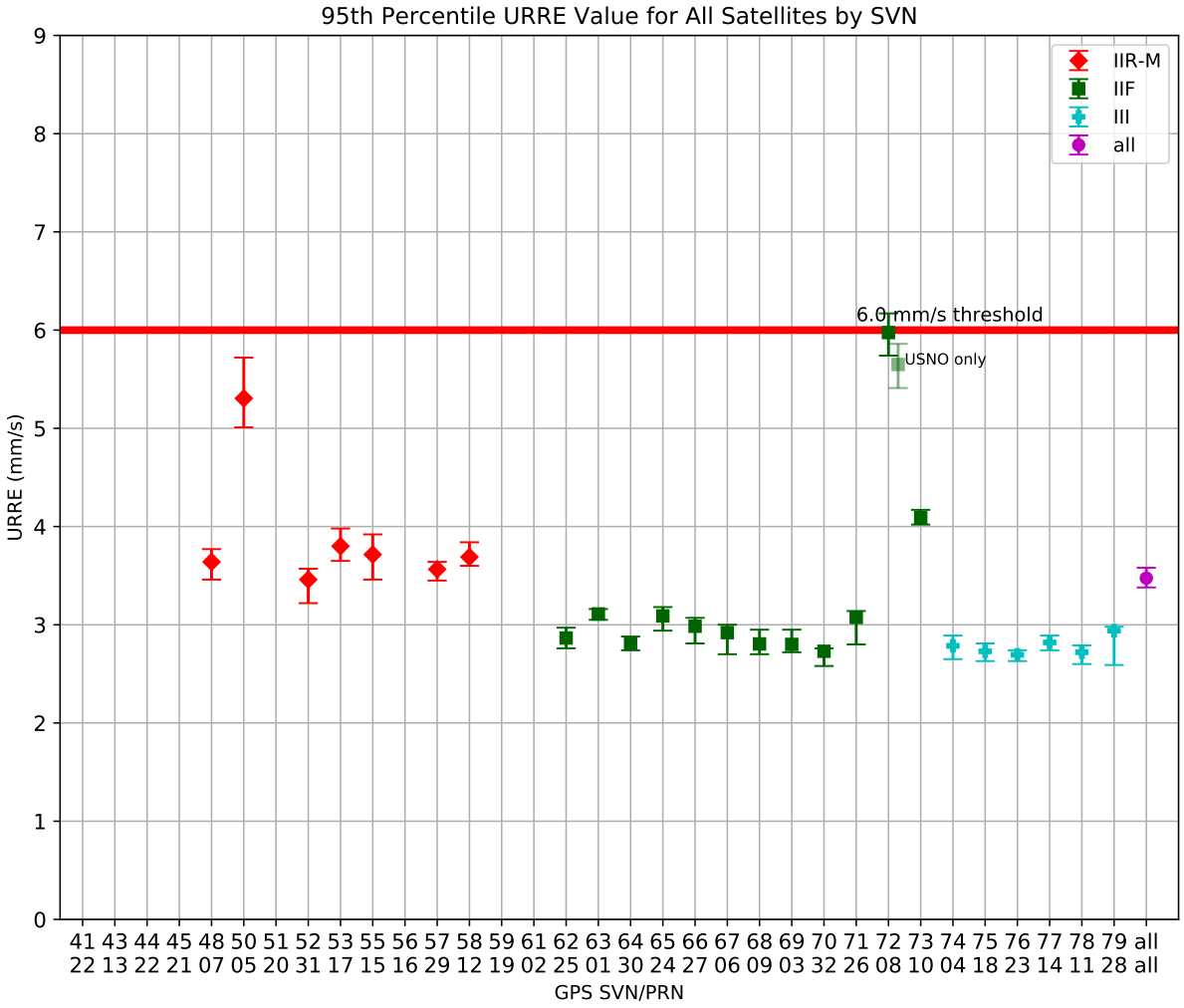

Figure 3.13: Range of the Monthly URRE 95th Percentile Values for All SVs

Notes: Each SVN with valid data is shown sequentially along the horizontal axis. The median value of the monthly 95th percentile URRE is displayed as a point on each of the vertical bars. The minimum and maximum of the monthly 95th percentile URRE for 2023 are shown by whiskers at the top and bottom of each vertical bar. Color distinguishes between the Block IIR-M, Block IIF, and GPS III SVs. The red horizontal line at 6.0 mm/s indicates the upper bound given by the SPSPS20 Section 3.4 performance metric. The marker for "all" represents the monthly 95th percentile values across all satellites. The marker for SVN 72/PRN 08 is duplicated to show both the range of values using all stations (unlabeled) and with only data from USNO considered (labeled "USNO only"). See Section 3.2.6 for details.

3.2.7 URAE Over All AOD

The SPS PS provides the following assertion for the user range acceleration error (URAE):

- *"≤0.002 m/sec/sec 95% Global Statistic URAE over any 3-second interval during Normal Operations at Any AOD"*

This is subject to the same general constraints from SPSPS20 Section 3.4 as the URE assertions.

The URAE is the time-derivative of the URRE. The URAE values were obtained by differencing the URRE values derived in support of the previous section. Table 3.6 contains the monthly 95$^{\text{th}}$ percentile values of the URAE based on the assumptions and constraints described above. For each SV, the worst value across the year is marked in red. Figure 3.14 provides a summary of these results for the entire constellation.

The values in Table 3.6 are all less than 2 mm/sec/sec except for the values associated with SVN 72/PRN 8 for all months and SVN 50/PRN 5 in February and March. As noted earlier, the values in the table are actually the user-equivalent range acceleration errors (UERAE) and include the noise of the receiver clock, as discussed in Section 3.2.6, which inflates the results. To explore this further, the URAE values were also computed using only data from the NGA monitor station at USNO. These results show 3-7% improvement over the values in Table 3.6. As a result, all the values are less than 2 mm/sec/sec except for SVN 72/PRN 8, which is still 5-14% above the threshold. Depending on the relative weight assumed for the receiver clock noise versus the satellite clock noise, SVN 72/PRN 8 may or may not be within the threshold.

This requirement is considered to be met in 2023 for all SVs other than Block IIR SVs and for SVN 72/PRN 8. It is not possible to make a statement regarding the Block IIR SVs for 2023 due to the lack of dual-frequency observations. For SVN 72/PRN 8, the results are inconclusive.

Table 3.6: Monthly 95th Percentile Values of L1 C/A + L2C SIS Instantaneous URAE for All SVs in mm/s/s

SVN	PRN	Block	Jan	Feb	Mar	Apr	May	Jun	Jul	Aug	Sep	Oct	Nov	Dec
48	7	IIR-M	1.51	1.55	1.57	1.54	1.56	1.54	1.56	1.59	1.58	1.58	1.58	1.51
50	5	IIR-M	1.81	2.00	2.03	1.92	1.92	1.91	1.87	1.92	1.89	1.79	1.77	1.73
50*	5*	IIR-M	1.63	1.73	1.89	1.81	1.76	1.75	1.72	1.77	1.69	1.64	1.71	1.69
52	31	IIR-M	1.52	1.59	1.58	1.55	1.55	1.53	1.54	1.56	1.56	1.49	1.44	1.42
53	17	IIR-M	1.53	1.58	1.55	1.53	1.52	1.54	1.57	1.58	1.58	1.56	1.47	1.46
55	15	IIR-M	1.59	1.68	1.63	1.58	1.58	1.60	1.62	1.64	1.64	1.56	1.49	1.48
57	29	IIR-M	1.47	1.51	1.51	1.47	1.46	1.48	1.51	1.52	1.52	1.47	1.44	1.42
58	12	IIR-M	1.42	1.51	1.47	1.45	1.46	1.45	1.49	1.50	1.49	1.48	1.46	1.44
62	25	IIF	1.42	1.47	1.49	1.46	1.44	1.43	1.48	1.50	1.49	1.43	1.40	1.39
63	1	IIF	1.54	1.59	1.57	1.56	1.58	1.56	1.58	–	–	–	–	–
64	30	IIF	1.37	1.38	1.39	1.37	1.40	1.39	1.41	1.42	1.42	1.42	1.41	1.37
65	24	IIF	1.54	1.60	1.57	1.54	1.57	1.55	1.59	1.60	1.58	1.52	1.49	1.48
66	27	IIF	1.47	1.50	1.51	1.49	1.50	1.49	1.52	1.52	1.53	1.45	1.41	1.41
67	6	IIF	1.45	1.48	1.47	1.46	1.46	1.46	1.48	1.50	1.50	1.43	1.40	1.37
68	9	IIF	1.36	1.40	1.41	1.38	1.42	1.39	1.43	1.45	1.45	1.48	1.38	1.36
69	3	IIF	1.37	1.42	1.42	1.40	1.43	1.40	1.46	1.49	1.47	1.44	1.41	1.40
70	32	IIF	1.35	1.39	1.39	1.37	1.37	1.35	1.37	1.37	1.37	1.32	1.30	1.29
71	26	IIF	1.54	1.58	1.58	1.56	1.55	1.56	1.58	1.59	1.58	1.51	1.43	1.43
72	8	IIF	2.26	2.29	2.30	2.30	2.32	2.34	2.36	2.37	2.40	2.41	2.32	2.34
72*	8*	IIF	2.10	2.13	2.16	2.16	2.17	2.20	2.18	2.20	2.23	2.24	2.24	2.27
73	10	IIF	1.71	1.75	1.75	1.72	1.72	1.71	1.74	1.75	1.77	1.73	1.74	1.71
74	4	III	1.33	1.38	1.40	1.36	1.39	1.37	1.40	1.42	1.43	1.44	1.32	1.32
75	18	III	1.34	1.38	1.39	1.34	1.35	1.34	1.37	1.38	1.39	1.36	1.34	1.31
76	23	III	1.33	1.37	1.36	1.32	1.33	1.34	1.36	1.37	1.37	1.35	1.35	1.32
77	14	III	1.43	1.46	1.38	1.39	1.41	1.40	1.43	1.44	1.43	1.39	1.37	1.38
78	11	III	1.36	1.39	1.40	1.36	1.34	1.36	1.37	1.38	1.39	1.33	1.32	1.31
79	28	III	–	1.49	1.47	1.47	1.46	1.45	1.47	1.47	1.47	1.39	1.33	1.30
All SVs			1.53	1.58	1.57	1.55	1.55	1.55	1.57	1.59	1.58	1.54	1.50	1.48

*Notes: The URAE evaluation could not be conducted for Block IIR SVs due to the lack of usable dual-frequency data. Values not present otherwise indicate that the satellite was not healthy throughout this period. Months during which an SV was healthy for less than 25 days are shown shaded. Months with the highest SIS Instantaneous URAE for a given SV are colored red. The row at the bottom is the monthly 95th percentile values over all SVs. The * on the second row for SVN 50/PRN 05 and SVN 72/PRN 08 indicates use of USNO data only. See Section 3.2.7 for more information.*

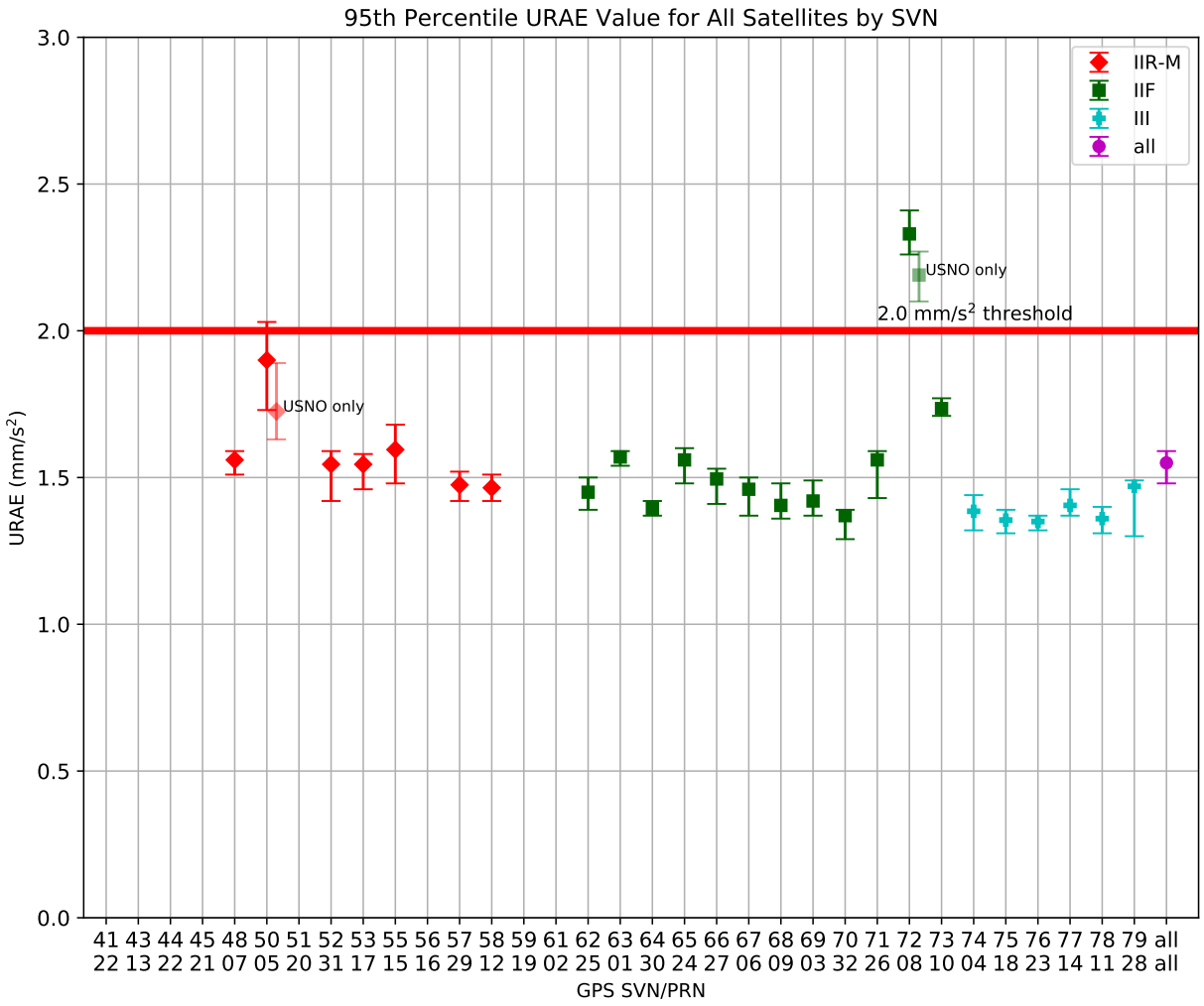

Figure 3.14: Range of the Monthly URAE 95$^{\text{th}}$ Percentile Values for All SVs

Notes: Each SVN with valid data is shown sequentially along the horizontal axis. The median value of the monthly 95th percentile URAE is displayed as a point on each of the vertical bars. The minimum and maximum of the monthly 95th percentile URAE for 2023 are shown by whiskers at the top and bottom of each vertical bar. Color distinguishes between the Block IIR-M, Block IIF, and GPS III SVs. The red horizontal line at 2.0 mm/s^2 indicates the upper bound given by the SPSPS20 Section 3.4 performance metric. The marker for "all" represents the monthly 95th percentile values across all satellites. The markers for SVN 50/PRN 05 and SVN 72/PRN 08 are duplicated to show both the range of values using all stations (unlabeled) and with only data from USNO considered (labeled "USNO only"). See Section 3.2.7 for details.

3.2.8 UTC Offset Error

The SPS PS Section 3.4.4, Table 3.4-4 provides the following assertion regarding the Coordinated Universal Time (UTC) offset error (UTCOE) accuracy:

- *"≤ 30 nsec 95% Global Statistic UTCOE during Normal Operations at Any AOD"*

The conditions and constraints state that this assertion should be true for any healthy SPS SIS.

This assertion was evaluated by calculating the global statistic UTCOE at each 15 minute interval in the year. The GPS-UTC offset available to the user was calculated based on the GPS broadcast navigation message data available from the SV at that time. The GPS-UTC offset truth information was provided by the U.S. Naval Observatory (USNO) daily GPS-UTC offset values. The USNO value for GPS-UTC at each evaluation epoch was derived from a multi-day spline fit to the daily truth values.

The global statistic at each 15 minute epoch is determined by evaluating the UTCOE across the surface of the earth at each point on a 111 km × 111 km grid. (This grid spacing corresponds to roughly 1° at the Equator.) At each grid point, the algorithm determines the set of SVs visible at or above the 5° minimum elevation angle that broadcast a healthy indication in the navigation message. For each of these SVs, the UTC offset information in the navigation message was compared to determine the data set that has an epoch time (t_{ot}) that is the latest of those that fall in the range $t_{current} \leq t_{ot} \leq t_{current}+72\ hours$. These data are used to form the UTC offset and UTCOE for that time-grid point. (The 72 hour value is derived from the 144 hour fit interval shown in IS-GPS-200 Table 20-XIII [2].)

The global statistics at each evaluation epoch are assembled into monthly data sets. The 95$^{\text{th}}$ percentile values are then selected from these sets.

The UTC offset parameters are contained in subframe 4, page 18 (data ID 56) of the GPS LNAV message transmitted on L1 C/A and in message type 33 of the GPS CNAV message transmitted on L2C and L5I. Typically, the values are identical across all three sources (within the precision provided). Because there are some differences between the LNAV and CNAV representations, the results were calculated for both LNAV and L2C CNAV. As a separate matter, we verified that the parameters transmitted on L2C CNAV and L5 CNAV for L5-capable SVs were identical. Therefore, the L5 results would be identical to the L2C results shown.

Figures 3.15 and 3.16 provide additional supporting information in the form of a time-history of global statistic UTCOE values at each 15 minute epoch for the year. Table 3.7 provides the results for each month of 2023. None of these values exceed the assertion of 30 nsec. Therefore, the assertion is verified for 2023.

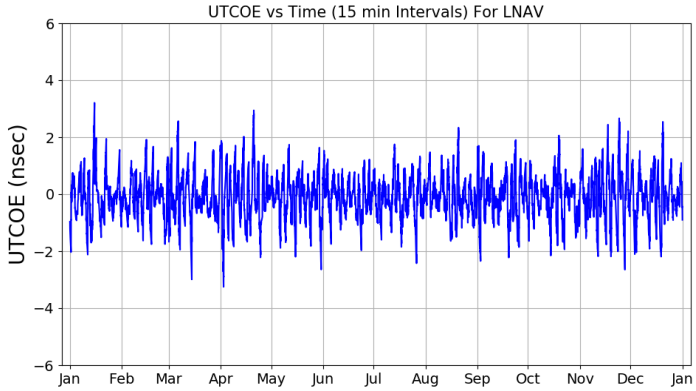

Figure 3.15: UTCOE LNAV Time Series for 2023

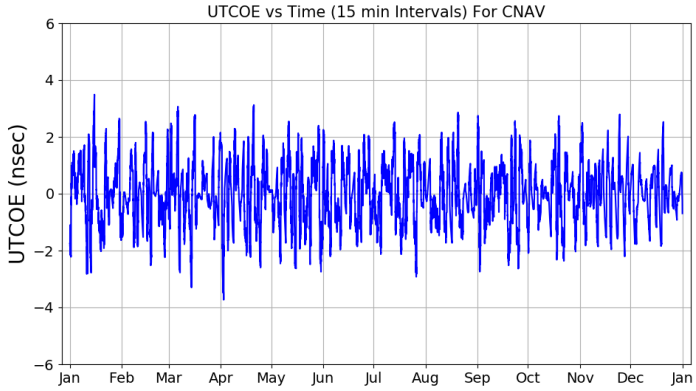

Figure 3.16: UTCOE CNAV Time Series for 2023

Table 3.7: 95th Percentile Global Statistic UTCOE for 2023

Month	**95th% Global Avg. UTCOE (nsec)**	
	LNAV	CNAV
Jan.	1.73	2.46
Feb.	1.44	2.15
Mar.	1.74	2.72
Apr.	1.84	2.41
May	1.60	2.30
Jun.	1.16	1.83
Jul.	1.35	2.08
Aug.	1.40	1.91
Sep.	1.64	2.30
Oct.	1.44	1.99
Nov.	1.98	1.94
Dec.	1.84	1.63

3.3 SIS Integrity

3.3.1 URE Integrity

Under the heading of SIS Integrity, the SPSPS20 makes the following assertion in Section 3.5.1, Table 3.5-1:

- *"$\leq 1 \times 10^{-5}$ Probability Over Any Hour of the SPS SIS Instantaneous URE Exceeding the NTE Tolerance Without a Timely Alert"*

The associated conditions and constraints include a limitation to a healthy SIS, a Not to Exceed (NTE) tolerance ±4.42 times the upper bound on the user range accuracy (URA) currently broadcast by the satellite, and a worst case for a delayed alert of 6 hours.

The reference to "a Timely Alert" in the assertion refers to any of a number of ways to issue an alert to the user through the GPS signal or navigation message. See SPSPS20 Section A.5.5 for a complete description.

The 2007 Precise Positioning Service (PPS) Performance Standard (PPSPS07) applies the following condition to the time period for the assertion:

- *"Applies to any satellite marked as healthy in the NAV message measured over any one-year interval"*

Technically, there is no time range for this assertion in the SPSPS20. However, we assert on the one-year interval in parallel to the PPSPS07.

This assertion was verified using two methods:

- The Instantaneous SIS URE values at the worst case location in view of each SV at each 5 minute interval were examined to determine the number of values that exceed ±4.42 times the URA. (The worst location was selected from the set of Instantaneous SIS URE values computed for each SV as described in Section 3.2.1.) The RMS UREs are also examined at a 30 second cadence to examine the results near where the threshold may be exceeded.
- ORDs at each 30 second interval from the NGA MSN tracking stations were examined to determine the number of values that exceed ±4.42 times the URA.

Two methods were used due to the fact that each method may result in false positives in rare cases. For example, the URE values may be incorrect near discontinuities in the TCP (as described in Appendix C.2.5). Similarly, the ORD values may be incorrect due to receiver or reception issues. Therefore, all reported events are examined manually to determine whether an integrity fault actually occurred, and if so, the extent.

Screening the Instantaneous SIS URE values and the ORD data revealed two events for which the URE exceeded NTE tolerance in 2023 across all signals. However, that does not mean that the assertion is met or unmet. Appendix A.6 contains additional information on these events.

There were 269128 healthy SV-hours for the year for L1 C/A. The resulting value of $2 / 269128 = 7.43 \times 10^{-6}$ does not violate the assertion. There were 212661 healthy SV-hours for the year for L1 C/A + L2C. The resulting value of $2 / 212661 = 9.40 \times 10^{-6}$ does not violate the assertion. There were 151408 healthy SV-hours for the year for L1 C/A + L5Q. The resulting value of $2 / 151408 = 1.32 \times 10^{-5}$ exceeds the assertion.

The assertion would be violated for L1 C/A + L5Q, however L5 is currently set unhealthy and is pre-operational. The assertion is verified for 2023 for L1 C/A and L1 C/A + L2C.

3.3.2 UTCOE Integrity

The SPS PS provides the following assertion regarding UTCOE Integrity in Section 3.5.4:

- *"$\leq 1 \times 10^{-5}$ Probability Over Any Hour of the SPS SIS Instantaneous UTCOE Exceeding the NTE Tolerance Without A Timely Alert during Normal Operations"*

The associated conditions and constraints include a limitation to a healthy SIS, and an NTE tolerance of ±120 nsec, given that the maximum SPS SIS instantaneous UTCOE did not exceed the NTE tolerance at the start of the hour. The reference to "a Timely Alert" in the assertion refers to any of a number of ways to issue an alert. See SPSPS20 Section A.5.5 for a complete description.

This assertion was evaluated by calculating the UTC offset for the navigation message subframe 4 page 18 data broadcast by each SV transmitting a healthy indication in the navigation message at each 15 minute interval. As in Section 3.2.8, only UTC offset information with an epoch time (t_{ot}) that is in the range $t_{current} \leq t_{ot} \leq t_{current} + 72\ hours$ were considered valid. That offset was used to compute the corresponding UTCOE from truth data obtained from USNO. If any UTCOE values exceed the NTE threshold of ±120 nsec, they would be investigated to determine if they represented actual violations of the NTE threshold or were artifacts of data processing.

No values exceeding the NTE threshold were found in 2023. The value farthest from zero for the year was 3.25 nsec for LNAV and 3.73 nsec for CNAV, both in April (see Figures 3.15 and 3.16). Therefore, the assertion is verified for 2023.

3.3.3 Instantaneous P_{sat} and P_{const}

The SPS PS provides the following assertions regarding P_{sat} and P_{const} in Section 3.5.5:

- *"$\leq 1 \times 10^{-5}$ Fraction of Time When the SPS SIS Instantaneous URE Exceeds the NTE Tolerance Without a Timely Alert (P_{sat})"*
- *"$\leq 1 \times 10^{-8}$ Fraction of Time When the SPS SIS Instantaneous URE from Two or More Satellites Exceeds the NTE Tolerance Due to a Common Cause Without a Timely Alert (P_{const})"*

These are closely related to the SIS URE integrity assertion discussed in Section 3.3.1. Technically, there is no time range for this assertion in the SPSPS20. However, we assert on the one-year interval in parallel to the process in Section 3.3.1.

As noted in Section 3.3.1, there were two events in which the SPS SIS Instantaneous URE exceeded the NTE tolerance on a single satellite. See Appendix A.6 for additional information.

P_{sat} is computed as a fraction of time, across the constellation. The combined duration of the events was 171 minutes for each signal.

There were 16147929 healthy SV-minutes for L1 C/A. The result of 171 / 16147929 is 1.06×10^{-5}, which violates the assertion. There were 12759666 healthy SV-minutes for L1 C/A + L2C. The result of 171 / 12759666 is 1.33×10^{-5}, which violates the assertion. There were 9084490 healthy SV-minutes for L1 C/A + L5Q. The result of 171 / 9084490 is 1.88×10^{-5}, which violates the assertion.

The P_{sat} assertion is violated for 2023 for all signals.

Each event was limited to a single satellite, thus P_{const} is 0 for the year, which fulfills the assertion.

3.4 SIS Continuity

3.4.1 Unscheduled Failure Interruptions

The SIS continuity metric for single frequency L1 C/A-code is stated in SPSPS20 Table 3.6-1 as follows:

- *"≥ 0.9998 Probability Over Any Hour of Not Losing the SPS SIS Availability from a Slot Due to Unscheduled Interruption"*

The conditions and constraints note the following:

- The empirical estimate of the probability is calculated as an average over all slots in the 24-slot constellation, normalized annually.
- The SPS SIS is available from the slot at the start of the hour.

There is some ambiguity in this metric, which is stated in terms of "a slot," while the associated conditions and constraints note that the assertion is an average over all slots. Therefore, both the per-slot and 24-slot constellation averages have been computed. As discussed below, while the per-slot values are interesting, the constellation average is the correct value to compare to the performance standard metric.

The notion of SIS continuity is slightly more complex for an expandable slot because multiple SVs are involved. Following SPSPS20 Section A.6.5, a loss of continuity is considered to occur when,

> *"The expandable slot is in the expanded configuration, and either one of the pair of satellites occupying the orbital locations defined in Table 3.2-2 for the slot loses continuity."*

Hence, the continuity of signal of the expanded slot will be determined by whether either SV loses continuity.

Three factors must be considered when looking at this metric:

1. Which SVs were assigned to which slots during the period of the evaluation.
2. When SVs were not transmitting, or were transmitting a PRN not available to users.
3. Which interruptions were scheduled vs. unscheduled.

The derivation of the SV/slot assignments is described in Appendix B.3.

For purposes of this report, interruptions were considered to have occurred if at least one of the following conditions is met:

1. One or more of the SVs assigned to the given slot are unhealthy as per SPSPS20 Section 2.3.2, which includes if the health bits in navigation message subframe 1 are set to anything other than all zeros.

2. If an appropriately distributed worldwide network of stations failed to collect any pseudorange data sets for a given SV for a given measurement interval. Failure to collect any data indicates that the satellite signal was removed from service (e.g., non-standard code or some other means).

The NGA MSN and IGS networks shown in Figure 1.1 provide continuous visibility from at least two stations with over 90% visibility from at least three stations. Therefore, if no data for a satellite are received for a specific time, it is highly likely that the satellite was not transmitting on the assigned PRN at that time. Receiver Independent Exchange format (RINEX) [7] observation files from these two networks were examined for each measurement interval (i.e., every 30 s) for each SV. If at least one receiver collected a pseudorange data set on LNAV with a signal-to-noise level of at least 25 dB-Hz on all frequencies and no loss-of-lock flags, the SV is considered trackable at that moment. This allows us to define an epoch-by-epoch availability for each satellite. For each slot, each hour in the year was examined. If an SV occupying the slot was not available at the start of the hour, the hour was not considered in the evaluation of the metric. If the slot was available at the start of the hour, the remaining data was examined to determine if an outage occurred during the hour.

The preceding criteria were applied to determine times and durations of interruptions. Subsequently, the Notice Advisories to Navstar Users (NANUs) effective in 2023 were reviewed to determine which of these interruptions could be considered scheduled interruptions, as defined in SPSPS20 Section 3.6. The scheduled interruptions were removed from consideration for purposes of assessing continuity of service. When a slot was available at the start of an hour but a scheduled interruption occurred during the hour, the hour was assessed based on whether data were available prior to the scheduled outage.

As defined in the ICD-GPS-240 [8], scheduled interruptions have a nominal notification time of 96 hours prior to the outage. Following the SPSPS20 Section 2.3.5, if the notification time for a scheduled interruption is less than 48 hours in advance of the interruption, the interruption will contribute to a loss of continuity.

The following NANU types are considered to represent (or modify) scheduled interruptions (assuming the 48-hour advance notice is met):

- FCSTDV - Forecast Delta-V
- FCSTMX - Forecast Maintenance
- FCSTRESCD - Forecast Rescheduled
- FCSTUUFN - Forecast Unusable Until Further Notice

We referenced the FCSTSUMM (Forecast Summary) NANU that occurs after the outage to confirm the actual beginning and ending time of the outage.

The results of the assessment of SIS continuity are summarized in Table 3.8. The metric is averaged over the constellation; therefore, the value in the bottom row (labeled "All Slots") must be greater than 0.9998 in order to meet the assertion.

Table 3.8: Probability Over Any Hour of Not Losing L1 C/A Availability Due to Unscheduled Interruption for 2023

Plane-Slot	**Count of Hours with the SPS SIS available at the start of the hour**[b]	**Count of Hours with Unscheduled Interruption**[c]	**Fraction of Hours in Which Availability was Maintained**
A1	8760	0	1.000000
A2[a]	8195	4	0.999512
A3	8755	0	1.000000
A4	8754	0	1.000000
B1[a]	8750	0	1.000000
B2	8754	0	1.000000
B3	8760	0	1.000000
B4	8754	0	1.000000
C1	8753	0	1.000000
C2	8724	1	0.999885
C3	8754	0	1.000000
C4[a]	8754	0	1.000000
D1	8754	0	1.000000
D2[a]	4592	3	0.999347
D3	8760	0	1.000000
D4	8755	0	1.000000
E1	8760	0	1.000000
E2	8760	0	1.000000
E3[a]	8754	0	1.000000
E4	8760	0	1.000000
F1	8755	0	1.000000
F2[a]	8732	1	0.999885
F3	8754	0	1.000000
F4	8760	0	1.000000
All Slots	205363	9	0.999956

[a] *When any of A2, B1, C4, D2, E3, and F2 are configured as expandable slots, both slot locations must be occupied by an available satellite for the slot to be counted as available.*

[b] *There were 8,760 hours in the evaluation period.*

[c] *Number of hours in which SPS SIS was available at the start of the hour and during the hour either (1) an SV transmitted navigation message with subframe 1 health bits set to anything other than all zeroes without a scheduled outage, or (2) signal lost without a scheduled outage.*

To put this in perspective, there are 8,760 hours in a year (8,784 for a leap year). The required probability of not losing SPS SIS availability over an hour is calculated as an average over all slots in the 24-slot constellation. The maximum number of hours that can experience unscheduled interruptions over the year is given by $8{,}760 \times (1 - 0.9998) \times 24 = 42$ hours. This is less than two unscheduled interruptions per SV per year, but allows for the possibility that some SVs may have no unscheduled interruptions while others may have more than one.

Returning to Table 3.8, across the slots in the constellation, the total number of hours lost was 9. This is smaller than the maximum number of hours of unscheduled interruptions (42) available to meet the metric and leads to the empirical value for the fraction of hours in which SPS SIS continuity was maintained of 0.999956. Therefore, this assertion is considered fulfilled in 2023.

3.4.2 Status and Problem Reporting Standards

3.4.2.1 Scheduled Events

The SPSPS20 makes the following assertion in Section 3.6.3 regarding notification of scheduled events affecting service to the Coast Guard and the Federal Aviation Administration (FAA):

- *"Appropriate NANU issued to the Coast Guard and the FAA at least 48 hours prior to the event for 95% of the events"*

While beyond the assertion in the performance standards, ICD-GPS-240 [8] states a threshold of no less than 48 hours and a nominal notification time of 96 hours prior to outage start.

This metric was evaluated by comparing the NANU periods to outages observed in the data. In general, scheduled events are described in a pair of NANUs. The first NANU is a forecast of when the outage will occur. The second NANU is provided after the outage and summarizes the actual start and end times of the outage. (This is described in ICD-GPS-240 Section 10.1.1).

Table 3.9 summarizes the pairs found for 2023. The two leftmost columns provide the SVN/PRN of the subject SV. The next three columns specify the NANU #, type, and release time of the forecast NANU. These are followed by three columns that specify the NANU #, the release date/time of the FCSTSUMM NANU provided after the outage, and the date/time of the beginning of the outage. The final column is the time difference between the time the forecast NANU was released and the beginning of the actual outage (in hours). This represents the length of time between the release of the forecast NANU and the actual start of the outage. Notice times less than 48 hours are shown in red. The average notice time in 2023 was over 148 hours.

Two satellites were decommissioned, one satellite was launched, and two satellites were set usable in 2023. Tables 3.10 and 3.11 provide the details on how this was represented in the NANUs.

To meet the assertion in the performance standard, at least 95% of the values in the rightmost column of Table 3.9 should be greater than 48.0. For 2023, all events had a notice time greater than 48 hours. Therefore, this assertion is satisfied.

Table 3.9: Scheduled Events Covered in NANUs for 2023

SVN	PRN	Forecast NANU			Summary NANU (FCSTSUMM)			Notice (hrs)
		NANU #	TYPE	Release Time	NANU #	Release Time	Start Of Outage	
41	22	2023001	FCSTDV	03 Jan 1905Z	2023002	11 Jan 0931Z	11 Jan 0344Z	176.65
62	25	2023004	FCSTDV	20 Jan 2227Z	2023009	26 Jan 2121Z	26 Jan 1535Z	137.13
56	16	2023012	FCSTDV	10 Feb 1757Z	2023014	17 Feb 0332Z	16 Feb 2152Z	147.92
52	31	2023015	FCSTDV	22 Feb 1711Z	2023016	28 Feb 1020Z	28 Feb 0015Z	127.07
48	07	2023017	FCSTDV	02 Mar 2023Z	2023018	10 Mar 0354Z	09 Mar 2149Z	169.43
61	02	2023019	FCSTDV	03 Apr 2255Z	2023020	06 Apr 1827Z	06 Apr 1034Z	59.65
57	29	2023021	FCSTDV	07 Apr 1800Z	2023022	14 Apr 0208Z	13 Apr 1948Z	145.80
51	20	2023025	FCSTDV	12 May 1620Z	2023026	19 May 0447Z	18 May 2243Z	150.38
52	31	2023027	FCSTDV	25 May 1625Z	2023028	02 Jun 2034Z	02 Jun 1332Z	189.12
61	02	2023029	FCSTDV	05 Jun 1539Z	2023030	09 Jun 0214Z	08 Jun 1934Z	75.92
78	11	2023031	FCSTDV	22 Jun 2003Z	2023032	30 Jun 1152Z	30 Jun 0528Z	177.42
53	17	2023033	FCSTDV	30 Jun 1523Z	2023034	07 Jul 0342Z	06 Jul 2117Z	149.90
64	30	2023035	FCSTDV	07 Jul 1747Z	2023041	14 Jul 0707Z	14 Jul 0148Z	152.02
70	32	2023045	FCSTDV	17 Aug 1816Z	2023049	25 Aug 0747Z	25 Aug 0234Z	176.30
58	12	2023050	FCSTDV	25 Aug 1512Z	2023052	01 Sep 0723Z	01 Sep 0137Z	154.42
61	02	2023053	FCSTDV	01 Sep 1739Z	2023054	08 Sep 0226Z	07 Sep 2023Z	146.73
68	09	2023055	FCSTDV	11 Sep 1429Z	2023056	15 Sep 0521Z	14 Sep 2352Z	81.38
45	21	2023058	FCSTDV	06 Oct 0308Z	2023060	13 Oct 1154Z	13 Oct 0646Z	171.63
44	22	2023061	FCSTDV	13 Oct 1441Z	2023062	19 Oct 2125Z	19 Oct 1559Z	145.30
55	15	2023063	FCSTDV	26 Oct 1428Z	2023064	03 Nov 0318Z	02 Nov 2124Z	174.93
61	02	2023065	FCSTDV	21 Nov 1548Z	2023067	28 Nov 1622Z	28 Nov 1052Z	163.07
79	28	2023066	FCSTDV	22 Nov 1849Z	2023068	30 Nov 1949Z	30 Nov 1319Z	186.50
72	08	2023069	FCSTDV	01 Dec 1559Z	2023071	08 Dec 0220Z	07 Dec 2010Z	148.18
71	26	2023070	FCSTDV	07 Dec 2200Z	2023072	14 Dec 2209Z	14 Dec 1723Z	163.38
67	06	2023073	FCSTDV	15 Dec 1610Z	2023074	21 Dec 1628Z	21 Dec 1123Z	139.22
Average Notice Period								148.38

Table 3.10: Decommissioning Events Covered in NANUs for 2023

SVN	PRN	FCSTUUFN/UNUSUFN NANU		DECOM NANU			Notice (hrs)
		NANU #	Release Time	NANU #	Release Time	End of Unusable Period	
41	22	2023003	19 Jan 1733Z	2023006	25 Jan 2330Z	23 Jan 2016Z	98.72
63	01	2023036	10 Jul 1020Z	2023044	11 Aug 0123Z	10 Jul 1020Z	0.00
Average Notice Period							49.36

Table 3.11: Usable Events Covered in NANUs for 2023

SVN	PRN	LAUNCH/GENERAL NANU		USABINIT NANU	
		NANU #	Launch Time	NANU #	Start Time
44	22	2023042	–	2023046	18 Aug 1605Z
79	28	2023007	18 Jan 1224Z	2023013	16 Feb 2056Z

3.4.2.2 Unscheduled Outages

The SPS PS provides the following assertion in Section 3.6.3 regarding notification of unscheduled outages or problems affecting service:

- *"Appropriate NANU issued to the Coast Guard and the FAA as soon as possible after the event"*

The ICD-GPS-240 states that the nominal notification time is 15 minutes after the start of an outage with a threshold of less than 1 hour.

This metric was evaluated by examining the NANUs provided throughout the year and comparing the NANU periods to outages observed in the data. Unscheduled events may be covered by either a single NANU or a pair of NANUs. In the case of a brief outage, a NANU with type UNUNOREF (unusable with no reference) is provided to detail the period of the outage. In the case of longer outages, a UNUSUFN (unusable until further notice) is provided to inform users of an ongoing outage or problem. This is followed by a NANU with type UNUSABLE after the outage is resolved. (This is described in detail in ICD-GPS-240 Section 10.1.2).

Table 3.12 provides a list of the unscheduled outages found in the NANU information for 2023. The two leftmost columns provide the SVN/PRN of the subject SV. The third column provides the plane-slot of the SV to assist in relating these events to the information in Table 3.8. The next two columns provide the NANU # and release date/time of the UNUSUFN NANU. These are followed by three columns that specify the NANU #, the release date/time of the UNUSABLE NANU provided after the outage, and the date/time of the beginning of the outage. The final column is the time difference between the outage start time and the UNUSUFN NANU release time (in hours). Values in the final column are shown in red if they have a lag time of greater than 60 minutes (1 hour).

Because the performance standard states only "as soon as possible after the event," there is no threshold check to be performed. However, the data are provided for information. With respect to the notification times provided in ICD-GPS-240, the threshold time was not met for one of the events listed in Table 3.12.

Table 3.12: Unscheduled Events Covered in NANUs for 2023

SVN	PRN	Plane-Slot[a]	UNUSUFN NANU		UNUSABLE/UNUNOREF NANU			Lag Time (minutes)
			NANU #	Release Time	NANU #	Release Time	Start Of Event	
63	01	D2A	2023005	25 Jan 1629Z	2023008	26 Jan 1543Z	25 Jan 1600Z	29.00
63	01	D2A	2023010	28 Jan 1541Z	2023011	02 Feb 2240Z	28 Jan 1500Z	41.00
79	28	A2F	2023023	19 Apr 1454Z	2023024	19 Apr 2216Z	19 Apr 1445Z	9.00
79	28	A2F	2023037	10 Jul 1125Z	2023038	10 Jul 1655Z	10 Jul 1110Z	15.00
79	28	A2F	2023039	10 Jul 2338Z	2023040	14 Jul 0111Z	10 Jul 2300Z	38.00
55	15	F2A	2023047	22 Aug 1631Z	2023048	23 Aug 1449Z	22 Aug 1611Z	20.00
79	28	A2F	2023043	11 Aug 0119Z	2023051	29 Aug 2309Z	10 Aug 2352Z	87.00
66	27	C2	2023076	30 Dec 1115Z	2024007	02 Feb 1853Z	30 Dec 1107Z	8.00
Average Lag Time								30.87

[a] *If an SV is not in a defined slot, only the plane is specified.*

3.5 SIS Availability

3.5.1 Per-Slot Availability

The SPS PS makes the following assertions in Section 3.7.1:

- *"≥ 0.957 Probability that a Slot in the Baseline 24-Slot Configuration will be Occupied by a Satellite Broadcasting a Healthy SF CA-code SPS SIS"*
- *"≥ 0.957 Probability that a Slot in the Expanded Configuration will be Occupied by a Pair of Satellites Each Broadcasting a Healthy SF CA-code SPS SIS"*

The constraints include the note that this is to be calculated as an average over all slots in the 24-slot constellation, normalized annually.

The derivation of the SV/slot assignments is described in Appendix B.3.

This metric was verified by examining the status of each SV in the 24-slot configuration (or pair of SVs in an expandable slot) at every 30 s interval throughout the year. The health status was determined from the subframe 1 health bits of the ephemeris being broadcast at the time of interest. In addition, data from both the MSN and the IGS networks were examined to verify that the SV was broadcasting a trackable signal at the time. The results are summarized in Table 3.13. The metric is averaged over the constellation; therefore, the value in the bottom row (labeled "All Slots") must be greater than 0.957 in order for the assertion to be met.

Slot D2 has a lower availability than the other slots due to the decommissioning of SVN 63/PRN 1 from D2A on 10 August 2023 (NANU 2023044). This left a gap in the defined constellation until the maneuver of SVN 61/PRN 02 into the slot was completed in late December 2023.

Regardless of the individual slot availabilities, the average availability for the constellation was 0.977, which is above the threshold of 0.957. Therefore, the assertion being evaluated in this section was met.

Table 3.13: Per-Slot L1 C/A Availability for 2023

Plane-Slot	**# Missing Epochs**[b]	**Availability**
A1	0	1.000000
A2[a]	67749	0.935551
A3	619	0.999411
A4	705	0.999329
B1[a]	1212	0.998847
B2	694	0.999340
B3	0	1.000000
B4	696	0.999338
C1	755	0.999282
C2	4427	0.995789
C3	733	0.999303
C4[a]	763	0.999274
D1	731	0.999305
D2[a]	500299	0.524069
D3	0	1.000000
D4	610	0.999420
E1	0	1.000000
E2	0	1.000000
E3[a]	721	0.999314
E4	0	1.000000
F1	610	0.999420
F2[a]	3417	0.996749
F3	625	0.999405
F4	0	1.000000
All Slots	585366	0.976798

[a] *When any of A2, B1, C4, D2, E3, and F2 are configured as expandable slots, both slot locations must be occupied by an available satellite for the slot to be counted as available.*

[b] *For each slot, there were 1,051,200 total 30 s epochs in the evaluation period.*

3.5.2 Constellation Availability

The SPSPS20 makes the following assertions in Section 3.7.2:

- *"≥ 0.98 Probability that at least 21 Slots out of the 24 Slots will be Occupied Either by a Satellite Broadcasting a Healthy SF CA-code SPS SIS in the Baseline 24-Slot Configuration or by a Pair of Satellites Each Broadcasting a Healthy SPS SIS in the Expanded Slot Configuration"*
- *"≥ 0.99999 Probability that at least 20 Slots out of the 24 Slots will be Occupied Either by a Satellite Broadcasting a Healthy SF CA-code SPS SIS in the Baseline 24-Slot Configuration or by a Pair of Satellites Each Broadcasting a Healthy SF CA-code SPS SIS in the Expanded Slot Configuration"*

To evaluate this metric, the subframe 1 health condition and the availability of signal were evaluated for each SV every 30 s for all of 2023. For non-expanded baseline slots, if an SV qualified as being in the slot and was transmitting a healthy signal, the slot was counted as occupied. For expanded slots, the slot was counted as occupied if two SVs were transmitting healthy signals in the slot, with one in each of the two portions of the expanded slot. If the count of occupied slots was greater than 20, the measurement interval was counted as a 1; otherwise, the measurement interval was assigned a zero. The sum was then divided by the total number of measurement intervals. The value for 2023 is 1.00. Thus, both requirements are satisfied.

While this satisfies the metric, it does not provide much information on exactly how many SVs are typically healthy. To address this, at each 30 s interval, the number of SVs broadcasting a healthy SIS was counted. This was done for both the count of occupied slots and for the number of SVs. The daily averages as a function of time are shown in Figure 3.17. The daily average number of occupied slots always exceeded 21.

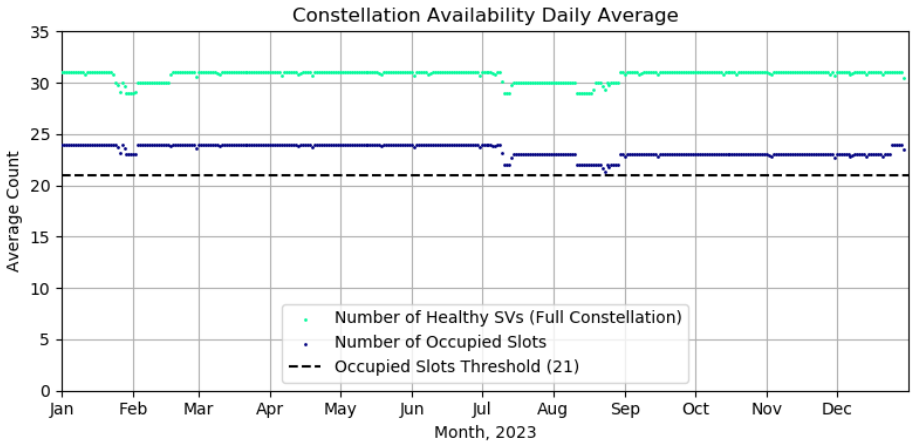

Figure 3.17: Daily Average Number of Occupied Slots

3.5.3 Operational Satellite Counts

Table 3.7-3 of the SPSPS20 states:

- *"≥ 0.95 Probability that the Constellation will Have at least 24 Operational Satellites Regardless of Whether Those Operational Satellites are Located in Slots or Not"*

Under "Conditions and Constraints" the term Operational is defined as

> *"any satellite which appears in the transmitted navigation message almanac... regardless of whether that satellite is currently broadcasting a healthy SPS SIS or not or whether the broadcast SPS SIS also satisfies the other performance standards in this SPS PS or not."*

Given the information presented in Sections 3.5.1 and 3.5.2, we conclude that at least 24 SVs were operational 100% of the time for 2023, thus meeting the assertion.

To evaluate this more explicitly, the almanac status was examined directly. IS-GPS-200 Section 20.3.3.5.1.3 [2] assigns a special meaning to the SV health bits in the almanac's subframe 4 page 25 and subframe 5 page 25 (Data ID 51 and 63). When these bits are set to all ones, it indicates "the SV which has that ID is not available, and there might be no data regarding that SV in that page of subframes 4 and 5..." Given this definition, the process examines the subframe 4 and 5 health bits for each day for the individual SVs and counts the number of SVs for which the health bits are other than "all ones."

The results are shown in Figure 3.18. This plot is very similar to the full constellation healthy satellite count shown in Figure 3.17. The almanac health data are not updated as frequently as those in subframe 1. The plot in Figure 3.18 contains only integer values. Therefore, on days when it appears the operational SV count is lower than the number of healthy SVs in the constellation, these reflect cases where an SV was set unhealthy for a small portion of the day. In Figure 3.17, such effects are averaged over the day, yielding a higher availability.

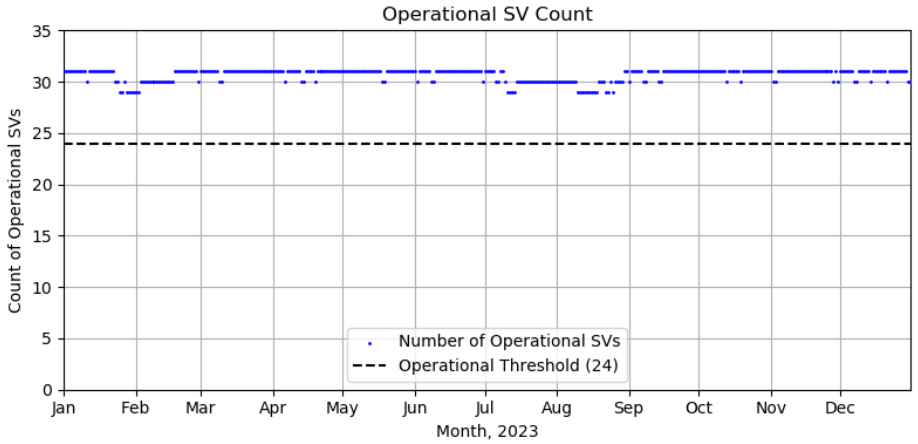

Figure 3.18: Count of Operational SVs by Day for 2023

3.6 Position/Velocity/Time Domain Standards

3.6.1 Evaluation of DOP Assertions

Dilution of precision (DOP) measures the geometric diversity of a set of observations. That is to say, the diversity of the lines of sight from a user to the observed usable SVs. There are a variety of types of DOP, including:

- position dilution of precision (PDOP),
- geometric dilution of precision (GDOP),
- horizontal dilution of precision (HDOP),
- vertical dilution of precision (VDOP), and
- time dilution of precision (TDOP).

Accurate position and time solutions require two components: a sufficient number of accurate signals, and an acceptable geometric diversity of those signals. The former requirement is addressed by the URE assertions in Section 3.4 of the SPSPS20, and the latter is addressed by the PDOP assertions in Section 3.8.1 of the SPSPS20.

Section 3.6.1.1 provides the evaluation of the PDOP assertions stated in SPSPS20. Appendix A.7 provides additional supporting information beyond the stated assertions and includes results specific to the various types of DOP to better explain how well the constellation meets the assertions.

3.6.1.1 PDOP Availability

The PDOP availability standards are stated in Table 3.8-1 of the SPSPS20 as follows:

- *"≥ 98% global PDOP of 6 or less"*
- *"≥ 88% worst site PDOP of 6 or less"*

Based on the definition of a representative receiver contained in SPS PS Section 3.8, a 5° minimum elevation angle is used for this evaluation.

These assertions were verified empirically throughout 2023 using a uniformly-spaced grid, containing N_{grid} points, to represent the terrestrial service volume at zero altitude, and an archive of the broadcast ephemerides transmitted by the SVs throughout the year. All healthy, transmitting SVs were considered. The grid was 111 km × 111 km (roughly $1^\circ \times 1^\circ$ at the Equator). The time started at 0000Z each day and stepped through the entire day at one minute intervals (1,440 points/day, defined as $1 \leq N_t \leq 1440$). The overall process followed is similar to that defined in Section 5.4.6 of the GPS Civil Monitoring Performance Specification (CMPS) [9].

The PDOP values were formed using the traditional PDOP algorithm [10], without regard for the effect of terrain. The coordinates of the grid locations provided the ground positions at which the PDOP was computed. The position of each SV was computed from the broadcast ephemeris available to a theoretical receiver at that grid point at the time of interest. The only filtering performed was the exclusion of any unhealthy SVs (those with subframe 1 health bits set to other than all zeroes). The results of each calculation were tested with respect to the threshold of PDOP ≤ 6. At each point in time, if the condition was violated, a bad PDOP counter associated with the particular grid point, b_i for $1 \leq i \leq N_{grid}$, was incremented. Once the summation over time is complete, b_i represents the number of bad PDOP flags observed at grid point i throughout the 24-hour period of interest.

At least four SVs must be available to a receiver for a valid PDOP computation. This condition was fulfilled for all grid points at all times in 2023.

Once the PDOPs had been computed across all grid points, for each of the 1,440 time increments during the day, the percentage of time PDOP ≤ 6 for the day was computed using the formula:

$$(\%PDOP \leq 6) = 100 \left(1 - \frac{\sum_{i=1}^{N_{grid}} b_i}{N_{grid} N_t} \right)$$

The worst site for a given day was identified from the same set of counters by finding the site with the maximum bad count: $b_{max} = \max_i(b_i)$. The ratio of b_{max} to N_t is an estimate of the fraction of time the worst site PDOP exceeds the threshold. This value was averaged over the year, and the percentage of time PDOP ≤ 6 was computed.

Table 3.14 summarizes the results of this analysis. The second column provides the values for the assertions. The third column is provided to verify that no single-day value actually dropped below the goal. From this table we conclude that the PDOP availability metrics are met for 2023.

Table 3.14: Summary of PDOP Availability

Metric	Average daily % over 2023	Minimum daily % over 2023
$\geq 98\%$ Global Average PDOP ≤ 6	100.000	99.985
$\geq 88\%$ Worst site PDOP ≤ 6	99.732	98.611

In addition to verifying the assertion, further DOP analyses were conducted which go beyond the assertion and speak to system performance on a more granular basis. The remainder of this chapter describes those analyses and results. For more additional DOP analysis, see Appendix A.7.

Behind the statistics are the day-to-day variations. Figure 3.19 provides a time history of PDOP metrics considering all satellites for 2023. Three metrics are plotted:

- Green: Average PDOP at Worst Site ($\langle PDOP_{worst\,site} \rangle$)
- Blue: Average Worst Site PDOP ($\langle PDOP \rangle_{worst\,site}$)
- Light Blue: Daily Global Average PDOP ($\langle PDOP \rangle$)

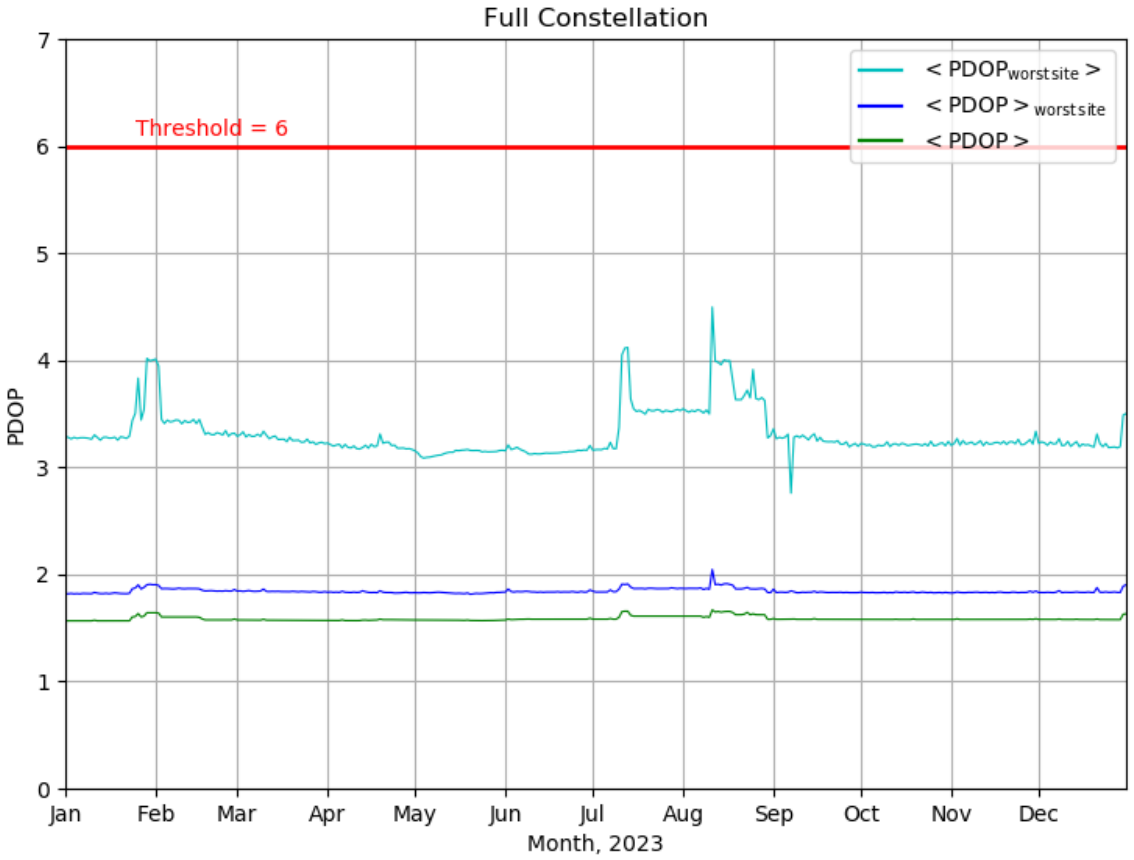

Figure 3.19: Daily PDOP Metrics Using All SVs for 2023

3.6.2 Position Service Availability

The positioning and timing availability standards are stated in Table 3.8-2 of the SPSPS20 as follows:

- *"≥ 99% Horizontal Service Availability, average location"*
- *"≥ 99% Vertical Service Availability, average location"*
- *"≥ 90% Horizontal Service Availability, worst-case location"*
- *"≥ 90% Vertical Service Availability, worst-case location"*

The conditions and constraints note that the percentages in the assertions are associated with the availability of a horizontal accuracy of 15 m (95th%, SIS only) and a vertical accuracy of 33 m (95th%, SIS only).

These values are derived as described in the sentence preceding SPSPS20 Table 3.8-2:

> *"The commitments for maintaining PDOP (Table 3.8-1) and SPS SIS URE accuracy (Table 3.4-1) result in support for position service availability standards as presented in Table 3.8-2."*

Because the commitments for PDOP and constellation SPS SIS URE have been met, this assertion in the SPSPS20 implies that the position and timing availability standards have also been fulfilled. A direct assessment of these metrics was not undertaken.

3.6.3 Position/Velocity Accuracy

The positioning accuracy standards are stated in Table 3.8-3 of the SPSPS20 as follows:

- *"≤ 8 m 95% Horizontal Error, Global Average Position Domain Accuracy"*
- *"≤ 13 m 95% Vertical Error, Global Average Position Domain Accuracy"*
- *"≤ 15 m 95% Horizontal Error, Worst Site Position Domain Accuracy"*
- *"≤ 33 m 95% Vertical Error, Worst Site Position Domain Accuracy"*
- *"≤ 0.2 m/s 95% velocity error, any axis, Global Average Velocity Accuracy"*

These values are derived as described in the sentence preceding SPSPS20 Table 3.8-3:

> *"The commitments for maintaining PDOP (Table 3.8-1), SPS SIS URE accuracy (Table 3.4-1), and SPS SIS URRE accuracy (Table 3.4-2), result in support for position/velocity/time accuracy standards as presented in Table 3.8-3."*

Because the commitments for PDOP, constellation SPS SIS URE, and constellation SPS SIS URRE have been met, the position, velocity, and timing accuracy standards have also been fulfilled.

While this verifies the assertion has been fulfilled, it is useful to corroborate that finding through examination of empirical results. We do this by evaluating position solutions (generated via the process described in Appendix C.5) for a set of continuously operating stations from both the MSN and IGS networks (see Figure 1.1). The process uses both a receiver autonomous integrity monitoring (RAIM) approach and a simplistic approach with no data editing. We conducted the elevation angle processing with a 5° minimum elevation angle in agreement with the standard.

Once the solutions are computed, two sets of statistics were developed for each approach, yielding 4 sets of results. The first set is a set of daily average position errors across all stations. In the second set, the worst site is determined on a day-to-day basis and the worst site 95th percentile position errors are computed.

These are empirical results and should not be construed to represent proof that the metrics presented in the standard have been met. Instead, they are presented as a means of corroboration that the standards have been met through the fulfillment of the more basic commitments of PDOP and SPS SIS URE.

3.6.3.1 Results for Daily Average

Using the approach outlined above, position solutions were computed at each 30 s interval for data from both the NGA and IGS stations. In the nominal case in which all stations are operating for a complete day, this yields 2,880 solutions per station per day. Truth positions for the IGS stations were taken from the weekly Station Independent Exchange format (SINEX) files. Truth locations for the NGA stations were taken from station locations defined as part of the latest World Geodetic System (WGS) 84 reference frame [11] with corrections for station velocities applied.

Residuals between estimated locations and the truth locations were computed in the form of North, East, and Up components in meters. The horizontal residual was computed from the root sum square (RSS) of the North and East components, and the vertical residual was computed from the absolute value of the Up component. As a result, the residuals will have non-zero mean values. The statistics on the residuals were compiled across all stations in a set for a given day. Figures 3.20 – 3.23 show the daily average for the horizontal and vertical residuals corresponding to the four cases.

The statistics associated with the processing are provided in Table 3.15. The table contains the mean, median, maximum, and standard deviation of the daily values across 2023. The results are organized in this fashion to facilitate comparison of the same quantity across the various processing options. The results are expressed to the centimeter level of precision. This choice of precision is based on the fact that the truth station positions are known only at the few-centimeter level.

The following observations regarding the quality of the daily average position solutions may be drawn from the charts and the supporting statistics in Table 3.15:

- Mean and Median values - The means and medians of the position residuals given in Table 3.15 are nearly identical for both the NGA and IGS data sets, suggesting that if there are any 30 s position residual outliers, they are few in number and not too large.
- Differences between NGA and IGS results - As reported in Table 3.15, the mean magnitude of the position residuals are similar between the NGA stations and the IGS stations. There are a number of differences between the two station sets. The NGA station set is more homogeneous in that the same receiver model is used throughout the data processed for this analysis, the data are derived from full-code tracking, and a single organization prepared all the data sets using a single set of algorithms. By contrast, the IGS data sets come from a variety of receivers and were prepared and submitted by a variety of organizations.

Table 3.15: Daily Average Position Errors for 2023

Statistic	**Data Editing**	**Horizontal**		**Vertical**	
		IGS	**NGA**	**IGS**	**NGA**
Mean (m)	RAIM	1.13	1.08	1.79	1.48
	None	1.13	1.09	1.80	1.50
Median (m)	RAIM	1.12	1.07	1.77	1.47
	None	1.12	1.08	1.78	1.48
Maximum (m)	RAIM	1.29	1.47	2.07	1.87
	None	1.30	3.04	2.08	2.98
Std. Dev. (m)	RAIM	0.05	0.04	0.09	0.07
	None	0.05	0.13	0.09	0.13

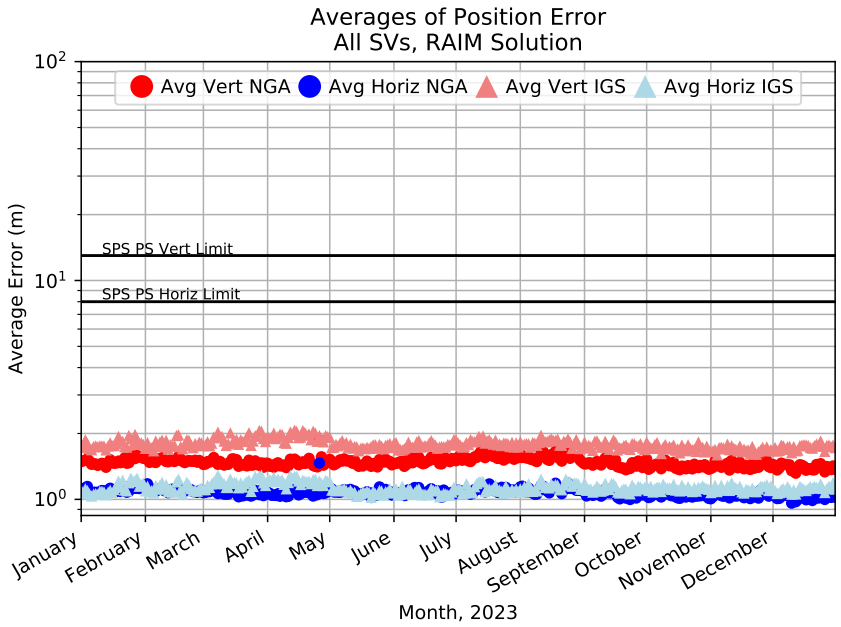

Figure 3.20: Daily Averaged Position Residuals Computed Using a RAIM Solution

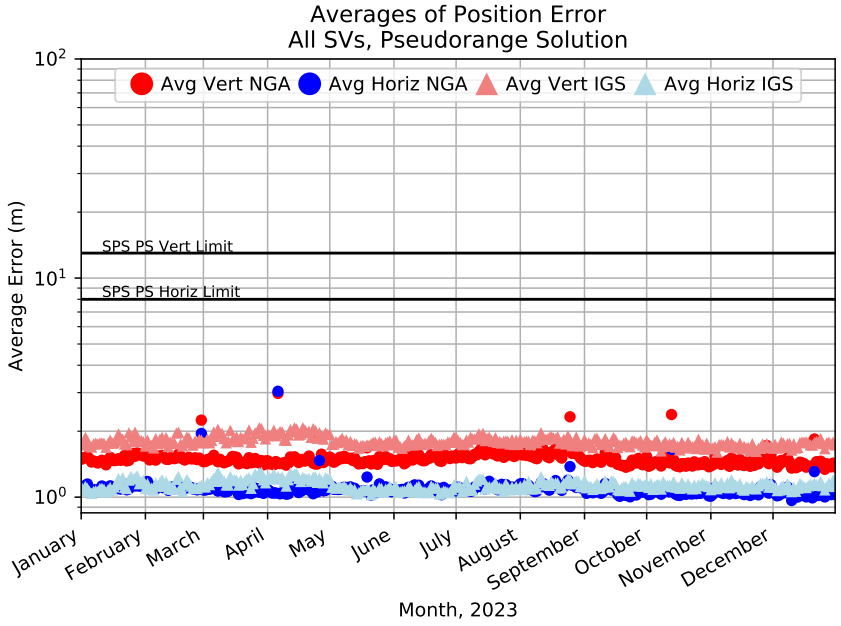

Figure 3.21: Daily Averaged Position Residuals Computed Using No Data Editing

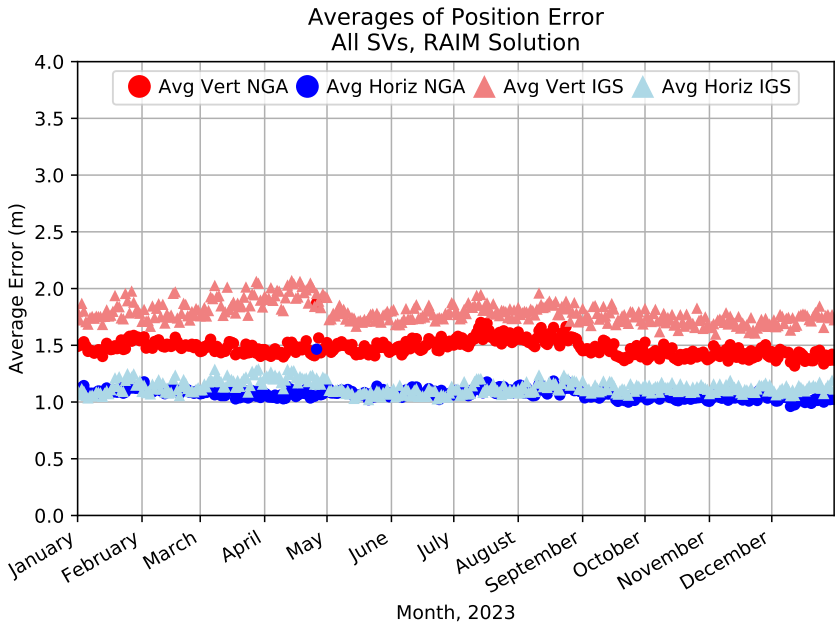

Figure 3.22: Daily Averaged Position Residuals Computed Using a RAIM Solution (enlarged)

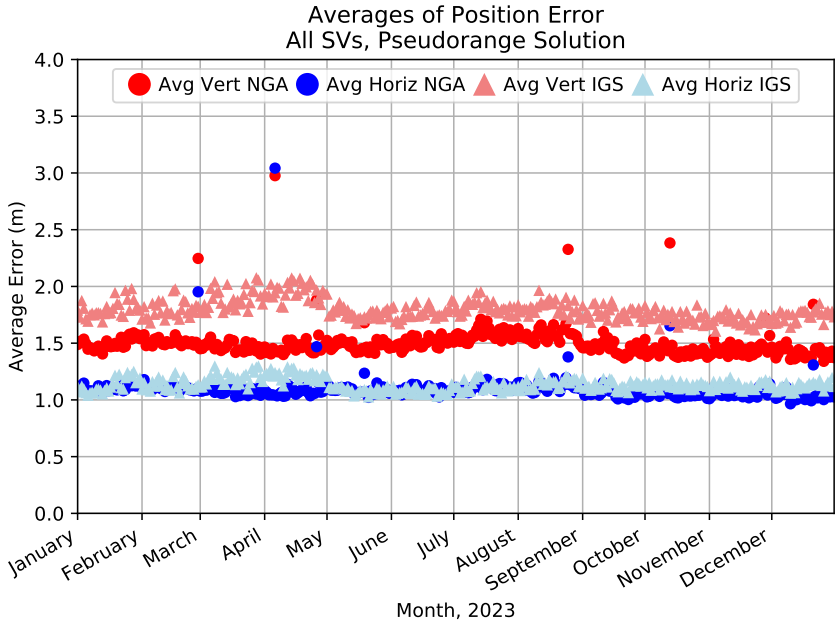

Figure 3.23: Daily Averaged Position Residuals Computed Using No Data Editing (enlarged)

3.6.3.2 Results for Worst Site 95th Percentile

The edited and non-edited 30 s position residuals were then independently processed to determine the worst site 95th percentile values. In this case, the 95th percentile was determined for each station in a given set, and the worst of these was used as the final 95th percentile value for that day. Figures 3.24-3.27 show these values for the various processing options described in the previous section. The plots are preceded by a table of the statistics for the mean, median, maximum, and standard deviation of the daily worst site 95th percentile values. Some general observations on the results are included following the tables.

The statistics associated with the worst site 95th percentile values are provided in Table 3.16. As before, the results are organized in this fashion to facilitate comparison of the same quantity across the various processing options. Values are reported with a precision of one centimeter due to (a) the magnitude of the standard deviation and (b) the fact that the station positions are known only at the few-centimeter level.

Most of the observations from the daily averaged position residuals hold true in the case of the result from the worst site 95th percentile case. However, there are a few additional observations that can be drawn from Figures 3.24-3.27 and Table 3.16 regarding the worst site 95th percentile position solutions:

- Comparison to threshold - The values for both mean and median of the worst 95th percentile for both horizontal and vertical errors are well within the standard for both solutions. Compared to the thresholds of 15 m 95th percentile horizontal and 33 m 95th percentile vertical, these results are outstanding.

- Comparison between processing options - For both data sets, the statistics between the RAIM and pseudorange solutions are similar. However, the maximum value is lower for RAIM solutions. This indicates the importance of data editing in position processing.

Table 3.16: Daily Worst Site 95th Percentile Position Errors for 2023

Statistic	Data Editing	Horizontal		Vertical	
		IGS	NGA	IGS	NGA
Mean (m)	RAIM	5.30	3.40	8.73	5.00
	None	5.35	3.48	8.86	5.04
Median (m)	RAIM	5.19	3.33	8.79	4.99
	None	5.24	3.39	8.96	5.01
Maximum (m)	RAIM	7.23	4.56	10.68	7.03
	None	7.30	8.61	10.70	7.16
Std. Dev. (m)	RAIM	0.59	0.37	0.87	0.53
	None	0.56	0.48	0.85	0.54

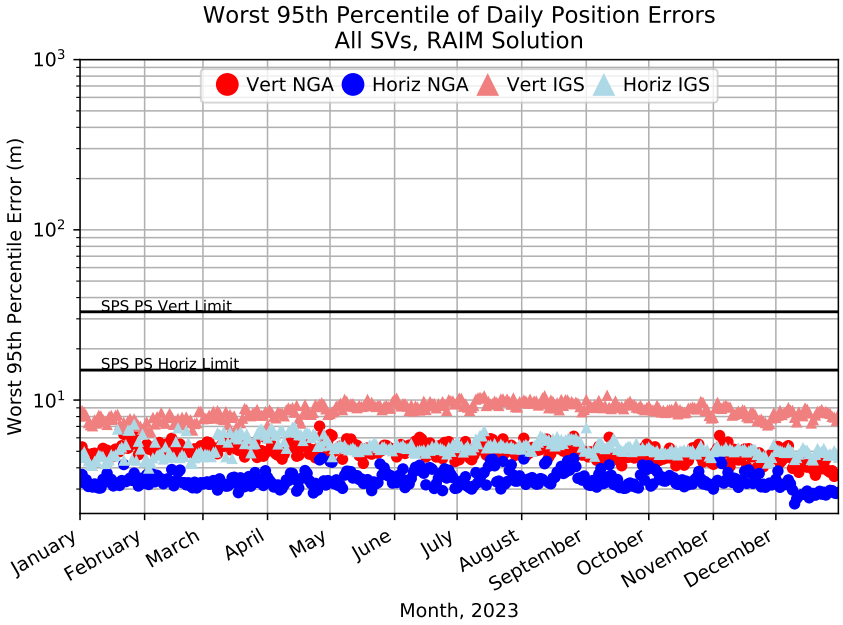

Figure 3.24: Worst Site 95th Daily Averaged Position Residuals Computed Using a RAIM Solution

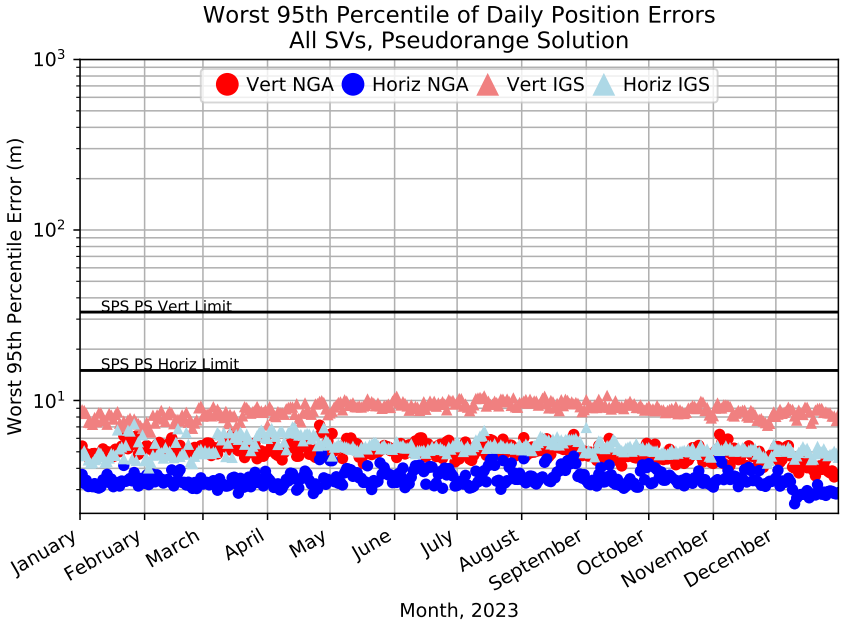

Figure 3.25: Worst Site 95th Daily Averaged Position Residuals Computed Using No Data Editing

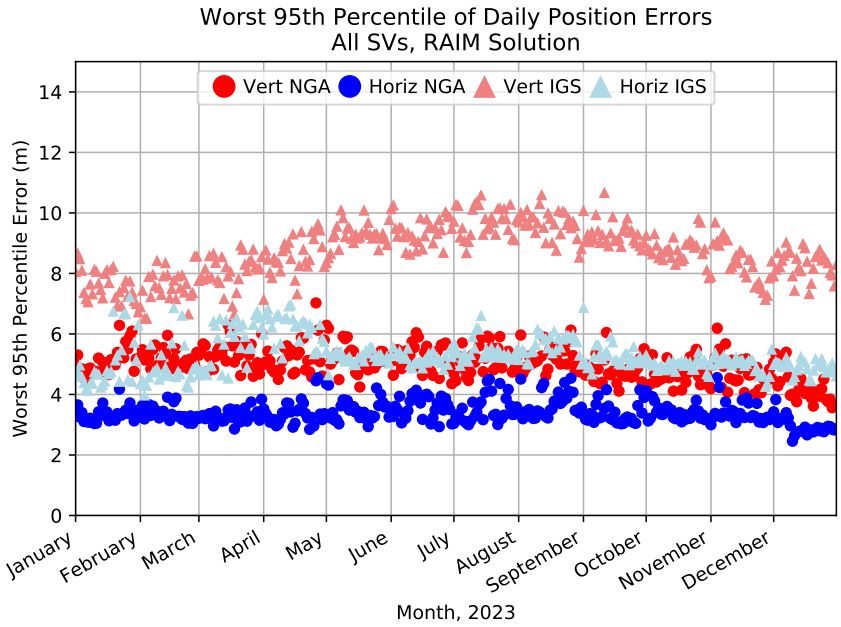

Figure 3.26: Worst Site 95th Daily Averaged Position Residuals Computed Using a RAIM Solution (enlarged)

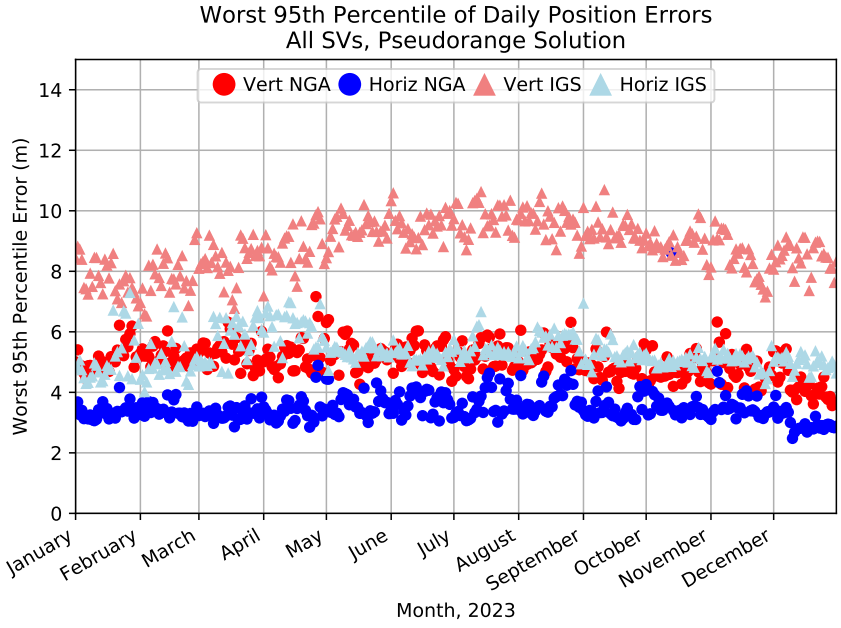

Figure 3.27: Worst Site 95th Daily Averaged Position Residuals Computed Using No Data Editing (enlarged)

3.6.4 Time Transfer Accuracy

The time transfer accuracy standard is stated in Table 3.8-3 of SPSPS20 as follows:

- *"≤ 30 nsec 95% Time Transfer error 95% of the time (SIS only)"*

The constraints define this standard as applicable to a time transfer solution "meeting the representative user conditions."

The equation for time transfer accuracy relative to UTC(USNO), referred to as user UTC(USNO) error (UUTCE), in GPS is found in the SPSPS20, Appendix B.2.2.

$$\text{UUTCE} = \sqrt{(\text{UERE} * \text{TTDOP}/c)^2 + (\text{UTCOE})^2)}$$

User-equivalent range errors (UERE) can be approximated with URE values. Time transfer dilution of precision (TTDOP) is $1/\sqrt{\text{N}}$, where N is the number of satellites visible to the user.[1] The UUTCE calculation was performed for each day of the year.

This computation was done only for satellites that meet the following criteria: healthy, trackable, operational, and having no NANU at each given time. To meet the requirement of an average over all points in the service volume, a worldwide grid with 425 points was created (see Figure 3.28). Because time transfer accuracy can be dependent on which SVs are in view of a given location, the grid was selected to provide a representative sampling of possible user locations around the world with a variety of possible SV combinations. The grid has 10° separation in latitude and longitude at the equator. This yields a spacing of roughly 1,100 km.

Statistics were performed for each day over the grid of 425 points and time step of 15 minutes, resulting in 40,800 points per day to determine the 95^{th} percentile UUTCE value.

The computation steps are:

1. Compute satellite positions for each time point in the day using the broadcast ephemeris,
2. For each time and grid point,
   (a) find visible satellites (above 5° elevation) that meet the above criteria,
   (b) determine the appropriate UTCO data set (UTCO_i). The appropriate data set is the valid data set that has the latest reference time (t_{ot}) of all valid data sets received at that location at that time. Calculate UTCOE_i = UTCO_i - USNO, where USNO is the daily truth value,
   (c) get the Instantaneous SIS URE for each visible satellite, then take the mean of all values (UERE_i) and assign as the value for that time and grid point,
3. Calculate all 40,800 UUTCE values for the day, find 95% containment of all values.

[1] *as per conversation with Mr. Karl Kovach, author of the SPS PS, 31 August 2017*

The daily UUTCE results over all grid points and times per day are shown in Figure 3.29. All of these results are well below 30 nsec. Therefore, this assertion is met.

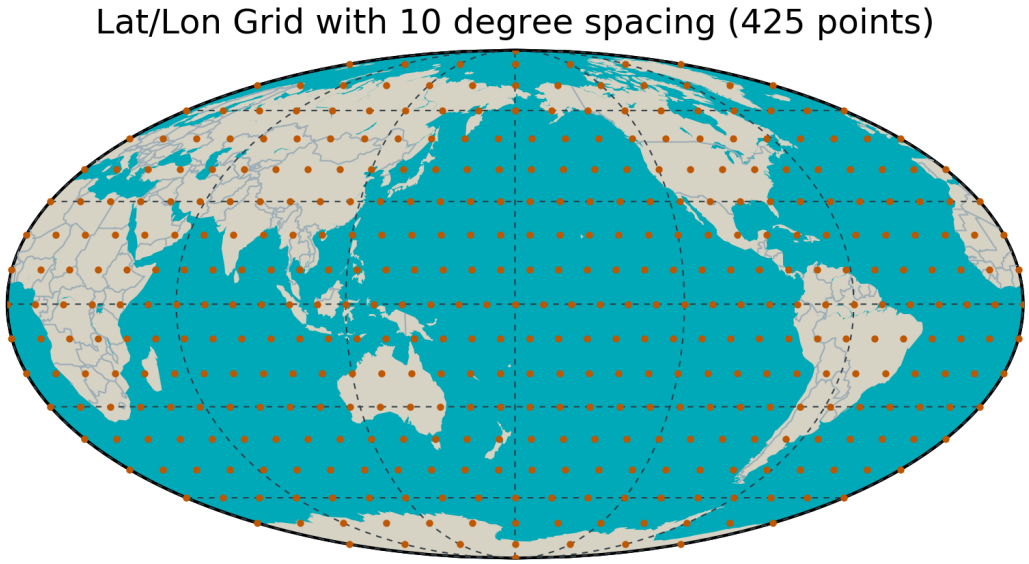

Figure 3.28: 10° Grid for UUTCE Calculation

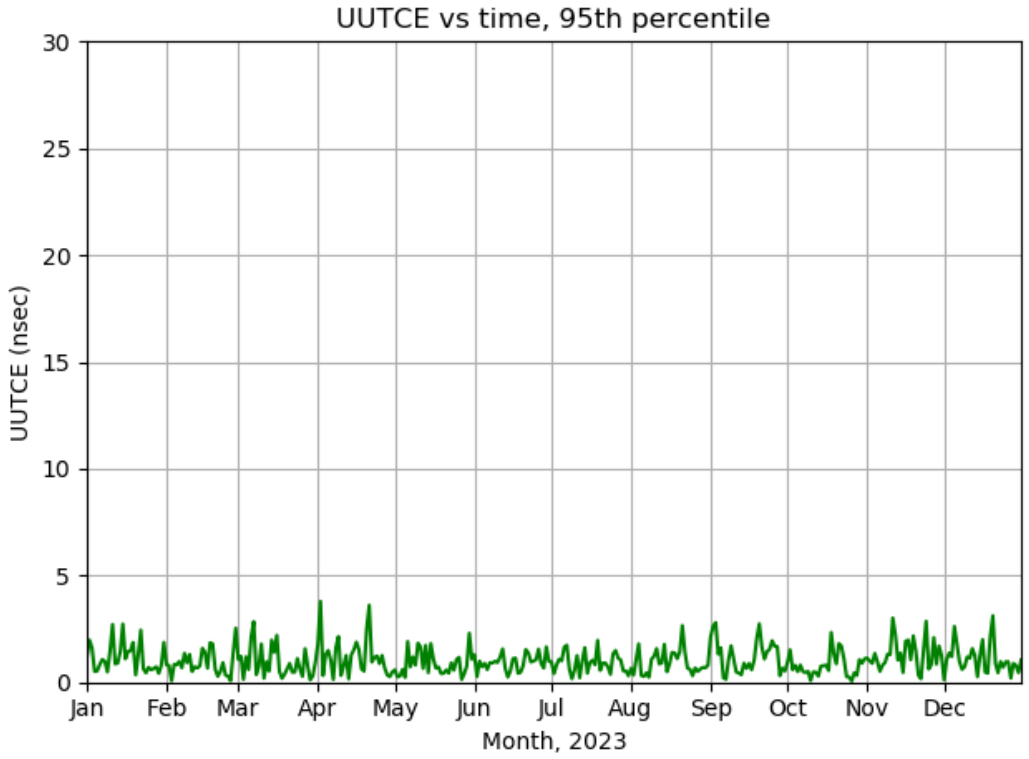

Figure 3.29: UUTCE 95th Percentile Values

Appendix A

Additional Results of Interest

This chapter provides additional results of interest. These results support the conclusions drawn earlier in the report while providing additional insight into satellite health values, age of data, user range accuracy values, extended mode operations, URE as a function of AOD, descriptions of notable events, and additional DOP analysis.

Contents

A.1 Health Values 67
A.2 Age of Data 69
A.3 User Range Accuracy Index Values 71
A.4 Extended Mode Operations 74
A.5 URE as a Function of AOD 76
A.5.1 SPS Results 76
A.5.1.1 Block IIR SVs 77
A.5.1.2 Block IIR-M SVs 79
A.5.1.3 Block IIF SVs 81
A.5.1.4 GPS III SVs 84
A.6 SVN 63/PRN 1 Integrity Fault Events 86
A.7 Additional DOP Analysis 88

A.1 Health Values

Several of the assertions require examination of the health information transmitted by each SV. We have found it useful to examine the rate of occurrence for all possible combinations of the six health bits transmitted in subframe 1. We examined all unique navigation messages received in 2023. There are typically 13 unique messages per day for each SV. This leads to approximately 4,750 unique messages for each year for an SV.

Table A.1 presents a summary of health bit usage in the ephemerides broadcast during 2023. Each row in the table presents a summary for a specific SV. The summary across all SVs is shown at the bottom. The table contains the number of times each unique health code was seen, the raw count of unique subframe 1 messages collected during the year, and the percentage of subframe 1 messages that contained specific health codes. Three unique health settings were observed throughout 2023: binary 111111_2 (0x3F), binary 111100_2 (0x3C), and binary 000000_2 (0x00).

Table A.1: Distribution of SV Health Values

SVN	PRN	Count by Health Code			Total # Subframe 1 Collected	% of Time by Health Code			Operational Days for 2023	Average # Subframe 1 per Operational Day
		0x3F	0x3C	0x00		0x3F	0x3C	0x00		
41	22	32	0	295	327	9.8	0.0	90.2	25	13.1
43	13	0	0	4748	4748	0.0	0.0	100.0	365	13.0
44	22	3	0	1756	1759	0.2	0.0	99.8	136	12.9
45	21	3	0	4736	4739	0.1	0.0	99.9	365	13.0
48	07	4	0	4749	4753	0.1	0.0	99.9	365	13.0
50	05	0	0	4740	4740	0.0	0.0	100.0	365	13.0
51	20	4	0	4734	4738	0.1	0.0	99.9	365	13.0
52	31	11	0	4736	4747	0.2	0.0	99.8	365	13.0
53	17	4	0	4745	4749	0.1	0.0	99.9	365	13.0
55	15	18	0	4732	4750	0.4	0.0	99.6	365	13.0
56	16	4	0	4741	4745	0.1	0.0	99.9	365	13.0
57	29	5	0	4752	4757	0.1	0.0	99.9	365	13.0
58	12	4	0	4737	4741	0.1	0.0	99.9	365	13.0
59	19	0	0	4738	4738	0.0	0.0	100.0	365	13.0
61	02	16	0	4740	4756	0.3	0.0	99.7	365	13.0
62	25	4	0	4745	4749	0.1	0.0	99.9	365	13.0
63	01	424	70	2402	2896	14.6	2.4	82.9	222	13.0
64	30	4	0	4739	4743	0.1	0.0	99.9	365	13.0
65	24	0	0	4746	4746	0.0	0.0	100.0	365	13.0
66	27	0	0	4734	4734	0.0	0.0	100.0	364	13.0
67	06	4	0	4743	4747	0.1	0.0	99.9	365	13.0
68	09	4	0	4743	4747	0.1	0.0	99.9	365	13.0
69	03	0	0	4982	4982	0.0	0.0	100.0	365	13.6
70	32	3	0	4743	4746	0.1	0.0	99.9	365	13.0
71	26	3	0	4746	4749	0.1	0.0	99.9	365	13.0
72	08	4	0	5031	5035	0.1	0.0	99.9	365	13.8
73	10	0	0	4765	4765	0.0	0.0	100.0	365	13.1
74	04	0	0	4688	4688	0.0	0.0	100.0	365	12.8
75	18	0	0	4716	4716	0.0	0.0	100.0	365	12.9
76	23	0	0	4698	4698	0.0	0.0	100.0	365	12.9
77	14	0	0	4727	4727	0.0	0.0	100.0	365	13.0
78	11	5	0	4720	4725	0.1	0.0	99.9	365	12.9
79	28	273	0	3817	4090	6.7	0.0	93.3	319	12.8
All SVs		836	70	146164	147070	0.6	0.0	99.4	365	402.9

A.2 Age of Data

The Age of Data (AOD) represents the elapsed time between the observations that were used to create the broadcast navigation message and the time when the contents of subframes 1, 2, and 3 became available to the user to estimate the position of an SV. The accuracy of GPS (for users that depend on the broadcast ephemeris) is indirectly tied to the AOD because the prediction accuracy degrades over time (see Section 3.2.2). This is especially true for the clock prediction. It has been recognized that reducing the AOD improves position, velocity, or time (PVT) solutions for autonomous users; however, there is an impact in terms of increased operations tempo at 2 SOPS.

Note that there is no need for a GPS receiver to refer to AOD in any PVT computation other than the optional application of the navigation message correction table (NMCT). (See IS-GPS-200 Section 20.3.3.5.1.9 for a description of the NMCT.) The AOD is computed here to validate that the operators at 2 SOPS are maintaining the URE accuracy with a normal operational tempo.

The daily average AOD throughout 2023 is shown in Table A.2, along with values for the previous three years. Details on how AOD was computed are provided in Appendix C.4. Figure A.1 illustrates the daily average AOD for the constellation and the various sub-constellations by SV type.

The average AOD is generally constant throughout 2023, which indicates that any variations in the URE results discussed earlier are not due to changes in operations tempo at 2 SOPS. The brief increase in AOD in August was due to some satellites entering short-term extended nav mode.

Table A.2: Age of Data of the Navigation Message by SV Type

	Average Age of Data (hrs)			
	2020	**2021**	**2022**	**2023**
Full Constellation	12.0	12.1	12.0	11.9
Block IIR/IIR-M	12.0	12.0	12.0	11.9
Block IIF	11.9	12.0	11.9	11.6
GPS III	11.9	12.3	12.3	12.1

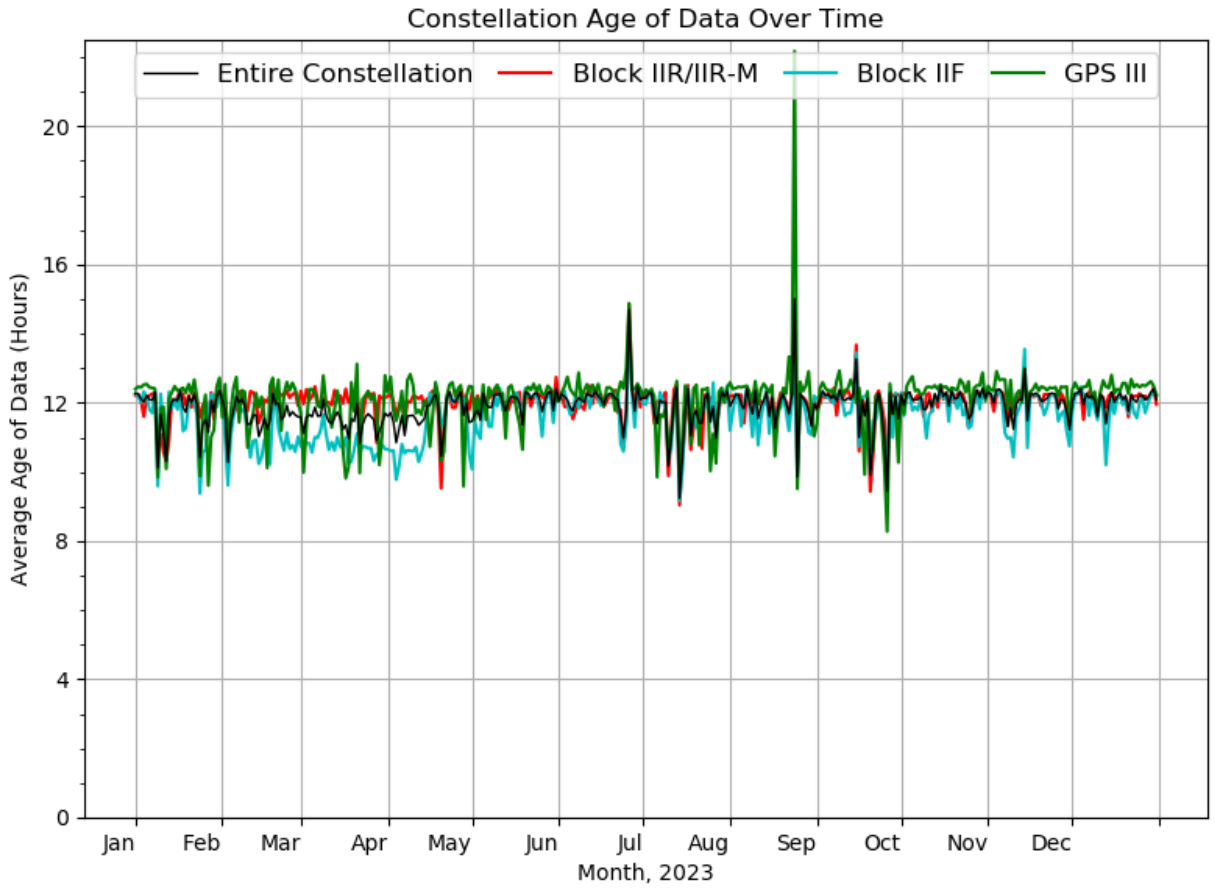

Figure A.1: Constellation Age of Data for 2023

A.3 User Range Accuracy Index Values

Figure A.2 presents the number of 30 s periods in the year in which an SV transmitted a given LNAV URA index. Only periods in which the SV was transmitting a healthy indication are included. SVs that were operational only part of the year have lower total counts.

The vast majority of the broadcast LNAV URA indices are 0, 1, or 2 (over 99.9%). Index values of 3 and 4 were very rare. No index values over 4 were observed.

Analysis of the URA values derived from the CNAV data requires a slightly different approach. Because the CNAV URA is a continuous function, we computed the CNAV URA value at each 30 s epoch, then binned those values corresponding to the range of LNAV URA values in IS-GPS-200 Section 20.3.3.3.1.3. That is to say, LNAV URA Index 1 has a range of 2.40 to 3.40 m; therefore, the CNAV URA values that fall into that range are assigned to Bin 1. CNAV URA values with values of 0.00 to 2.40 m are assigned to Bin 0.

Figure A.3 presents the number of 30 s periods in the year in which an SV transmitted a CNAV URA value that falls into the specified bins. There are a smaller number of SVs due to the fact the Block IIR SVs do not transmit a CNAV message.

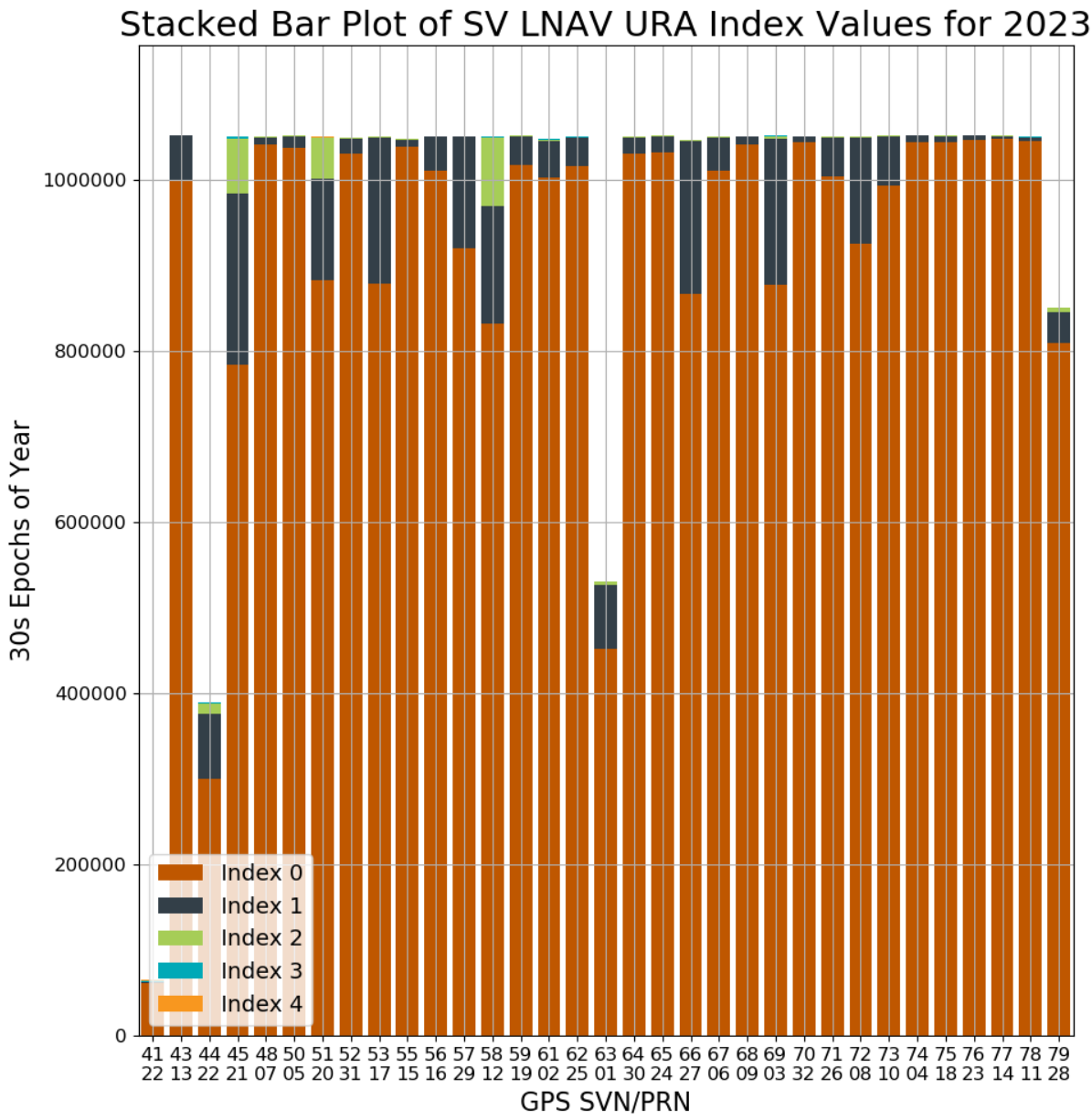

Figure A.2: Stacked Bar Plot of SV LNAV URA Index Values for 2023

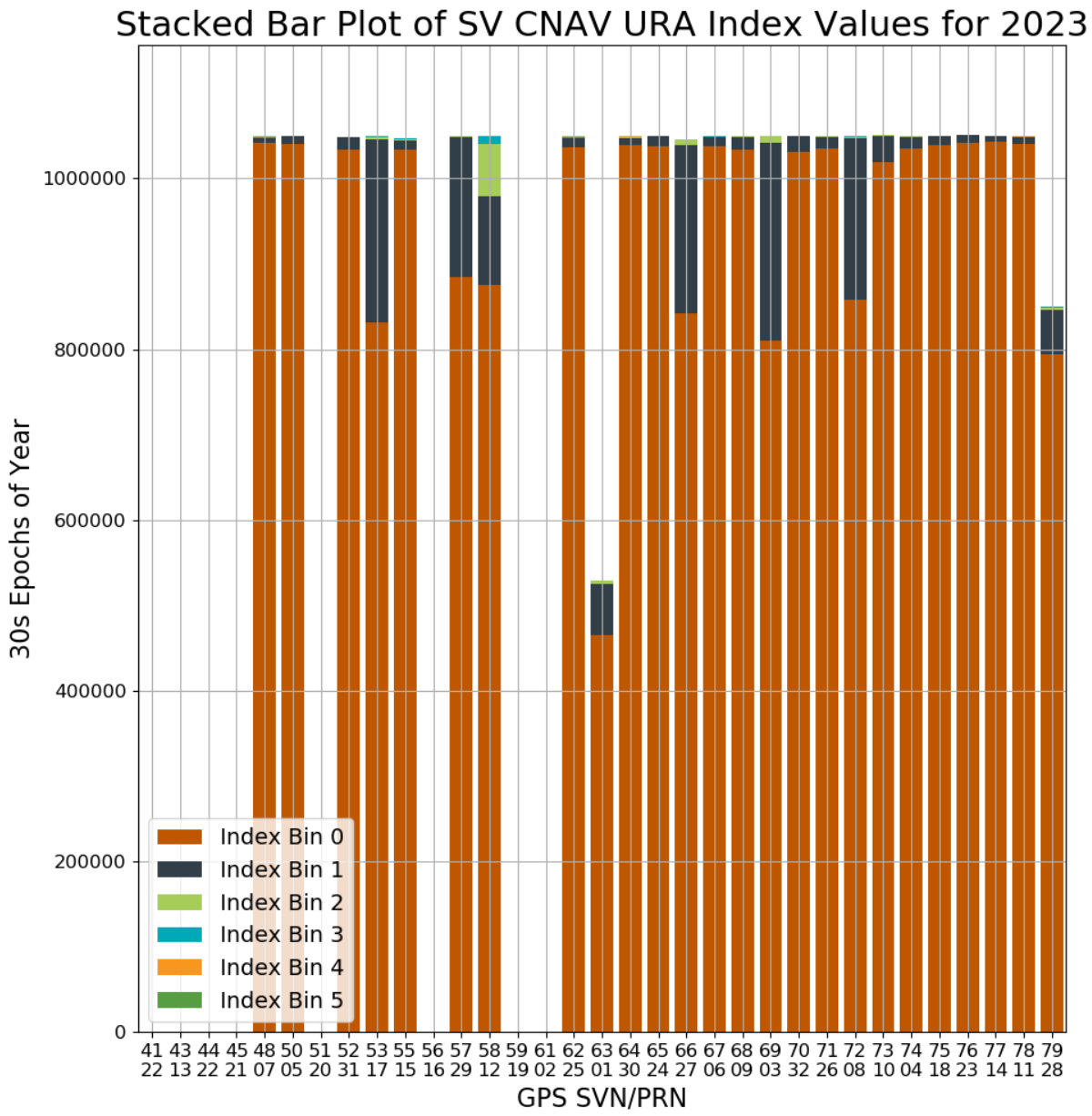

Figure A.3: Stacked Bar Plot of Binned SV CNAV URA Index Values for 2023

A.4 Extended Mode Operations

IS-GPS-200 defines Normal Operations as the period of time when subframe 1, 2, and 3 data sets are transmitted by the SV for periods of two hours with a curve fit interval of four hours (IS-GPS-200 Section 20.3.4.4). This definition is taken to be the same as the definition of Normal Operations in SPSPS20 for the URE metrics. To determine if any SV operated outside of Normal Operations at any time in 2023, the broadcast ephemerides were examined to determine if any contained fit interval flags that were set to 1. (See IS-GPS-200 20.3.3.4.3.1 for definition of the fit interval flag).

The analysis found a total of 52 examples of extended operations for satellites set healthy. The examples were distributed across 13 days. The average time of an occurrence was 4 hours 24 minutes. The minimum duration was 30 seconds and the maximum duration was 13 hours 50.5 minutes. These results are summarized in Table A.3. Only satellites with healthy extended operations events were included in the table.

Given the relative rarity of occurrence, the URE values for the periods summarized in Table A.3 are included in the statistics presented in Section 3.2.1, even though a strict interpretation of the SPSPS20 would suggest that they be removed. However, the SVs involved were still set healthy and (presumably) being used by user equipment, so it is appropriate to include these results to reflect performance seen by the users.

Examination of the ephemerides from past years reveals that 2023 is not an anomaly. Such periods have been found in all years checked, dating back to 2005.

Past discussions with the operators have revealed several reasons for these occurrences. Some are associated with Alternate MCS (AMCS) testing. When operations are transitioned from the MCS to the AMCS (and reverse), it is possible that SVs nearing the end of their daily cycle may experience a longer-than-normal upload cycle. Other occurrences may be caused by delays due to ground antenna maintenance or due to operator concentration on higher-priority issues with the constellation at the time.

Table A.3: Summary of Occurrences of Extended Mode Operations

SVN	PRN	# of Occurrences		Duration (minutes)	
		Healthy	Unhealthy	Healthy	Unhealthy
41	22	1	0	63	0
43	13	1	0	239	0
44	22	2	0	295	0
45	21	4	0	1047	0
48	07	2	0	175	0
50	05	2	0	468	0
51	20	2	0	956	0
52	31	2	0	870	0
53	17	1	0	452	0
55	15	2	0	168	0
56	16	1	0	258	0
57	29	1	0	267	0
58	12	3	0	879	0
59	19	3	0	522	0
61	02	1	0	100	0
62	25	2	0	633	0
64	30	2	0	441	0
65	24	2	0	733	0
66	27	3	0	442	0
67	06	2	0	609	0
68	09	2	0	646	0
69	03	3	0	1364	0
70	32	1	0	148	0
71	26	2	0	622	0
72	08	2	0	406	0
73	10	3	0	920	0
Totals		52	0	13723	0

A.5 URE as a Function of AOD

This appendix contains supporting information for the results presented in Section 3.2.2. Charts of SIS RMS URE vs. AOD similar to Figures 3.5 - 3.12 are presented for each GPS SV. The charts are organized by SV block and by ascending SVN within each block. These charts are based on the set of 30 s Instantaneous RMS SIS URE values computed as described in Appendix C.2.4.

For each SV, the entire year of 30 s URE values was grouped by AOD in bins of 15 minutes each. For satellites operating on the normal pattern (roughly one upload per day), the count of points in each bin is roughly constant from the time the upload becomes available until about 24 hours AOD. The nominal number of points can be calculated by multiplying the number of expected 30 s estimates in a 15 minute bin (30 estimates per bin) by the number of days in the year. There are just under 11,000 points in each bin. The URE values in each bin were sorted and the 95th percentile was determined. Since GPS SVs are typically uploaded daily, bins beyond 24 hours of AOD are sparsely populated. Bins with few points tend to be dominated by occasional high-value outliers that can lead to erroneous conclusions about behavior. Therefore, bins containing fewer than 10% of points relative to the maximum populated bin were dropped before plotting.

The count of points in each bin as a function of AOD for L1 C/A are plotted. This is representative of the curves for other signal combinations for a given SV as the unhealthy periods for all signals for a given SV are very nearly coordinated. Note that for most SVs, the counts curve has a well-defined horizontal plateau that begins near zero AOD, continues for roughly 24 hours, and then drops quickly toward zero. The location of the right-hand drop of the counts curve toward zero provides an estimate of the typical upload period for the SV. For SVs that are uploaded more frequently, the green curve will show a left-hand peak higher than the nominal count decreasing to the right.

Where multiple curves are present, the biases between the curves are a result of the influence of the ISC and DCB values on the URE calculation process. See Appendix C.2.2, Appendix C.2.5, and Appendix C.2.6 for details.

SVN 79/PRN 28 (GPS III), which was set operational February 2023, had larger URE values February through May than in the remainder of the year. These were likely related to early estimates of T_{GD} and ISC values as these were updated in May 2023.

A.5.1 SPS Results

The figures on the following pages each show up to four curves:

- 95th percentile URE vs. AOD for:
  - Blue: L1 C/A
  - Magenta: L1 C/A + L2C
  - Cyan: L1 C/A + L5Q
- Green: count of points in each bin vs. AOD for L1 C/A

A.5.1.1 Block IIR SVs

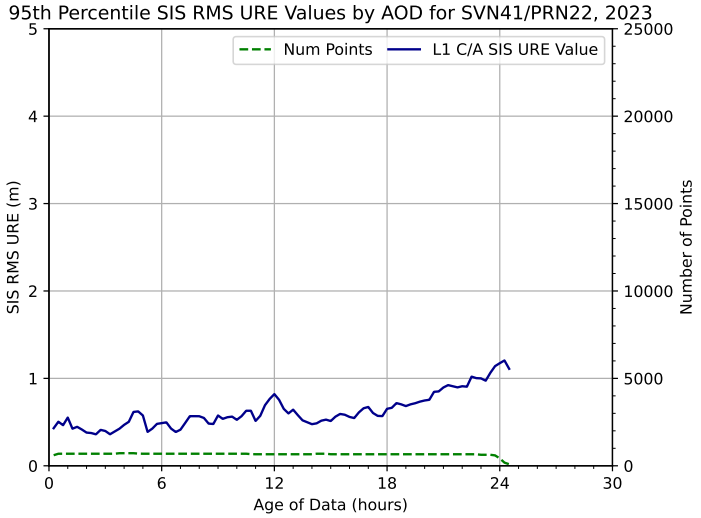

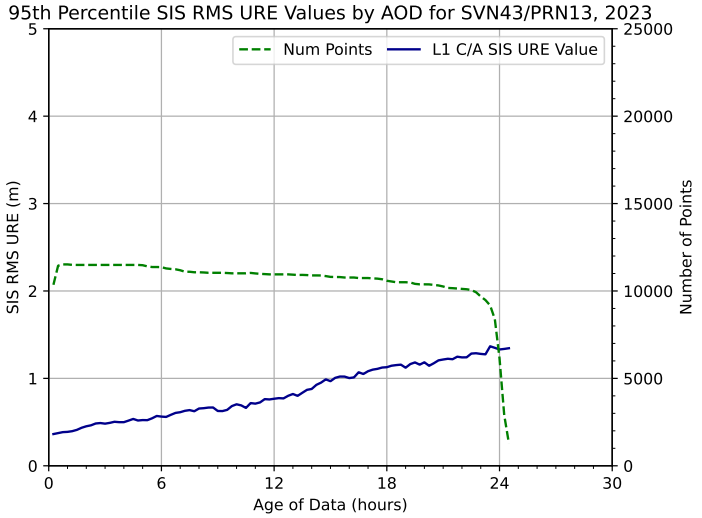

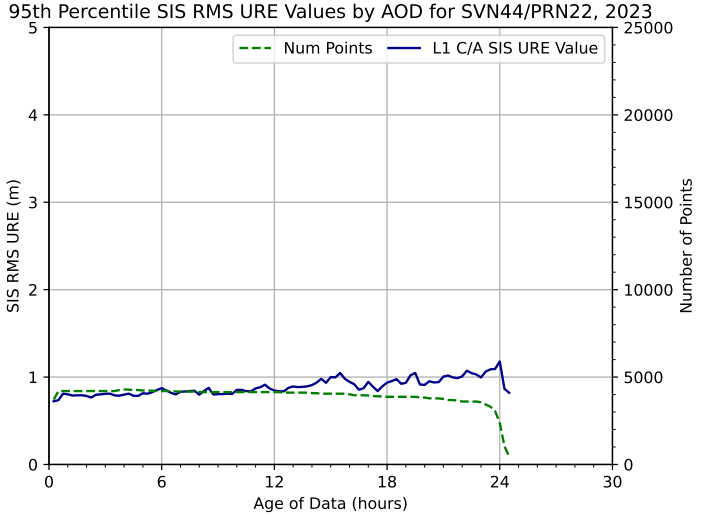

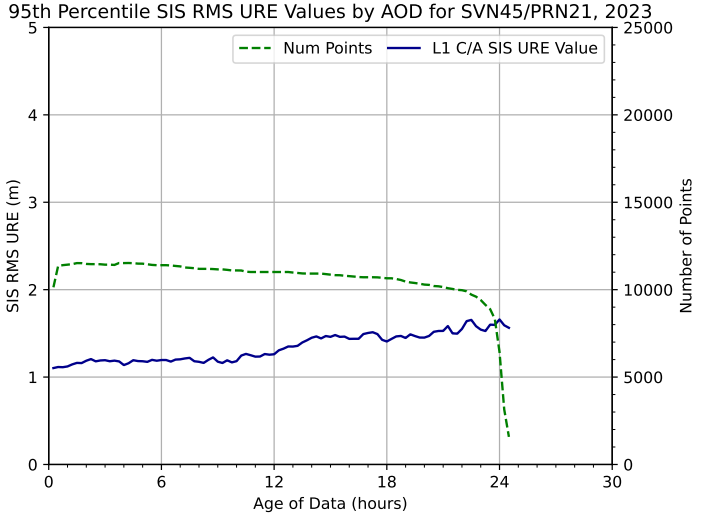

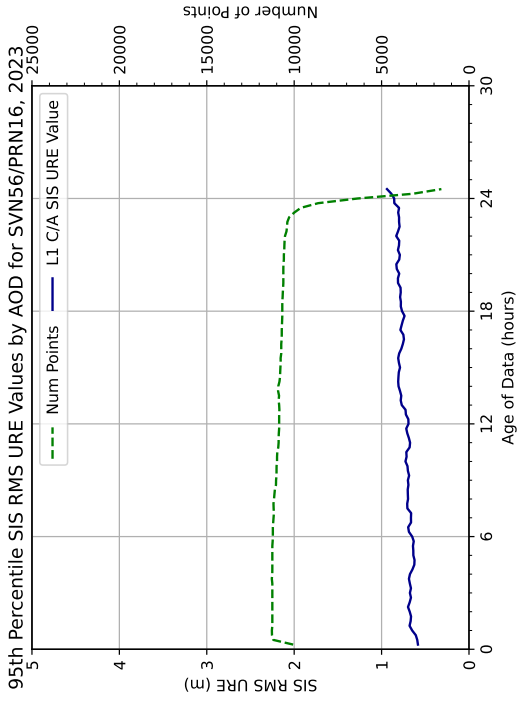
95th Percentile SIS RMS URE Values by AOD for SVN56/PRN16, 2023
Num Points
L1 C/A SIS URE Value
SIS RMS URE (m)
Number of Points
Age of Data (hours)

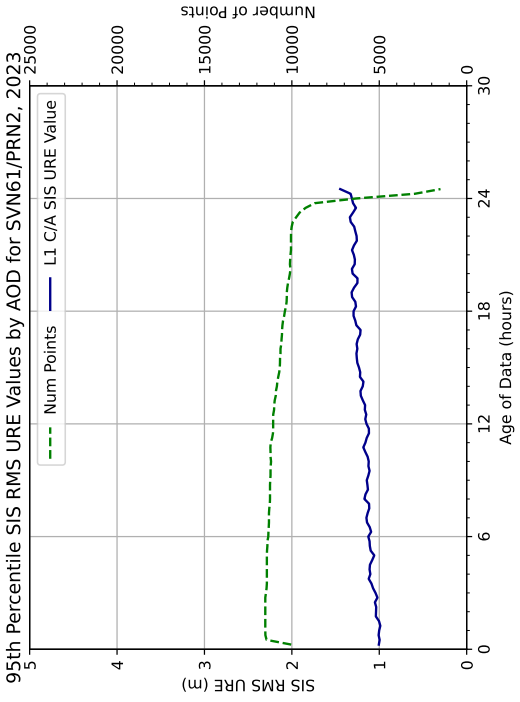
95th Percentile SIS RMS URE Values by AOD for SVN61/PRN2, 2023
Num Points
L1 C/A SIS URE Value
SIS RMS URE (m)
Number of Points
Age of Data (hours)

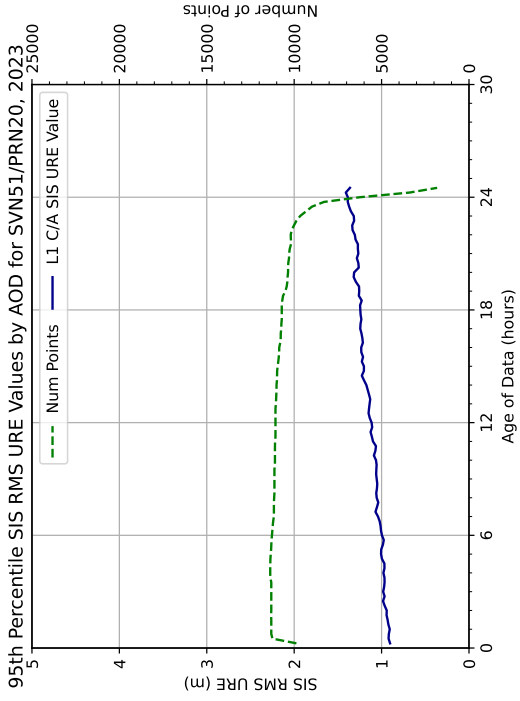
95th Percentile SIS RMS URE Values by AOD for SVN51/PRN20, 2023
Num Points
L1 C/A SIS URE Value
SIS RMS URE (m)
Number of Points
Age of Data (hours)

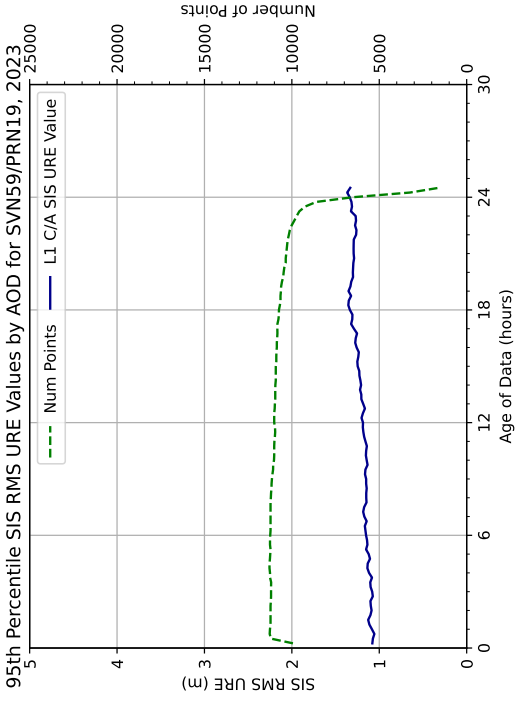
95th Percentile SIS RMS URE Values by AOD for SVN59/PRN19, 2023
Num Points
L1 C/A SIS URE Value
SIS RMS URE (m)
Number of Points
Age of Data (hours)

A.5.1.2 Block IIR-M SVs

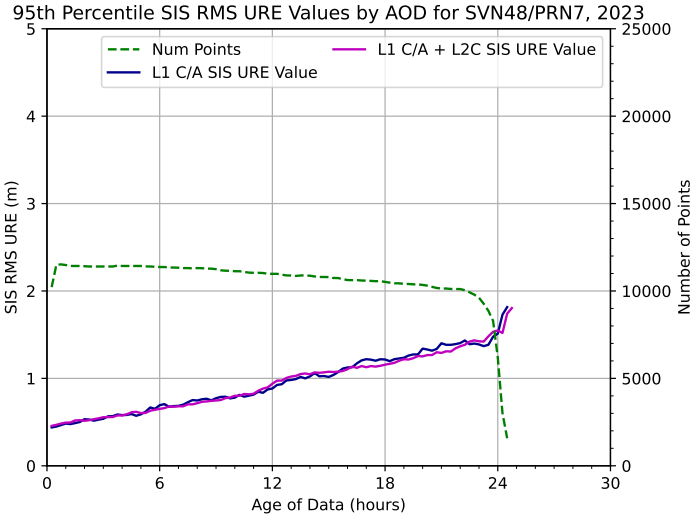

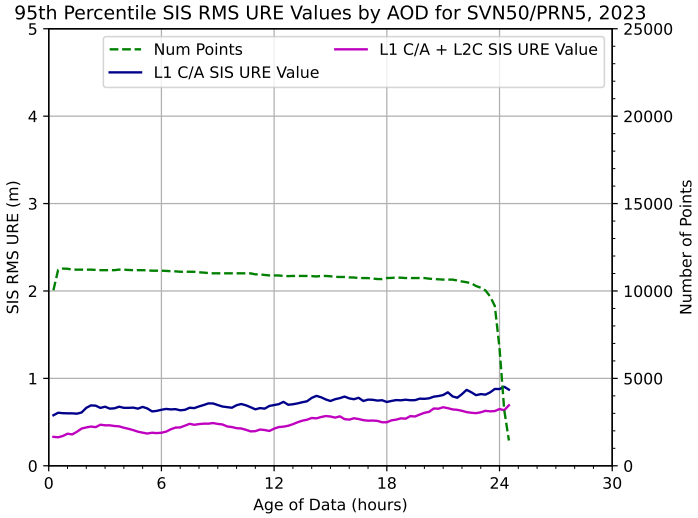

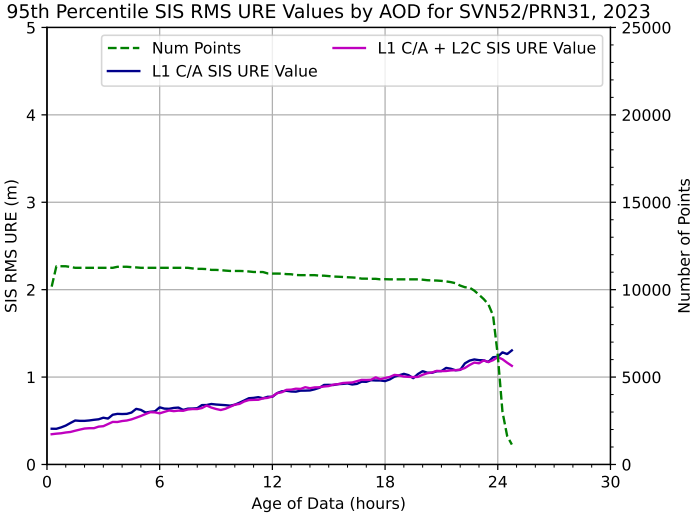

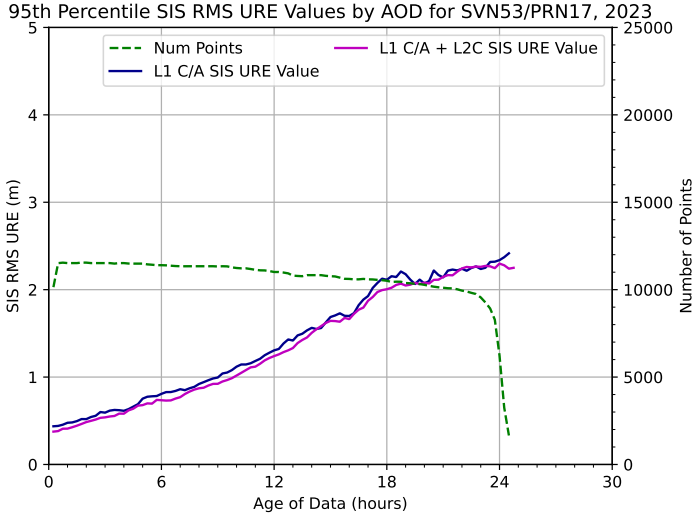

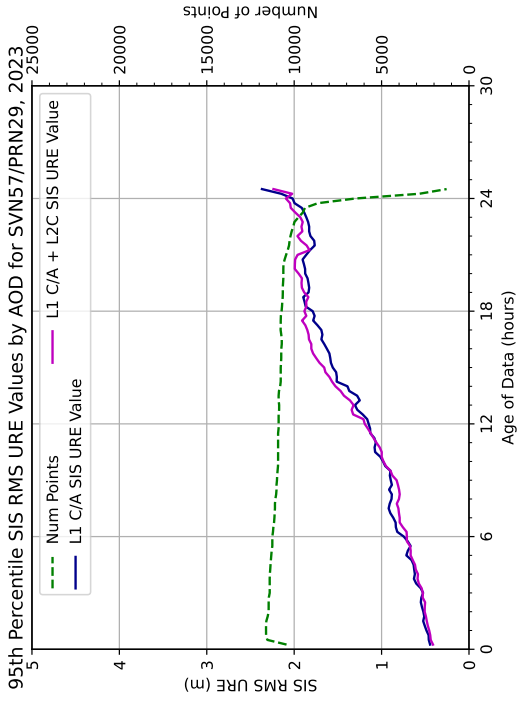
95th Percentile SIS RMS URE Values by AOD for SVN57/PRN29, 2023
Num Points
L1 C/A SIS URE Value
L1 C/A + L2C SIS URE Value
SIS RMS URE (m)
Number of Points
Age of Data (hours)

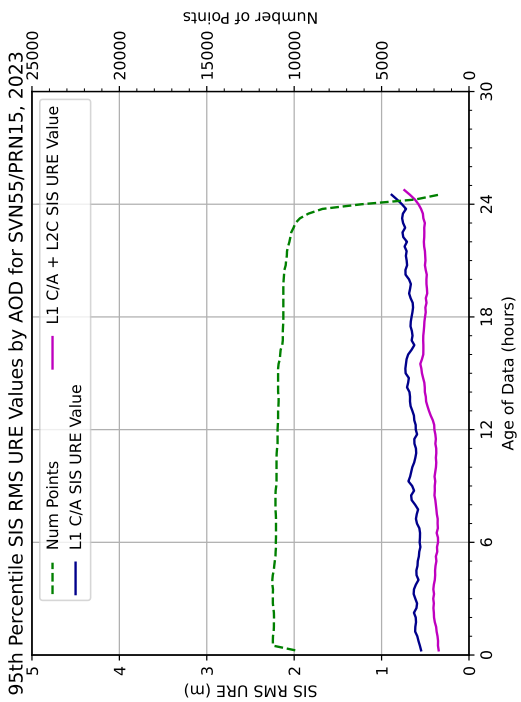
95th Percentile SIS RMS URE Values by AOD for SVN55/PRN15, 2023
Num Points
L1 C/A SIS URE Value
L1 C/A + L2C SIS URE Value
SIS RMS URE (m)
Number of Points
Age of Data (hours)

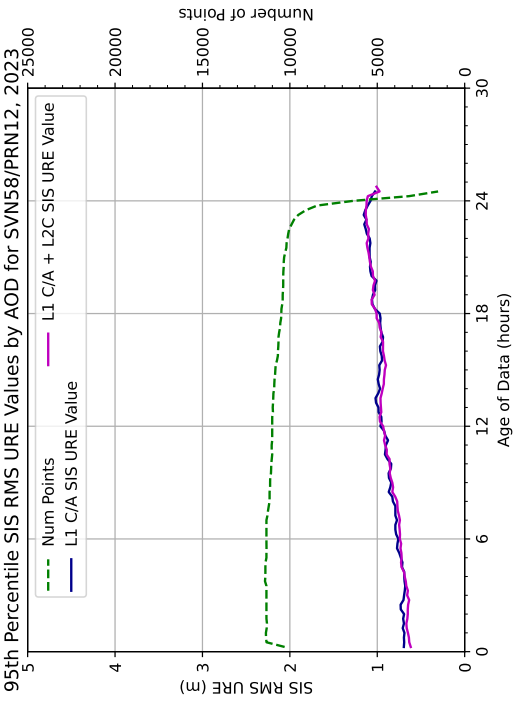
95th Percentile SIS RMS URE Values by AOD for SVN58/PRN12, 2023
Num Points
L1 C/A SIS URE Value
L1 C/A + L2C SIS URE Value
SIS RMS URE (m)
Number of Points
Age of Data (hours)

A.5.1.3 Block IIF SVs

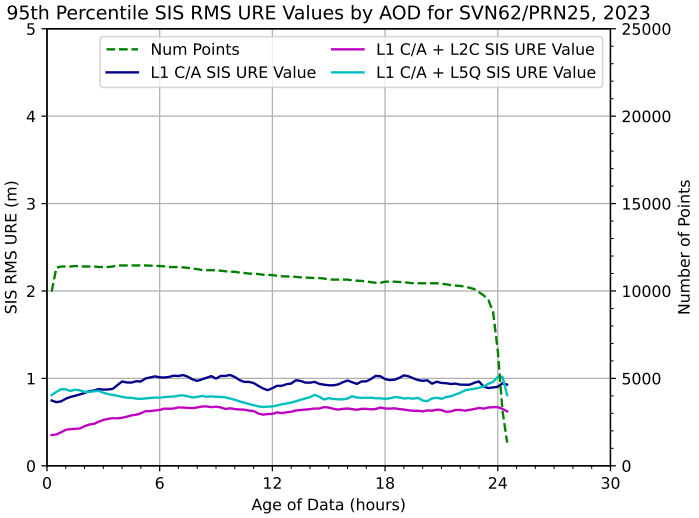

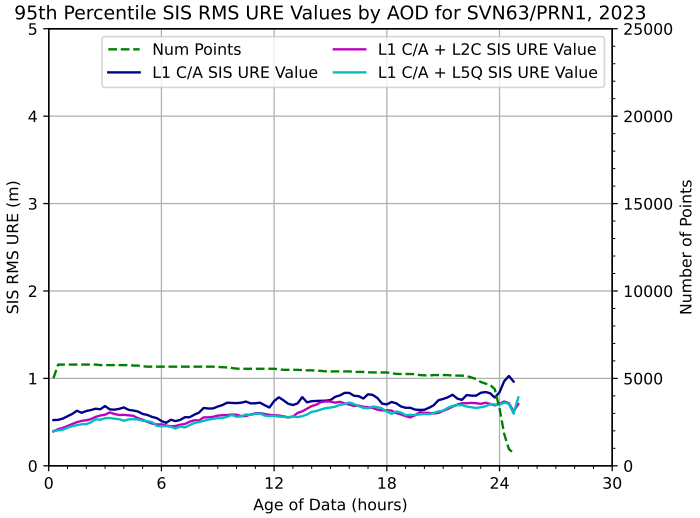

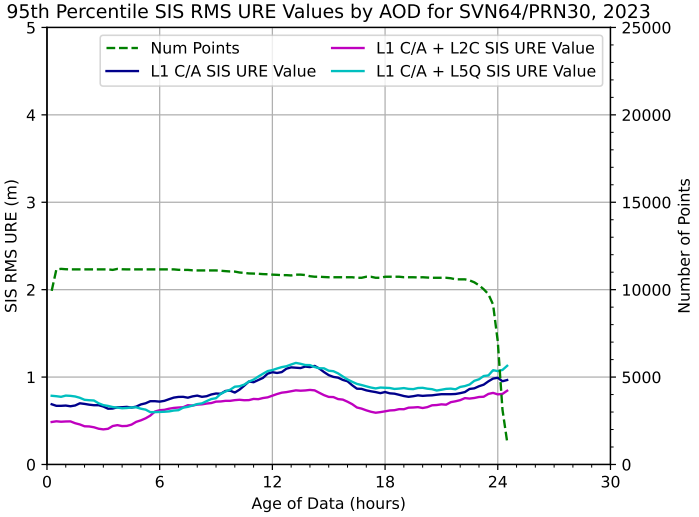

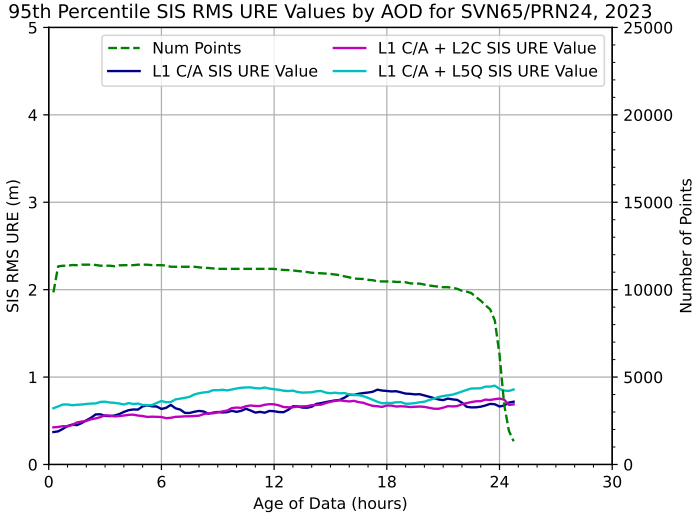

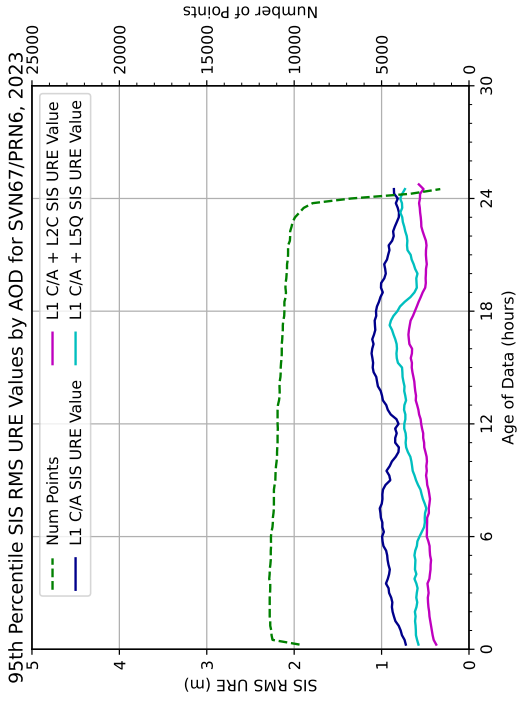
95th Percentile SIS RMS URE Values by AOD for SVN67/PRN6, 2023
Num Points
L1 C/A SIS URE Value
L1 C/A + L2C SIS URE Value
L1 C/A + L5Q SIS URE Value
SIS RMS URE (m)
Number of Points
Age of Data (hours)

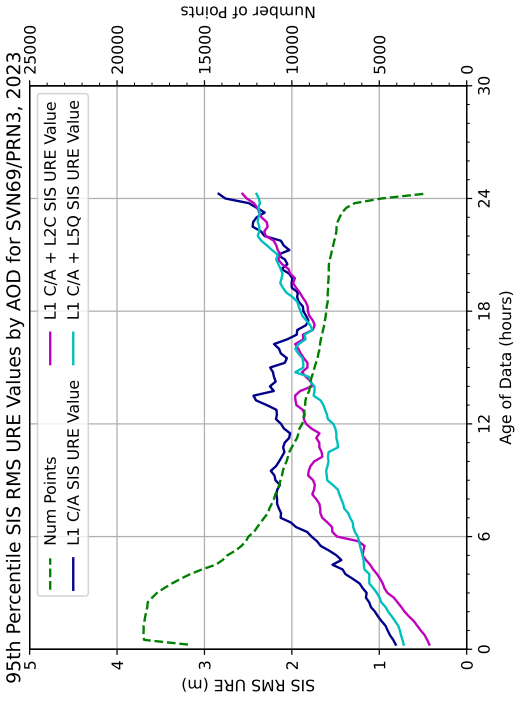
95th Percentile SIS RMS URE Values by AOD for SVN69/PRN3, 2023
Num Points
L1 C/A SIS URE Value
L1 C/A + L2C SIS URE Value
L1 C/A + L5Q SIS URE Value
SIS RMS URE (m)
Number of Points
Age of Data (hours)

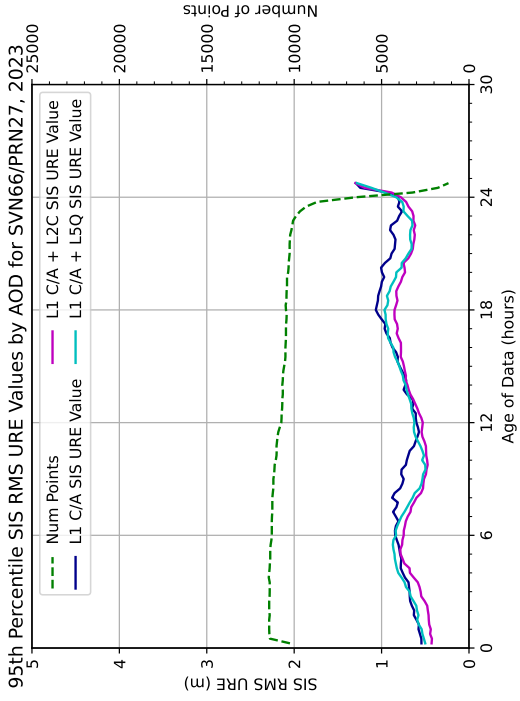
95th Percentile SIS RMS URE Values by AOD for SVN66/PRN27, 2023
Num Points
L1 C/A SIS URE Value
L1 C/A + L2C SIS URE Value
L1 C/A + L5Q SIS URE Value
SIS RMS URE (m)
Number of Points
Age of Data (hours)

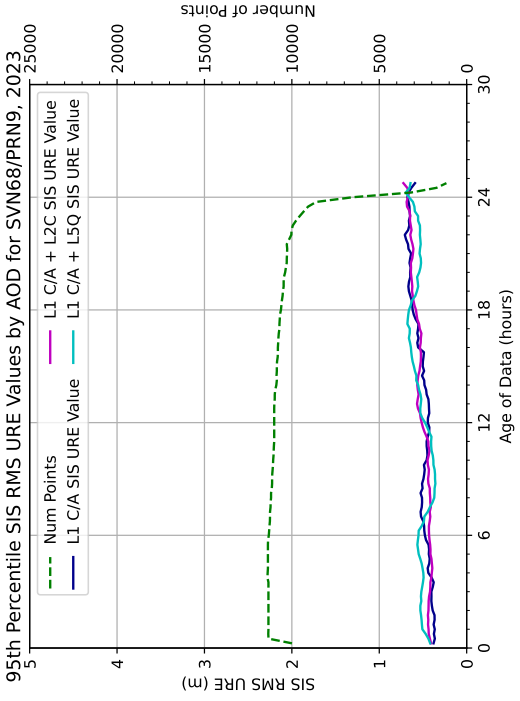
95th Percentile SIS RMS URE Values by AOD for SVN68/PRN9, 2023
Num Points
L1 C/A SIS URE Value
L1 C/A + L2C SIS URE Value
L1 C/A + L5Q SIS URE Value
SIS RMS URE (m)
Number of Points
Age of Data (hours)

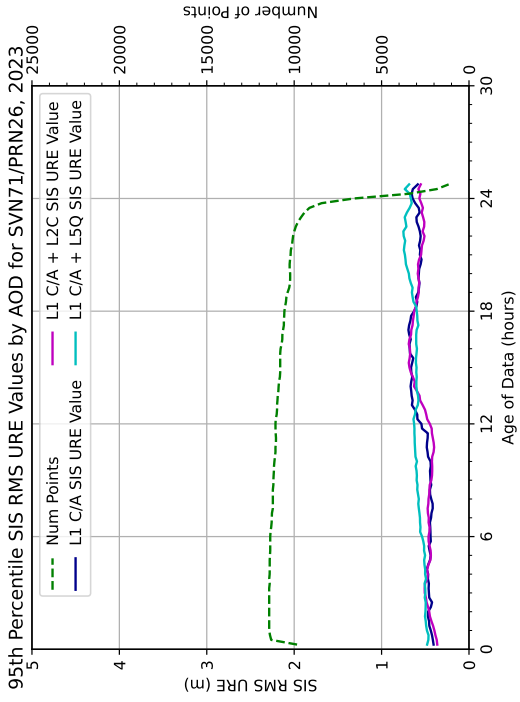
95th Percentile SIS RMS URE Values by AOD for SVN71/PRN26, 2023
Num Points
L1 C/A SIS URE Value
L1 C/A + L2C SIS URE Value
L1 C/A + L5Q SIS URE Value
SIS RMS URE (m)
Number of Points
Age of Data (hours)

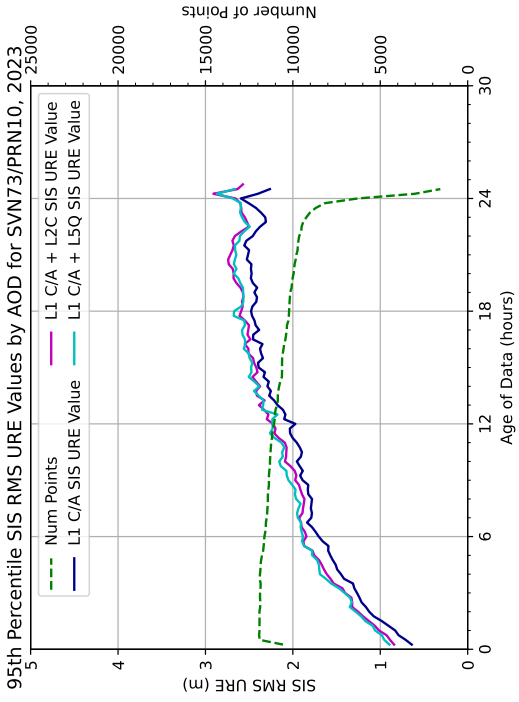
95th Percentile SIS RMS URE Values by AOD for SVN73/PRN10, 2023
Num Points
L1 C/A SIS URE Value
L1 C/A + L2C SIS URE Value
L1 C/A + L5Q SIS URE Value
SIS RMS URE (m)
Number of Points
Age of Data (hours)

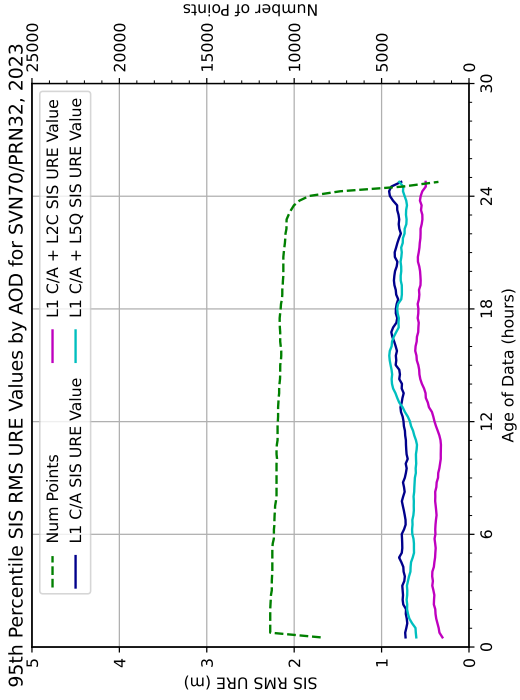
95th Percentile SIS RMS URE Values by AOD for SVN70/PRN32, 2023
Num Points
L1 C/A SIS URE Value
L1 C/A + L2C SIS URE Value
L1 C/A + L5Q SIS URE Value
SIS RMS URE (m)
Number of Points
Age of Data (hours)

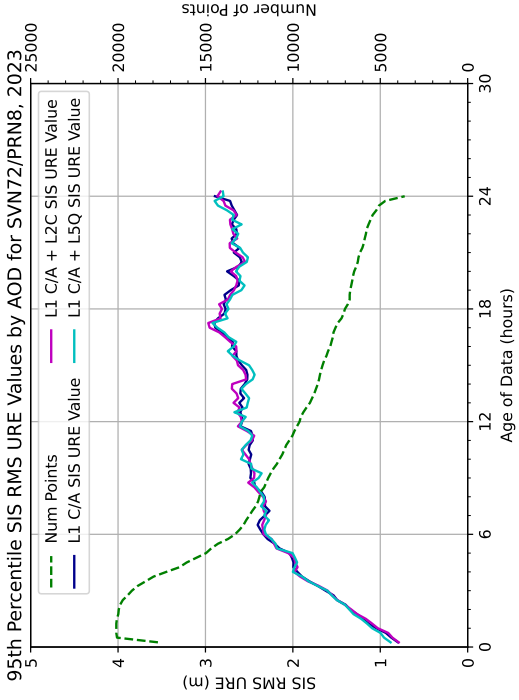
95th Percentile SIS RMS URE Values by AOD for SVN72/PRN8, 2023
Num Points
L1 C/A SIS URE Value
L1 C/A + L2C SIS URE Value
L1 C/A + L5Q SIS URE Value
SIS RMS URE (m)
Number of Points
Age of Data (hours)

A.5.1.4 GPS III SVs

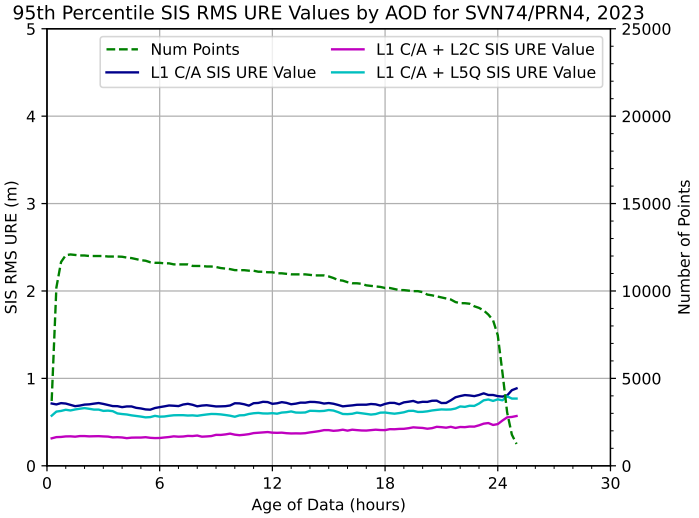

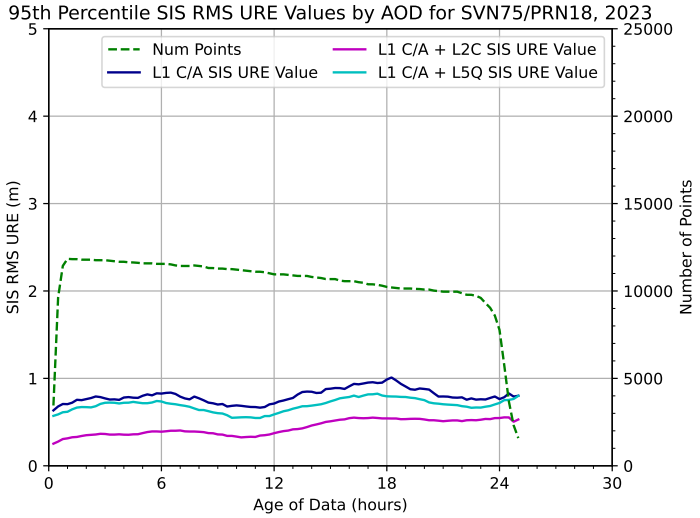

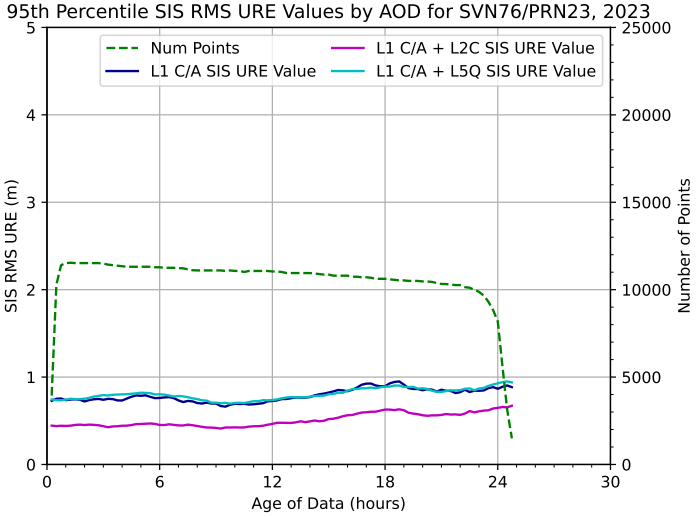

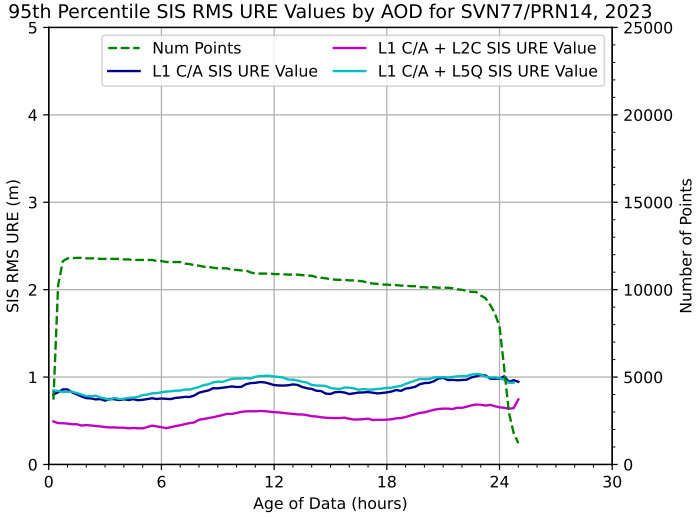

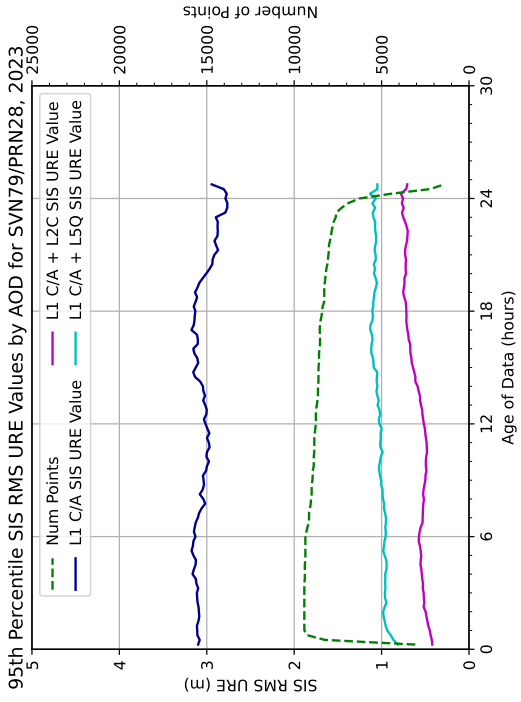
95th Percentile SIS RMS URE Values by AOD for SVN79/PRN28, 2023
Num Points
L1 C/A SIS URE Value
L1 C/A + L2C SIS URE Value
L1 C/A + L5Q SIS URE Value
SIS RMS URE (m)
Number of Points
Age of Data (hours)

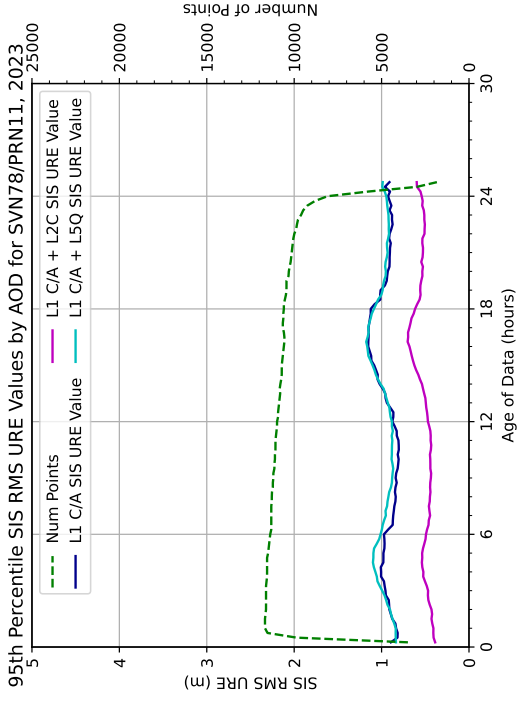
95th Percentile SIS RMS URE Values by AOD for SVN78/PRN11, 2023
Num Points
L1 C/A SIS URE Value
L1 C/A + L2C SIS URE Value
L1 C/A + L5Q SIS URE Value
SIS RMS URE (m)
Number of Points
Age of Data (hours)

A.6 SVN 63/PRN 1 Integrity Fault Events

During 2023, SVN 63/PRN 1 exceeded the not-to-exceed (NTE) URE integrity threshold during two events. As discussed in Section 3.3.1 and Section 3.3.3, the assertions on integrity in the SPSPS20 define an integrity fault event as any line-of-sight SIS Instantaneous URE exceeding the ±4.42 times broadcast maximum URA threshold.

Figures A.4 and A.5 show the SIS RMS URE and the range of SIS Instantaneous URE values for L1 C/A, and the 4.42 times broadcast maximum URA NTE threshold for the period of interest. Note there is a difference in cadence between the RMS (30 s) and line-of-sight UREs (5 min).

The first event occurred on 25 January 2023. The fault period lasted for 148 minutes between 1602Z and 1830Z. The URA index broadcast by the SV was 0 during this event, corresponding to a maximum URA threshold of 2.4 m and an NTE threshold of 10.61 m. At 1602Z, a clock phase event resulted in a jump in URE from sub-1 m to around 27 m, with a maximum line-of-sight URE of 27.59 m during the event. Note that, due to the location of the clock event in the precise ephemeris data, the increase in UREs is not visible in Figure A.4 until after 1610Z. The start time of the event was instead determined through analysis of carrier phase data. The fault period continued until transmission from the satellite ceased at 1830Z. Broadcast resumed at 1915Z with an unhealthy indication, with an upload at 2316Z correcting the broadcast clock bias term and lowering the URE values. The satellite was set healthy again the next day at 1541Z.

The second event occurred on 10 July 2023. The fault period lasted for 23 minutes between 0957Z and 1020Z. The URA index broadcast by the SV was 1 during this event, corresponding to a maximum URA threshold of 3.4 m and an NTE threshold of 15.03 m. At 0957Z, a clock phase event resulted in a jump in URE from sub-1 m to around 40 m, with a maximum line-of-sight URE of 40.80 m during the event. Note that, due to the location of the clock event in the precise ephemeris data, the increase in UREs is not visible in Figure A.5 until after 1000Z. The start time of the event was instead determined through analysis of ORD data. The fault period continued until transmission from the satellite ceased at 1120Z. Broadcast resumed at 1106Z with an unhealthy indication, with an upload at 1550Z correcting the broadcast clock bias term and lowering the URE values. The satellite was not set healthy again following this event, and was decommissioned on 10 August 2023.

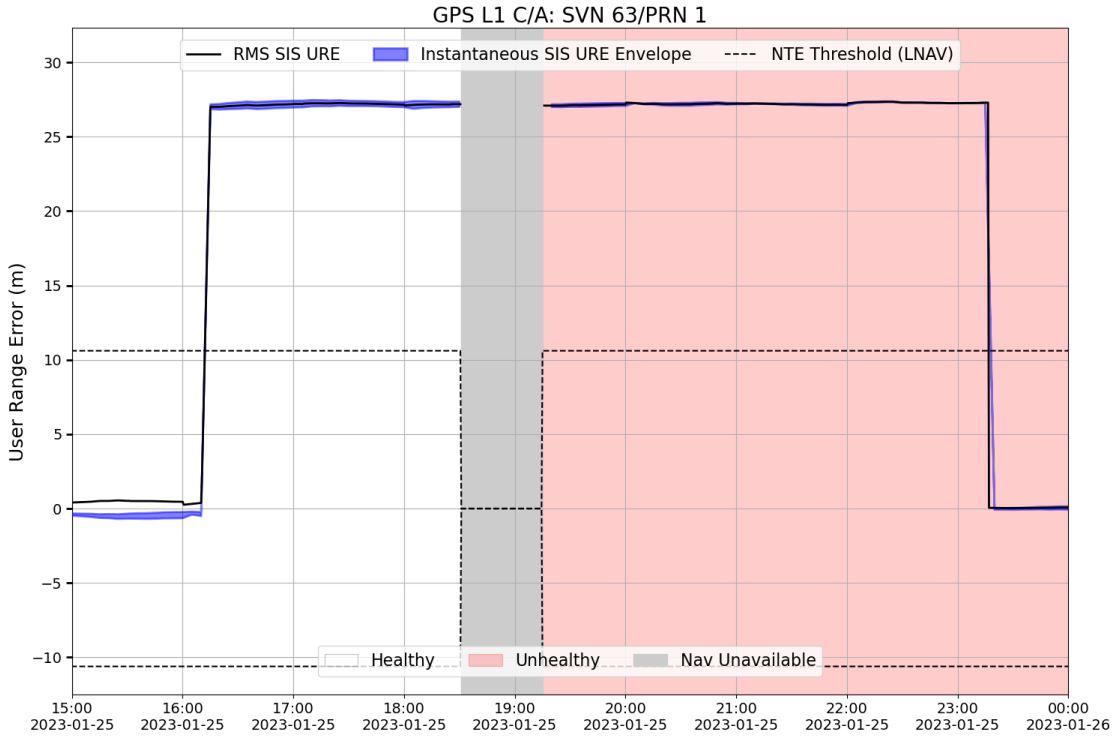

Figure A.4: Integrity Fault Event on 25 January 2023, SVN 63/PRN 1

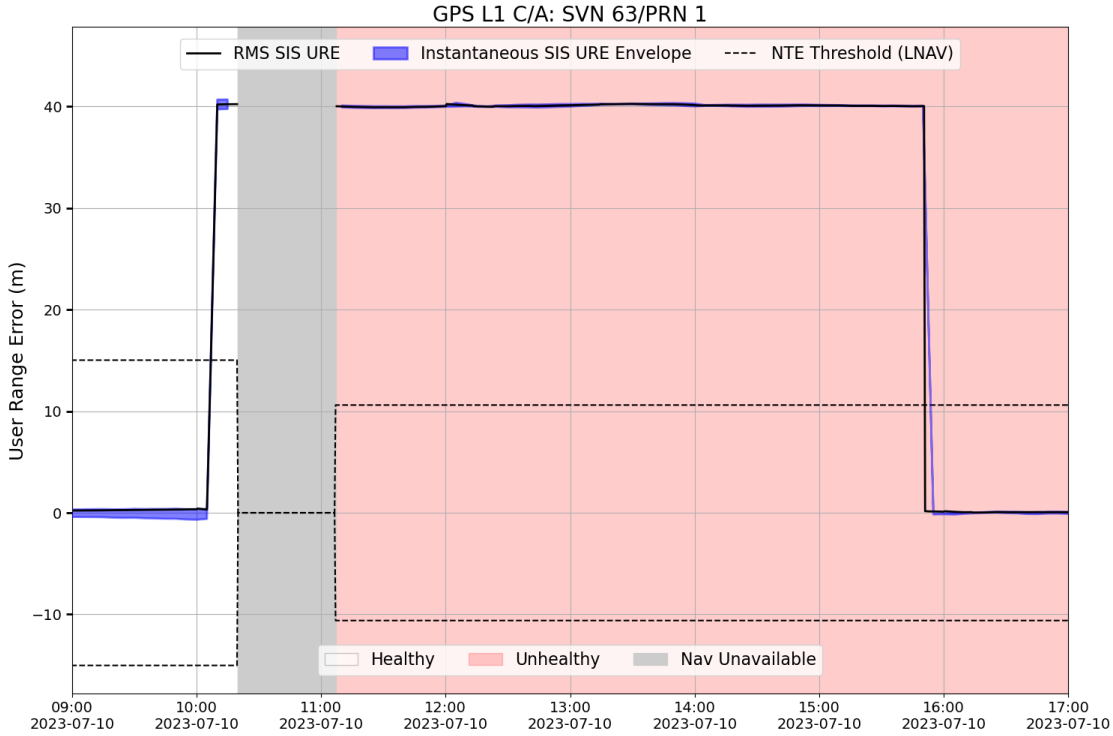

Figure A.5: Integrity Fault Event on 10 July 2023, SVN 63/PRN 1

A.7 Additional DOP Analysis

There are several ways to look at DOP values when various averaging techniques are taken into account. Assuming a set of DOP values, each identified by latitude (λ), longitude (θ), and time (t), then each individual value is represented by $DOP_{\lambda,\theta,t}$.

The global average DOP for a day, $\langle DOP \rangle(day)$, is defined to be:

$$\langle DOP \rangle(day) = \frac{\sum_t \sum_\theta \sum_\lambda DOP_{\lambda,\theta,t}}{N_{grid} \times N_t}$$

Another measure of performance is the average DOP over the day at the worst site, $\langle DOP \rangle_{worst\,site}$. In this case, the average over a day is computed for each unique latitude/longitude combination and the worst average of the day is taken as the result.

$$\langle DOP \rangle_{worst\,site}(day) = \max_{\lambda,\theta} \left(\frac{\sum_t DOP_{\lambda,\theta,t}}{N_t} \right)$$

This statistic is the most closely related to the description of worst site used in Section 3.6.1.1.

The average of worst site DOP, $\langle DOP_{worst\,site} \rangle$, is calculated by obtaining the worst DOP in the latitude/longitude grid at each time, then averaging these values over the day.

$$\langle DOP_{worst\,site} \rangle(day) = \frac{\sum_t \max_{\lambda,\theta} (DOP_{\lambda,\theta,t})}{N_t}$$

Given that the $\langle DOP \rangle_{worst\,site}(day)$ is most closely related to the worst site definition used in Section 3.6.1.1, this is the statistic that will be used for "worst site" in the remainder of this section. For 2023, both $\langle DOP \rangle_{worst\,site}(day)$ and $\langle DOP_{worst\,site} \rangle(day)$ satisfy the SPS PS assertions.

It is worth noting the following mathematical relationship between these quantities:

$$\langle DOP \rangle \leq \langle DOP \rangle_{worst\,site} \leq \langle DOP_{worst\,site} \rangle$$

In general, this relationship serves as a sanity check on the DOP results and establishes that these metrics are increasingly sensitive to outliers in $DOP_{\lambda,\theta,t}$.

In calculating the percentage of the time that the $\langle DOP \rangle$ and $\langle DOP \rangle_{worst\,site}$ are within bounds, several other statistics were calculated which provide insight into the availability of the GPS constellation throughout the world. Included in these statistics are the annual means of the daily global average DOP and the $\langle DOP \rangle_{worst\,site}$ values. These values are presented in Table A.4, with values for 2020 through 2022 provided for comparison.

The average number of satellites and the fewest satellites visible across the grid are calculated as part of the DOP calculations. Also shown in Table A.4 are the annual means of the global average number of satellites visible to grid cells on a 111 km × 111 km (latitude by longitude) global grid and the annual means of the number of satellites in the worst-site grid cell (defined as seeing the fewest number of satellites). It should be noted that the worst site for each of these values was not only determined independently from day-to-day, but was also determined independently for each metric. That is to say, it is not guaranteed that the worst site with respect to Horizontal DOP (HDOP) is the same as the worst site with respect to PDOP. For all quantities shown in Table A.4, the values are very similar across all four years.

Table A.4: Additional DOP Annually-Averaged Visibility Statistics for 2020 – 2023

	$\langle$**DOP**$\rangle$				$\langle$**DOP**$\rangle_{\textbf{worst site}}$			
	2020	**2021**	**2022**	**2023**	**2020**	**2021**	**2022**	**2023**
Horizontal DOP	0.84	0.84	0.83	0.83	0.95	0.95	0.95	0.95
Vertical DOP	1.35	1.37	1.35	1.35	1.70	1.70	1.69	1.69
Time DOP	0.79	0.80	0.79	0.78	0.90	0.90	0.90	0.90
Position DOP	1.60	1.61	1.59	1.59	1.85	1.86	1.85	1.84
Geometry DOP	1.78	1.80	1.78	1.77	2.06	2.07	2.05	2.05
Number of visible SVs	10.32	10.25	10.32	10.41	5.77	5.89	5.95	5.83

There are a few other statistics that can add insight regarding the GPS system availability. The primary availability metric requires that the globally averaged PDOP be in-bounds at least 98% of the time. There are two related values: the number of days for which the PDOP is in bounds and the 98$^{\text{th}}$ percentile of the daily globally averaged PDOP values. Similarly, calculations can be done for $\langle DOP \rangle_{worst\,site}$ criteria of having the PDOP ≤ 6 greater than 88% of the time. Table A.5 presents these values for 2023 and the previous three years.

Table A.5: Additional PDOP Statistics

	2020	**2021**	**2022**	**2023**
% of Days with the $\langle PDOP \rangle \leq 6$	100.00	100.00	100.00	100.00
% of Days with the $\langle PDOP \rangle$ at Worst Site ≤ 6	100.00	100.00	100.00	100.00
98$^{\text{th}}$ Percentile of $\langle PDOP \rangle$	1.63	1.69	1.64	1.65
88$^{\text{th}}$ Percentile of $\langle PDOP \rangle_{worst\,site}$	1.88	1.90	1.86	1.87

Table A.5 shows that the average DOP values for 2023 are nearly identical to the previous three years.

Appendix B

Supporting Data

This chapter includes supporting data for the analysis, including PRN to SVN mapping, NANU activity, and SVN to Plane-Slot mapping.

Contents

B.1 PRN to SVN Mapping for 2023 92
B.2 NANU Activity in 2023 92
B.3 SVN to Plane-Slot Mapping for 2023 95

B.1 PRN to SVN Mapping for 2023

Throughout the report, SVs have been referred to by both PRN and SVN. The PRN to SVN mapping is time dependent as PRN assignments change. Keeping track of this relationship has become more challenging over the past few years as the number of operational SVs is typically very close to the number of available PRNs. Therefore, it is useful to have a summary of the PRN to SVN mapping as a function of time. Figure B.1 presents that mapping for 2023. SVNs on the right vertical axis appear in the order in which they were assigned the PRN values in 2023. Colored bars indicate the range of time each relationship was in effect. Start and end times of relationships are indicated by the dates at the top of the chart.

These data are assembled by ARL:UT from the NANUs and the operational advisories, and confirmed by discussion with The Aerospace Corporation staff supporting 2 SOPS.

B.2 NANU Activity in 2023

Several sections in the report make use of NANUs. It is useful to have a time history of the relevant NANUs sorted by SVN. This makes it convenient to determine which NANU(s) should be examined if an anomaly is observed for a particular satellite at a particular time.

Figure B.2 presents a plot of the NANU activity in 2023. Blue bars represent scheduled outages and red bars represent unscheduled outages. Gray bars represent SVs that were decommissioned in 2023. Light green bars represent SVs after launch prior to a NANU declaring initial usability. NANU numbers are indicated next to each bar. In the event there is more than one NANU for an outage, the last NANU number is displayed.

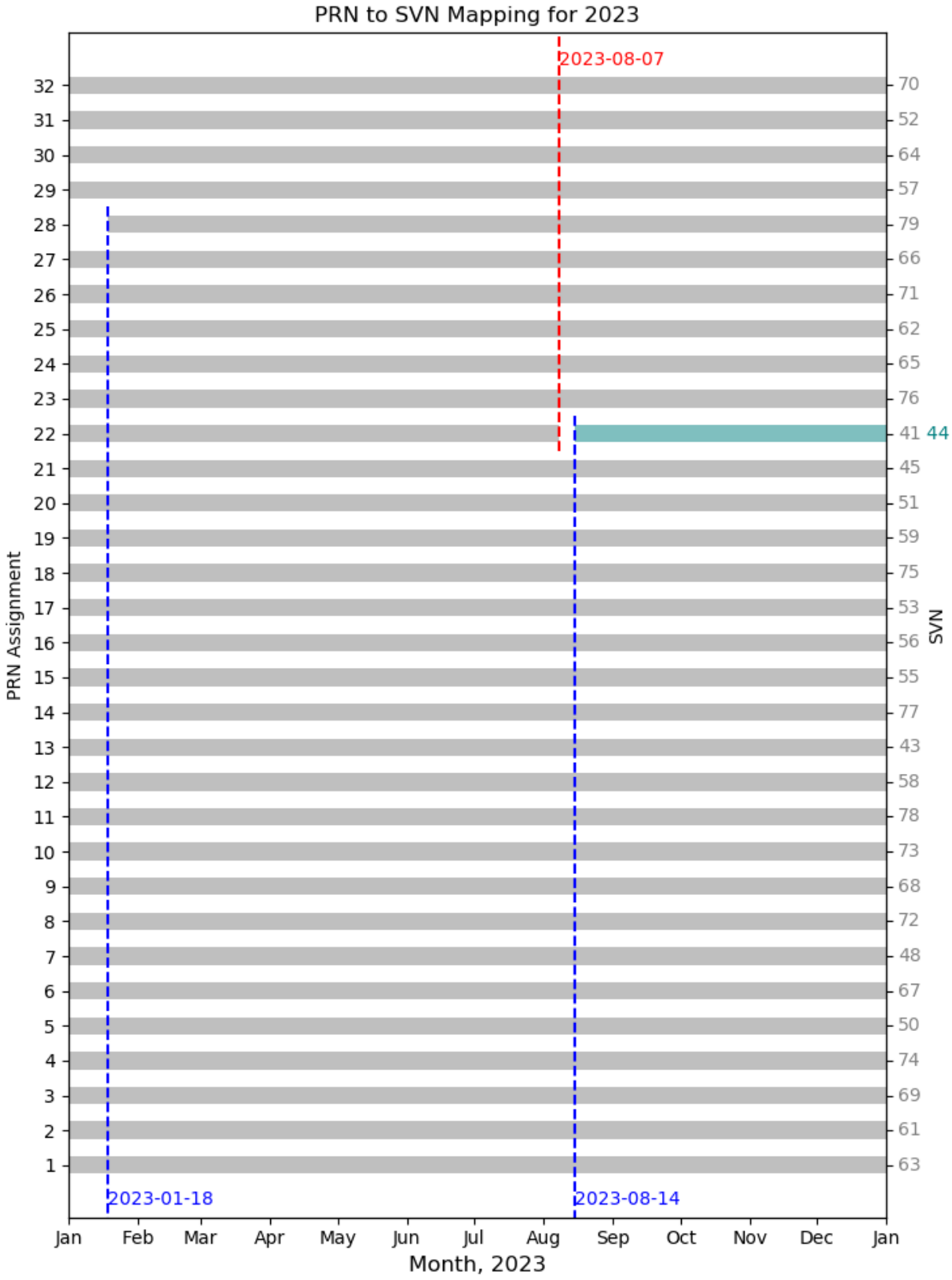

Figure B.1: PRN to SVN Mapping for 2023

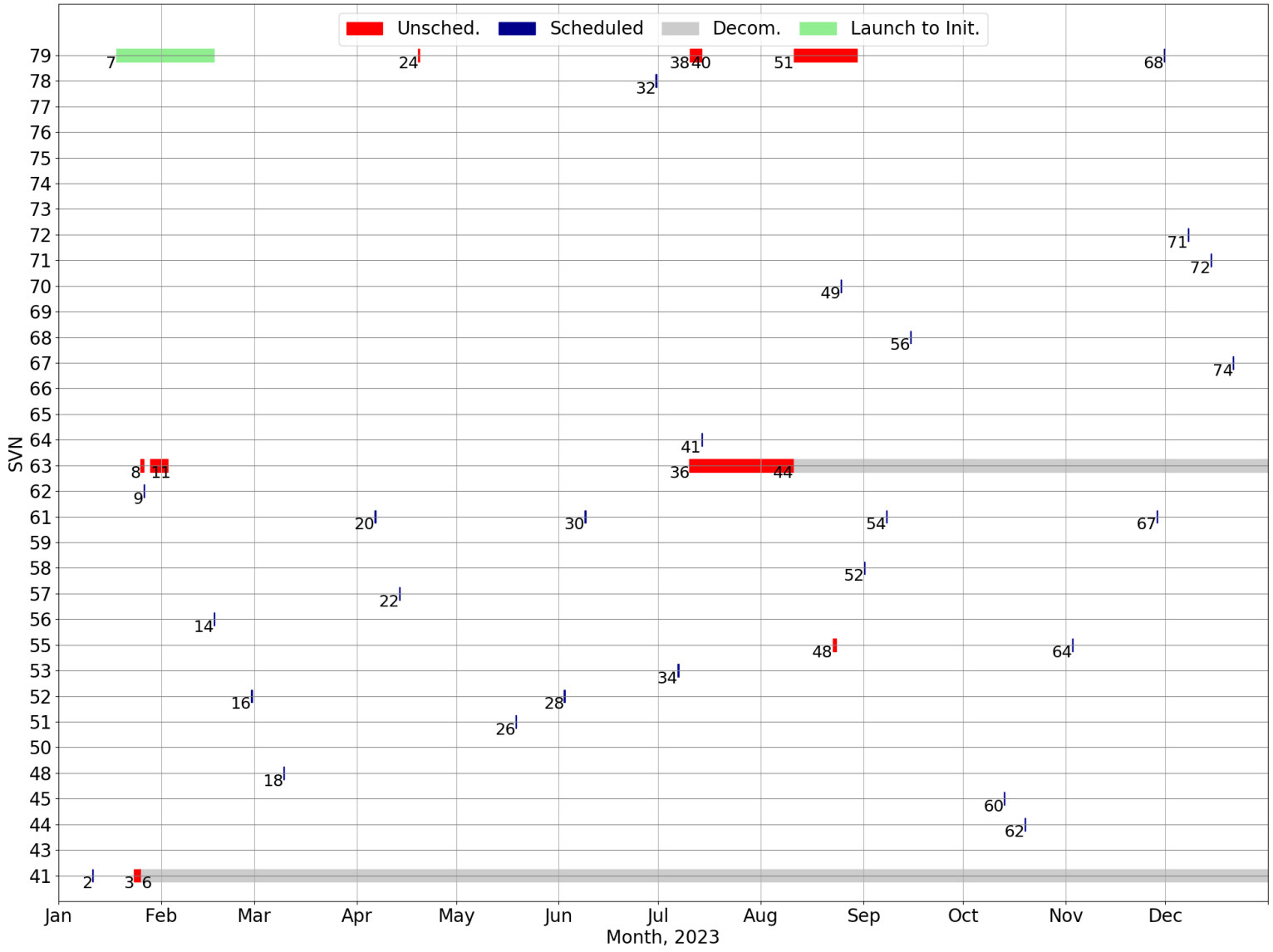

Figure B.2: Plot of NANU Activity for 2023

B.3 SVN to Plane-Slot Mapping for 2023

Several assertions are related to the performance of the constellation as defined by the plane-slot arrangement specified in the SPSPS20. Six planes lettered A-F are defined. Each plane contains four slots numbered 1-4. For each plane, one slot may be expanded into a pair of locations designated by the addition of the letters F (fore) or A (aft). The possible plane-slot designators appear on the vertical axis of Figure B.3. Evaluation of these assertions requires information on the plane-slot occupancy during the year.

The constellation definition located in Section 3.2 of the SPSPS20 that provides the plane-slot definitions is an ideal model in the sense that it assumes all SVs have zero eccentricity and nominal inclination. Slots within a plane are defined in terms of the Right Ascension of the Ascending Node (RAAN) and the Argument of Latitude of a hypothetical nominal satellite at a specified epoch. Appendix A.2.4 of the SPSPS20 defines how to propagate these nominal slot centers in time. Appendix A.7.4 of the SPSPS20 defines a slot as occupied when the footprint of a satellite (or combined footprint of a pair of satellites, for expanded slots) on the surface of the Earth overlaps at least 95% of the nominal slot's footprint, averaged over an orbit revolution, and provides an inequality in terms of RAAN and Argument of Latitude offset as a conservative approximation of the 95% footprint overlap condition.

Information on plane-slot assignment appears in the operational advisory (OA) provided by 2 SOPS to the U.S. Coast Guard (USCG) Navigation Center, defined in ICD-GPS-240. However, the format does not permit clarity for expanded slots: there is no provision for fore or aft designations. Also, OA designations for slots contain numbers beyond the slots defined in the performance standard. The operators define these "slots of convenience" without fixed meaning for constellation position. As a result, OA interpretation can be challenging. During 2023, the Navigation Center also posted a graphic depicting the SV locations in terms of plane and slot. This graphic shows the status at a particular epoch.

As satellites are moved within the constellation, there exist occasional periods when more than one SV may be present within the defined boundaries of a slot. From the user's point of view, the slot should be counted as occupied if a satellite transmitting a healthy signal, or a combination of multiple satellites each transmitting a healthy signal, cover the area visible from the designated primary slot locations. Additionally, Appendix A.7.2.4 and Appendix A.7.2.5 of the SPSPS20 define "equivalent-or-better" non-standard configurations of expanded slots which meet the 95% overlap condition but may not have the nominal fore or aft slots themselves meet the individual overlap conditions. These circumstances require particular care to properly determine plane-slot assignments.

Figure B.3 presents a plot of the plane-slot relationships throughout 2023, including start and end dates of slot occupancy. The contents of Figure B.3 are determined by assessing the 95% footprint overlap criterion for the actual satellite positions as compared to the nominal constellation. Refer to Appendix C.6 for more information on this process. In the cases where an SV is decommissioned or a new SV is launched, the appropriate NANUs were also checked to confirm dates. The dates when satellites are judged to be present in a slot location are noted only when a change occurs in the plane-slot during the year. This allows the reader to determine when multiple satellites occupied the same slot.

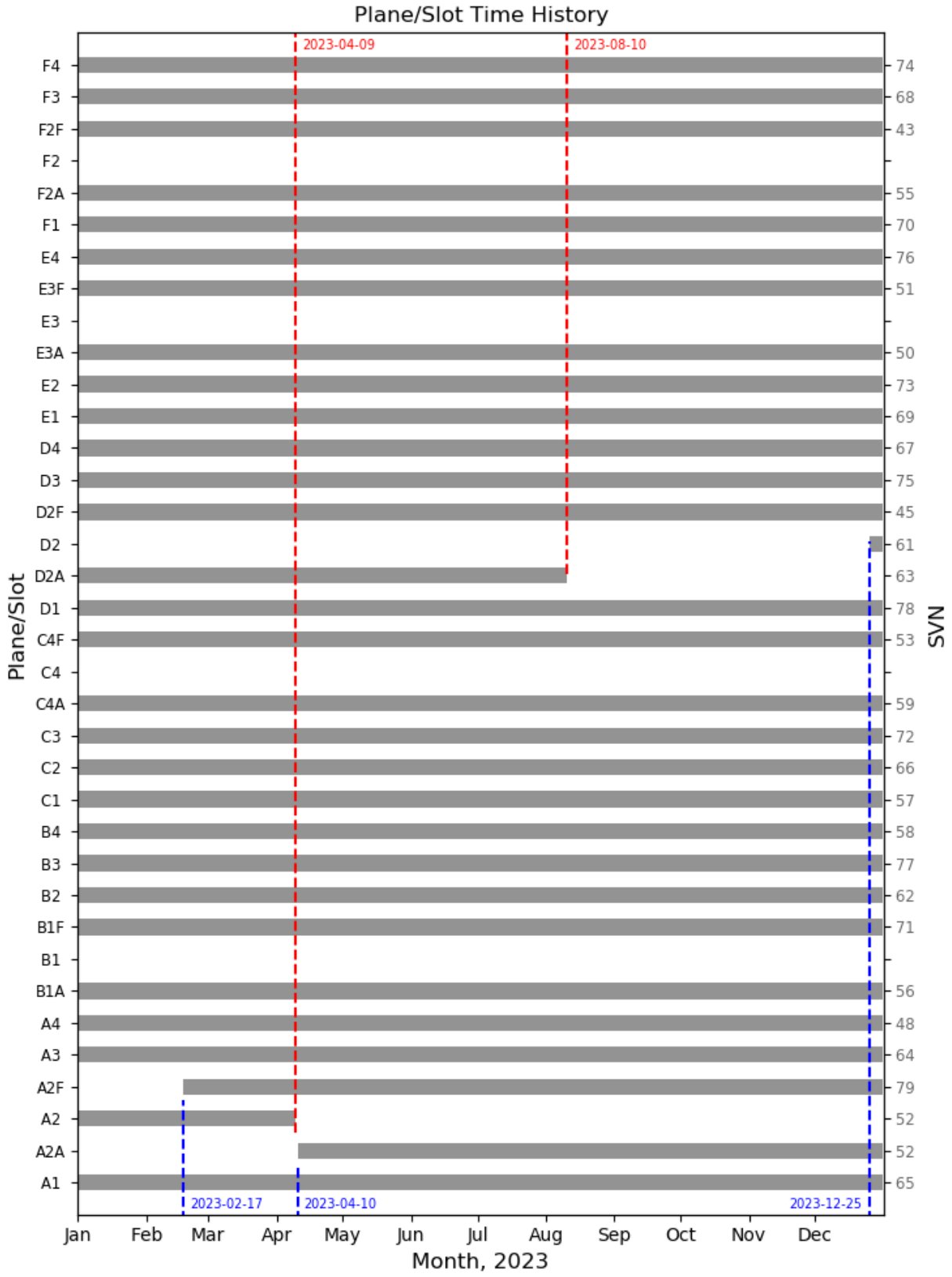

Figure B.3: Time History of Satellite Plane-Slots for 2023

Appendix C

Analysis Details

This chapter provides details on the analysis process. Topics include the motivation behind selected signal combinations, the methodology of the URE process, the process by which navigation message data are selected, the means by which AOD is computed, and the determination of plane-slot assignments.

Contents

C.1 Signals Used 99
C.2 URE Methodology 100
C.2.1 Clock and Position Values for Broadcast and Truth 101
C.2.2 ISCs and DCBs 102
C.2.3 Definition of 95^{th} Percentile Global Statistic 105
C.2.4 Definition of 95^{th} Percentile Global Average 107
C.2.5 Limitations of URE Analysis 108
C.2.6 Challenges of Comparing UREs Between Signal Combinations 109
C.3 Selection of Broadcast Navigation Message Data 110
C.4 AOD Methodology 111
C.5 Position Methodology 112
C.6 Plane/Slot Methodology 115

C.1 Signals Used

The signals and signal combinations defined in the SPS PS are listed in Table 1.1 and replicated below. While it is possible to generate results to test all assertions directly, this would result in a large duplication of effort. What is necessary is to cover the signals of interest and the navigation messages of interest. If no assertion violations are found for such a subset, then assertions for the other signal combinations can be assumed to be satisfied. However, if any violation of assertions is detected within this subset, it may be necessary to compute results for additional signal combinations to verify the results.

Table C.1: SPS SIS Signal Combinations Covered by SPSPS20

One Carrier Single Frequency (SF)	**Two Carriers Dual Frequency (DF)**	**Three Carriers Triple Frequency (TF)**
C/A-code + LNAV Data	(C/A + CM)-codes + CNAV Data	(C/A + CM + I5)-codes + CNAV Data
CM-code + CNAV Data	(C/A + CL)-codes + CNAV Data	(C/A + CL + I5)-codes + CNAV Data
CL-code + CNAV Data	(C/A + CM+CL)-codes + CNAV Data	(C/A + CM+CL + I5)-codes + CNAV Data
(CM+CL)-codes + CNAV Data	(C/A + I5)-codes + CNAV Data	(C/A + CM + Q5)-codes + CNAV Data
I5-code + CNAV Data	(C/A + Q5)-codes + CNAV Data	(C/A + CL + Q5)-codes + CNAV Data
Q5-code + CNAV Data	(C/A + I5+Q5)-codes + CNAV Data	(C/A + CM+CL + Q5)-codes + CNAV Data
(I5+Q5)-codes + CNAV Data		(C/A + CM+CL + I5+Q5)-codes + CNAV Data

The signal combinations selected for evaluation are summarized in Table C.2. This selection of signal combinations includes all unique signals at least once and all navigation messages (LNAV, CNAV-L2C, CNAV-L5I). Table C.2 notes whether or not T_{GD} and ISC values are included in the URE computation.

Table C.2: Rationale for Selection of Signal Combinations

Signal Combination	**Navigation Message**	**Rationale**	**T_{GD}**	**ISC**
L1 C/A	LNAV	Primary SPS signal; checks L1 C/A and LNAV	✔	✗
L1 C/A + L2C	CNAV from L2C	SPS dual-frequency combination; checks L2C CNAV message	✔	✔
L1 C/A + L5Q	CNAV from L5I	SPS dual-frequency combination; checks L5I CNAV message	✔	✔

C.2 URE Methodology

User range error (URE) represents the accuracy of the broadcast navigation messages. URE values are central to several of the assertions evaluated in this report. The concept of URE is simple, but the execution is dependent on many details. This section provides an overview of the methodology used in determining URE values.

The URE statistics presented in this report are based on a comparison of the BCP against the TCP. This is a useful approach, but one that has specific limitations. The most significant limitation is that the TCP may not capture the effect of individual discontinuities or large effects over short time scales (e.g., a frequency step or clock run-off). Nonetheless, this approach is appropriate given the 30-day period of averaging implemented in determining URE compared to brief (less than an hour) periods of the rare discontinuities. Briefly, this approach allows the computation of URE *without direct reference to observations* from any particular ground sites, though the TCP carries an implicit network dependency based on the set of ground stations used to derive the precise orbits from which the TCP is derived.

Throughout this report, there are references to several distinct SIS URE expressions. Each of these SIS URE expressions means something slightly different. It is important to pay careful attention to the particular SIS URE expression being used in each case to avoid misinterpreting the associated results.

Throughout this section, there are references to the "Instantaneous RMS SIS URE." This is a statistical basis SIS URE (note the "RMS" statistical qualifier), where the measurement quantity is the Instantaneous SIS URE, and the span of the statistic covers that one particular point ("instant") in time across a large range of spatial points. This is effectively the evaluation of the Instantaneous SIS URE across every spatial point in the area of the service volume visible to the SV at that particular instant in time.

Put another way, consider the signal from a given SV at a given point in time. That signal intersects the surface of the Earth over an area, and at each point in that area there is a unique Instantaneous SIS URE value based on geometric relationship between the SV and the point of interest. In the name "Instantaneous RMS SIS URE," the "Instantaneous" means that no time averaging occurs. The "RMS" refers to taking the RMS of all the individual Instantaneous SIS URE values across the area visible to the SV for a single time. This concept is explained in SPSPS20 Section A.4.11, and the relevant equation is presented in Appendix C.2.4 of this report.

Appendix A.4.11 of the SPSPS20 defines two types of SIS URE values:

- Instantaneous SIS URE values which express the URE at a given moment along a specific line of sight, and
- Statistical SIS URE values which express the URE across the SV field of view for a time period.

The Instantaneous SIS URE values are most useful for describing the largest errors in the field of view from the SV or to establish the URE to a particular user at a particular point in time. The Statistical SIS URE values allow discussion of the overall accuracy across the entire field of view at a given point in time or over a period in time.

When the BCP and TCP are used to estimate the range residual along a satellite-to-receiver line-of-sight vector at a given instant in time, the result is an Instantaneous SIS URE. Some of the primary differences between Instantaneous SIS UREs and Statistical SIS UREs are given in Table C.3.

Table C.3: Characteristics of SIS URE Methods

Instantaneous SIS URE	**Statistical SIS URE**
Always algebraically signed (±) number	Never algebraically signed
Never a statistical qualifier	Always a statistical qualifier (RMS, 95%, etc.)
Specific to a particular time and place	Statistic over span of times, or places, or both

C.2.1 Clock and Position Values for Broadcast and Truth

The BCP values used in this report are derived from multiple GPS navigation messages (see Table C.2). This verifies that all available navigation message data sets fulfill the relevant assertions.

The broadcast navigation message data were collected by the National Geospatial-Intelligence Agency (NGA) GPS Monitor Station Network (MSN) (see Section C.3). The message data provide a set of parameters that are used in conjunction with equations in the signal interface specifications [2], [3] to derive the SV position and clock offset at a given time. The signal interface specifications and the data allow the user to determine the period of time for which the data are valid. Our process evaluates the parameters at either a 30 s or 1 min cadence depending on the process. In all cases, our processes use the most recently transmitted navigation message in order to best replicate the user experience.

The TCP values used in this report are derived from the NGA antenna phase center (APC) precise ephemeris (PE). This PE product is available from the NGA public website [12]. We use the APC version, as opposed to the center of mass (COM) version, due to the fact that both the GPS LNAV/CNAV messages and the NGA APC precise orbits are referenced to the L1 P(Y) + L2 P(Y) phase center for both orbit and clock. This removes the need to use antenna phase offset data to move the TCP positions from the COM to the APC.

The NGA PE products are synchronized with GPS system time based on coordination with the GPS MCS. This is another advantage of the NGA PE products in that it minimizes the need to solve for a system time bias between the BCP and the TCP.

The NGA product is published in tabular SP3 format, with positions and clocks provided at a 5 min cadence. Lagrange interpolation is used for calculating SV position, using the five points prior to and after the desired epoch. Linear interpolation is used for the clock values.

C.2.2 ISCs and DCBs

When computing UREs from signal combinations other than the primary signal combination, it is necessary to account for the effective phase center differences between each. The primary signal combination is the combination from which the BCP and TCP were derived. In this case, L1 P(Y) + L2 P(Y) is the primary signal combination.

The differences cause range errors that manifest as clock errors. These differences are quantified in the broadcast inter-signal correction (ISC) values. The interface specifications provide equations for adjusting the pseudorange values such that they appear to have been collected from the phase center of the primary signal combination.

A result of this process is that any errors in a given broadcast ISC value will be reflected in pseudoranges for all signal combinations to which that ISC value applies. (For the purpose of this section, the T_{GD} is regarded as an additional ISC value). The extent to which the errors affect the result will vary based on scale factors related to the frequencies involved. These effects must be accounted for when UREs are evaluated.

The broadcast ISC values are typically updated no more than four times a year. The updates are not aligned with quarters and are only approximately spaced. Few SVs are updated each quarter and several do not require updates for over a year. Therefore, the ISC values are constant over long periods.

The URE process may mitigate ISC errors in the following manner[1]:

- Compute the SV position and clock error at a given moment using both the broadcast orbit and the NGA PE.
- Adjust the clock error derived from the broadcast orbit from the phase center of the primary signal combination to the phase center of the signal combination of interest using the inverse of the process defined in the interface specification.
- Adjust the clock error derived from the precise orbit in a similar manner, but using a source of ISC truth.
- Continue with the regular URE evaluation process using the adjusted clock errors.

Note the reliance on ISC truth values. The evaluation of ISC values is a challenging task. The quantity of interest is not directly observable. As a result, the calculation typically requires a large amount of data and some assumptions. For example, some ISC calculations assume a zero-mean error across the constellation. This is likely not the case, but it is assumed common errors will be removed from the process.

There are several organizations within the IGS that regularly evaluate the ISC values (described as diffferential code bias (DCB) values). For the remainder of this section, the DCB values produced by DLR (Germany) will be considered. This choice is based on the fact that there is a paper describing how the DCB values are derived [13].

[1]This process differs from the process used prior to 2020. The earlier process used constant factors that were applied across all the results in an RSS fashion.

In 2021 [14] and 2022 [15], the IGS provided updated guidance on how DCB are to be calculated. The change meant DCBs and the antenna phase center (APC) offset corrections (PCO) are handled separately. Until 27 November 2022, the DLR DCB combined these two terms. From that date forward the PCO adjustment has been removed from the DCB values. The change meant the PCOs are considered as an additional component to the clock.

This is done though use of the standard dual-frequency correction equation:

$$PCO = (f_1^2\ PCO_{z,f_1} - f_2^2\ PCO_{z,f_2})/(f_1^2 - f_2^2)$$

Where:

- f_1 is the first frequency
- f_2 is the second frequency
- PCO_{z,f_1} is the PCO at f_1
- PCO_{z,f_2} is the PCO at f_2

Table C.4 is a summary of the ISC accounting process. Table C.4 is organized in a manner similar to Table 3 of Montenbruck (2018) [16]. Table C.4 contains the same GPS signal combinations but is expanded to include the other signal combinations of interest.

Table C.4: GPS Signal Combinations of Interest and Orbit Adjustments

Msg.	Signals	BCP Correction to Clock Error	TCP Correction to Clock Error
LNAV	L1 P(Y) + L2 P(Y)	0	0
	L1 P(Y)	T_{GD}	- γ_{L2L1} $DCB_{C1W\text{-}C2W}$
	L1 C/A	T_{GD}	- γ_{L2L1} $DCB_{C1W\text{-}C2W}$ + $DCB_{C1C\text{-}C1W}$
CNAV	L1 C/A	T_{GD} - ISC_{L1CA}	- γ_{L2L1} $DCB_{C1W\text{-}C2W}$ + $DCB_{C1C\text{-}C1W}$
	L1 C/A + L2C	T_{GD} - γ_{L1L2} ISC_{L1CA} + γ_{L2L1} ISC_{L2C}	γ_{L1L2} $DCB_{C1W\text{-}C2W}$ - γ_{L2L1} $DCB_{C2L\text{-}C2W}$
	L1 C/A + L5Q	T_{GD} - γ_{L1L5} ISC_{L1CA} + γ_{L5L1} ISC_{L5Q}	γ_{L1L5} $DCB_{C1W\text{-}C2W}$ - γ_{L1L5} $DCB_{C1C\text{-}C5Q}$

Where:

$$\begin{aligned}
\gamma_{L1L2} &= f_{L1}^2/(f_{L1}^2 - f_{L2}^2),\\
\gamma_{L2L1} &= f_{L2}^2/(f_{L1}^2 - f_{L2}^2),\\
\gamma_{L1L5} &= f_{L1}^2/(f_{L1}^2 - f_{L5}^2),\ \text{and}\\
\gamma_{L5L1} &= f_{L5}^2/(f_{L1}^2 - f_{L5}^2).
\end{aligned}$$

Note that the first row of Table C.4 has zero for both values. This row represents the primary signal combination for GPS. The equations in the column labeled "BCP Correction to Clock Error" are in IS-GPS-200 and IS-GPS-705.

There are some matters to consider when looking at the DLR DCB values:

- The DLR DCB data set contains the following values: C1C-C1W, C1C-C2W, C2W-C2S, C2W-C2L, C2W-C2X, C1C-C5Q, C1C-C5X, C1C-C1L, C1C-C1X. The names use RINEX signal nomenclature. As expected, there are no DCBs based on Y-code. However, the data set does contain DCBs based on codeless tracking (i.e., C1W and C2W). (The X suffix refers to combined signal tracking: e.g., C2M/C2L or L5I/L5Q).

- In addition, the list does not include all the needed DCBs. For example, there is no C1W-C5I (L1 codeless to L5I). If we assume both transitive and associative properties hold for DCB values, then some of the missing combinations may be derived. However, this also means the noise of DCBs so combined will be conflated.

- DLR produces both one-day and seven-day DCB values. These are usually published one to two months after the end of each quarter. Unless there are changes in the signal generation chain, the ISCs should be reasonably stable. However, the seven-day DCB values do shift from week to week. Frequently, shifts are aligned with SV outages or other changes in the composition of the SVs used in the derivation. This is an unfortunate side effect of the estimation process.

- The DCB values are derived including a zero-mean assumption. The GPS T_{GD} values are also biased in that any common group delay across the constellation is handled in the GPS system time estimate. However, there is no way of knowing the actual bias in either case.

- The various biases are addressed in a two-step process:

  - The first step is to compute the average bias between the BCP correction and the TCP correction across all SVs for the day. The TCP corrections are then adjusted by this value to roughly overlay the BCP corrections. There will still be non-zero variations between individual SVs.
  - The second step is to remove the common clock bias across the SVs at each epoch. This addresses the remaining bias between the zero-mean assumptions.
  - This process allows us to observe any large errors in the ISC values, however, the scale factor on the ISC and DCB values places a limit on the observability of the differences.
    - For the T_{GD}, the least significant bit (lsb) scale factor is 0.5 nsec (15 cm).
    - For the remaining ISC values, the scale factor is 0.029 nsec (0.9 cm).
    - The standard deviation on the DCBs is in the range 0.01 – 0.10 nsec (0.3 – 3 cm).
  - Note that the GPS ISC values change infrequently (typically no more often than every three months) and we are using the 7-day average DCB values. Therefore, the ISC values and the DCB values will be constant for a given SV for a given day. As a result, the BCP correction term and the TCP correction term will be constant across a day but biased differently.
  - Note that all this is done without reference to actual observations. If the ISC values and the DCB values were perfectly correct, the adjustments would cancel and the UREs for any signal-combination would be identical to the L1 P(Y) + L2 P(Y) URE values. Any differences are due to the relative errors in the ISC and DCB values.

C.2.3 Definition of 95th Percentile Global Statistic

Where the SPSPS20 uses the term "95th% Global Statistic" and the assertion includes a time period, it is interpreted to mean the description of "Brute Force 95th%" in SPSPS20 Appendix A.4.11 extended over time, as suggested by Note 1 in the same section. This is different than the interpretation of the phrase "95th% Global Average" from the 2008 SPS PS. The interpretation of that term is discussed in C.2.4. The Instantaneous SIS URE value is calculated for a large number of locations for each time in a series of times. The 95th percentile value is then selected from the entire set.

For each SV, this is done for a series of time points at a 5 min cadence. At each time point, the components of the URE (i.e., the radial, along-track, cross-track, and clock offset errors) are projected along the line of sight to each location to form a SIS Instantaneous URE value. The collection of SIS Instantaneous URE values at each time point are stored. Once the values for all the time points for a month have been computed, the absolute values of SIS Instantaneous URE values for all time points are gathered together in a monthly set. The 95th percentile value is selected from that set.

This method uses an approximation of an equidistant grid over the portion of the Earth visible to the SV with a spacing of roughly 550 km (5° latitude on the surface of the Earth). Considering those points at or above a 5° elevation angle with respect to the SV, this yields a set of 577 SIS Instantaneous URE values for each SV for each evaluation time. Figure C.1 illustrates this set of grid points for a particular SV-time shown as a projection onto the surface of the Earth.

This was done at a cadence of 5 min for each SV for all of 2023, and all 577 values were stored for all time points. Sets of values corresponding to each month were extracted (approximately 5 million values per SV-month). The absolute values and 95th percentile values for each month were selected as the result for the SV-month. This is the basis for Table 3.1.

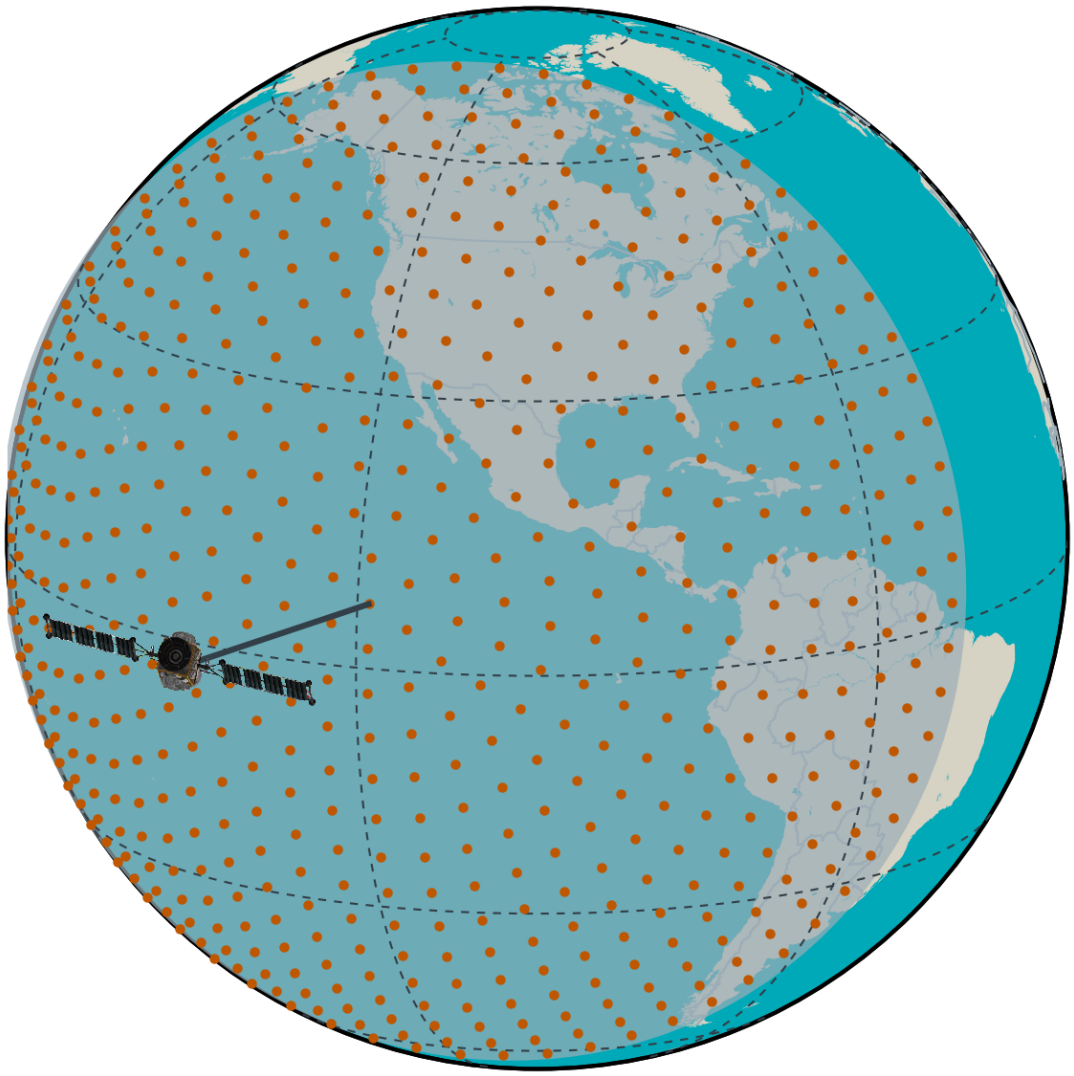

Figure C.1: Illustration of the 577 Point Grid

C.2.4 Definition of 95th Percentile Global Average

Where the 2008 SPS PS uses the term "95th% Global Average" and the assertions includes a time period, it is interpreted to mean a two-part process in which:

1. the description of "Piecewise RMS" in 2008 SPS PS Appendix A.4.11 is applied to obtain the Instantaneous SIS RMS URE at a series of time points, then
2. the 95th percentile of the collection of Instantaneous SIS RMS URE values is selected as the statistic.

This is different than the interpretation of the phrase "95th% Global Statistic" from SPSPS20. The interpretation of that term is discussed in C.2.3. The first part of the process is illustrated in Figure C.2.

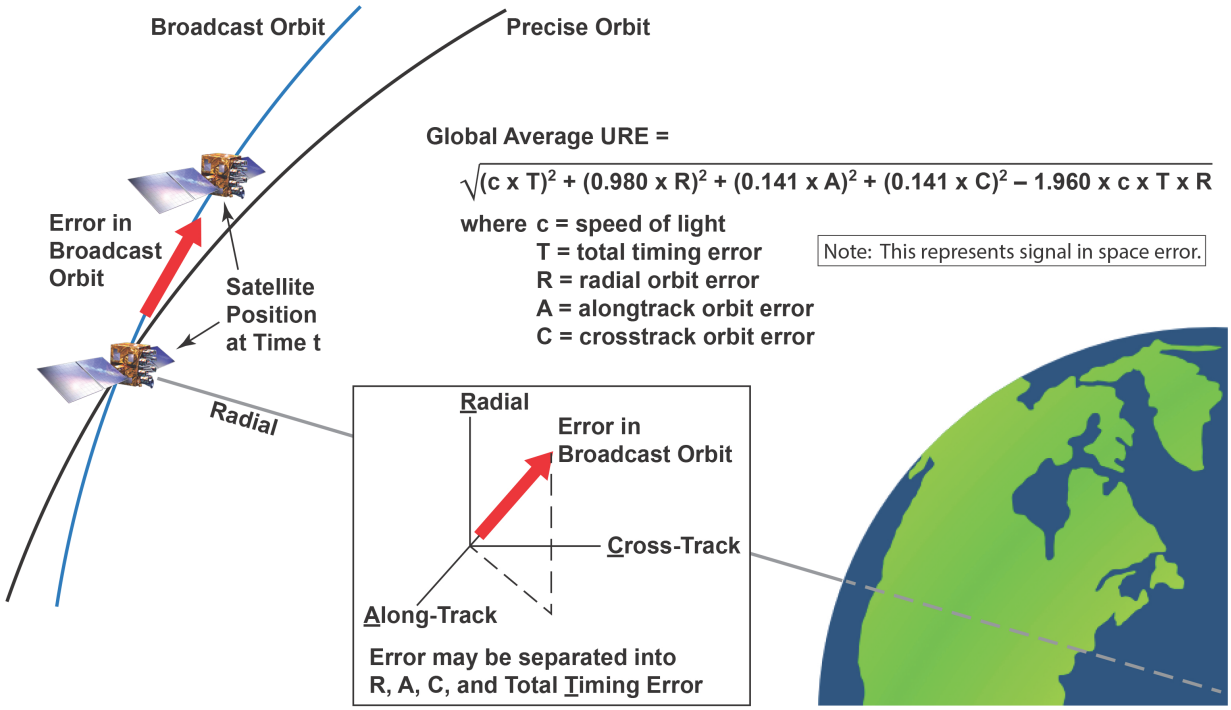

Figure C.2: Global Average URE as defined in 2008 SPS PS

The equation shown in Figure C.2 is Equation A-1 of 2008 SPS PS Section A.4.11. The derivation for the generalized form of this equation can be found in the referenced paper [17]. This expression allows the computation of the URE from known errors. Based on the coefficients of this equation, the URE is calculated for a surface corresponding to the mean curvature of WGS 84.

For purposes of this report, the Instantaneous RMS SIS URE values were generated at 30 s intervals for all of 2023. The URE was formed by differencing the BCP and TCP to obtain the radial, along-track, cross-track, and time errors at each epoch. These errors were used as inputs to the 2008 SPS PS Equation A-1.

After the Instantaneous RMS SIS URE values were computed, values for periods when each SV was unhealthy or not broadcasting were discarded. The remaining values were then grouped by monthly period for each SV and sorted; the 95^{th} percentile values within a given month were identified for each SV. The monthly grouping corresponds closely to the 30-day period suggested in Note 2 of 2008 SPS PS Section 3.4, while being more intuitive to the reader.

C.2.5 Limitations of URE Analysis

The methods described above work well when the estimated URE accuracy is below the required thresholds, as it verifies that the system is operating as expected. However, experience has shown that when an actual problem arises, the use of these procedures, without other cross-checking mechanisms, can create some issues and may lead to incorrect results. Consider the following two cases:

- The precision with which we can identify the time at which the URE values for an SV exceed a given threshold is limited by the cadence at which the UREs are calculated. We use a cadence of 30 s for the method described in Section C.2.4, which is a satisfactory granularity for nearly all cases. We use a cadence of 5 min for the method described in Section C.2.3, which may require additional examination of the results to determine the 30 s epoch at which a threshold was exceeded.
- When an SV is set unhealthy or cannot be tracked, the TCP may provide misleading results. There are several options for handling discontinuities that occur during outages, which are implemented by the creators of the TCP. Therefore, the URE values generated near such events may be incorrect. As a result, it is necessary to avoid accepting UREs into the statistical process under conditions in which the SV could not be tracked or was set unhealthy. This has been done for all the results presented here.

In all cases, when an apparent violation of the URE limit is encountered, we chose to reconcile the analysis described above with the behavior of ORDs formed from the data collected at NGA and IGS sites. Because the observational data used is collected at a 30 s cadence, we obtain a much higher resolution insight into the details of the actual event than we do with the interpolated TCP.

C.2.6 Challenges of Comparing UREs Between Signal Combinations

The reader may expect that some signal combinations will have lower URE values than others for a variety of reasons. For example, a L1 C/A user using CNAV data has access to both T_{GD} and ISC values; whereas, a L1 C/A user using LNAV data has only T_{GD}.

However, such an expectation contains several hidden assumptions:

- If the T_{GD} and ISC values were perfect, the UREs would be identical for all signal combinations. However, the T_{GD} and ISC values contain errors, some of which are likely systematic while others are SV-dependent.
- The "truth data" which are used to check the T_{GD} and ISC values (see Appendix C.2.2) are also the result of an analysis process that yields less-than-perfect results.
- The broadcast orbits are derived from a large state estimator that considers a variety of factors. As a result, while the collection of UREs across the constellation for a given month will have a mean close to zero, the mean for a given SV over a month will be non-zero.

When all these error sources are combined, they add and cancel in a manner that may lead to non-intuitive results. Therefore, some signal-combinations may have URE values that appear non-intuitively lower than signal-combinations that might be expected to be "better." However, this is actually due to limits in our observability.

Finally, recall that the performance standards provide assertions against which performance may be verified. The performance standards do not focus on the relative accuracy of any pair of signal combinations, but establish the threshold to be achieved for each signal-combination.

C.3 Selection of Broadcast Navigation Message Data

Several of the processes used in deriving the results in this report are dependent on the broadcast navigation message data. In most cases, the clock, ephemeris, and integrity (CEI) data are required. These are contained in subframes 1, 2, and 3 of the GPS LNAV message and in Message Type (MT) 10, MT 11, and the front portion of MT 30-37 of the GPS CNAV messages. A CEI data set is broadcast by a given SV for a period in time. The CEI data sets nominally change every two hours for both LNAV and CNAV. The position and health status of the transmitting SV are derived from the CEI data.

The goal in selecting a CEI data set for a given SV at a given time of interest is to reproduce what the user would have experienced had they been collecting data from that SV at that time. To accomplish this, the process must have access to a complete time-history of navigation message data and it must properly select specific sets of CEI data from that time-history.

The CEI data sets supporting this analysis were collected from the NGA MSN, which has complete dual-station visibility to all GPS SVs (and generally, much better). The MSN data collection process captures the earliest transmission of each unique CEI data set. We investigated any gaps in the CEI data set time-history and filled such gaps, if practical. The result is a time-history of the unique CEI data sets transmitted by each SV.

Wherever the analysis process requires CEI data for a given SV at a given time, it selects the CEI data set that corresponds to what was being transmitted from the SV at that time. During periods in which new data is being transmitted (data set cutovers), the preceding CEI data set is used until the time the new CEI data set had been completely transmitted and available to the user.

It must be recognized that this may be an inexact reproduction of the experience of any given user. Users may experience delays in the receipt of newly transmitted navigation message data due to obstructions, atmospheric issues, or receiver problems. However, our process is deterministic and reproducible.

C.4 AOD Methodology

The AOD was calculated by finding the upload times based on the t_{oe} offsets as defined in IS-GPS-200 Section 20.3.4.5 and then examining the t_{nmct} under the following assumptions:

- A complete set of the subframe 1, 2, and 3 data broadcast by all SVs of interest is available throughout the time period of interest.
- The term t_{nmct} defined in IS-GPS-200 Section 20.3.3.4.4 represents the time of the Kalman state used to derive the corresponding navigation message.

Given these assumptions, the AOD at any point in time can be determined by the following process:

- Working backward from the time of interest to finding the time when the most recent preceding upload was first broadcast
- Finding the AOD offset (AODO) of the associated subframe 2
- Subtracting the AODO from the t_{oe} (as described in IS-GPS-200 20.3.3.4.4) to determine the time of the Kalman state parameters
- Calculating the difference between the time of interest and the Kalman state parameter time

The search for the preceding upload is necessary because the AODO has a limited range and is not sufficient to maintain an accurate count for a complete upload cycle.

The results of this algorithm are generally consistent with the results provided by MCS analysis. The first assumption is fulfilled by the NGA MSN archive. The remaining assumption was discussed with systems engineers supporting 2 SOPS and is believed to be valid.

The exception to this process is PRN 32. PRN 32 does not have the AODO term described due to limitations in the navigation message format. As a result, we cannot directly derive the AOD for PRN 32. For purposes of this report, we examined all upload cutovers through 2023 for all SVs except SVN 70/PRN 32. We computed the AOD at the time of each upload cutover. We then computed the mean of these samples to determine an average AOD at the time of the upload cutover. There were 11,736 samples with an average AOD of 951 s (about 16 minutes). We assumed this average holds true for SVN 70/PRN 32 and conducted the analysis accordingly.

Note that there is no need for a GPS receiver to calculate AOD. The URE as a function of AOD is one of the metrics evaluated for this report but is not a concern for a real-time user.

C.5 Position Methodology

Section 2.4.5 of SPSPS20 provides usage assumptions for the SPS PS, and some of the notes in Section 2.4.5 are relevant to the question of position determination. The following is quoted from Section 2.4.5:

The performance standards in Section 3 of this SPS PS do not take into consideration any error source that is not under direct control of the Space Segment or Control Segment. Specifically excluded errors include those due to the effects of:

- *Signal distortions caused by ionospheric and/or tropospheric scintillation*
- *Residual receiver ionospheric delay compensation errors*
- *Residual receiver tropospheric delay compensation errors*
- *Receiver noise (including received signal power and interference power) and resolution*
- *Multipath and receiver multipath mitigation*
- *User antenna effects*
- *Operator (user) error*

In addition, at the beginning of Section 3.8, the SPSPS20 explains that in addition to the error exclusions listed in Section 2.4.5, the following assumptions are made regarding the SPS receiver:

The use of a representative SPS receiver that:

- *is designed in accordance with IS-GPS-200.*
- *is tracking the SPS SIS from all satellites in view above a* 5° *mask angle... It is assumed the receiver is operating in a nominal noise environment...*
- *accomplishes satellite position and geometric range computations in the most current realization of the WGS 84 Earth-Centered, Earth-Fixed (ECEF) coordinate system.*
- *generates a position and time solution from data broadcast by all satellites in view.*
- *compensates for dynamic Doppler shift effects on nominal SPS ranging signal carrier phase and C/A-code measurements.*
- *processes the health-related information in the SIS and excludes marginal and unhealthy SIS from the position solution.*
- *ensures the use of up-to-date and internally consistent ephemeris and clock data for all satellites it is using in its position solution.*
- *loses track in the event a GPS satellite stops transmitting a trackable SIS.*
- *is operating at a surveyed location (for a time transfer receiver).*

To address these assumptions, we adopted the following approach for computing a set of accuracy statistics:

1. 30 s GPS observations were collected from the NGA GPS monitor station network (MSN) and a similar set of IGS stations. This decision addressed the following concerns:
   (a) All stations selected collect dual-frequency observations. Therefore, the first-order ionospheric effects can be eliminated from the results.
   (b) All stations selected collect weather observations. The program that generates the positions uses the weather data to eliminate first-order tropospheric effects.
   (c) The receiver thermal noise will not be eliminated, but both the NGA and IGS stations are equipped with the best available equipment, so effects will be limited.
   (d) Similarly, multipath cannot be eliminated, but both networks use antennas designed for multipath reduction, and station sites were chosen to avoid the introduction of excessive multipath.
   (e) Antenna phase center locations for such stations are precisely surveyed. Therefore, position truth is readily available.
   (f) Despite the similarities, the two networks are processed separately for a variety of reasons.
      i. The NGA MSN uses receivers capable of tracking the Y-code. As a result, the individual observations have somewhat better SNR than the observations from the IGS stations.
      ii. By contrast, the IGS stations are tracking L1 C/A and L2 codeless, then averaging their observations over 30 s in order to reduce noise on the data.
      iii. The NGA MSN uses a single receiver type which limits the number of receiver-specific traits but leaves open the possibility that a systemic problem could affect all receivers. The IGS network uses a variety of receivers, which is some protection against systemic problems from a single receiver type, but requires that the processing address a variety of receiver-specific traits.
      iv. The NGA MSN is operated and maintained by a single organization. Changes are planned and well-controlled. The IGS network is cooperative in nature. While policies are in place to encourage operational standards, changes in station behavior are not as well-coordinated.
2. Process the data using a comprehensive set of broadcast ephemerides collected as described in Appendix C.3.

3. Process the collected observations using the PRSOLVE program of the ARL:UT-hosted open source GNSS Toolkit (GNSSTk, formerly GPSTk)[18]. Note:

   (a) PRSOLVE meets the relevant requirements listed above. For example, SV positions are derived in accordance with IS-GPS-200, the elevation mask is configurable, weather data is used to estimate tropospheric effects, and WGS 84 [11] conventions are used. Data from unhealthy SVs were removed from PRSOLVE using an option to exclude specific satellites.

   (b) PRSOLVE is highly configurable. Several of the items in the preceding list of assumptions are configuration parameters to PRSOLVE.

   (c) Any other organization that wishes to reproduce the results should be able to do so. (Both the algorithm and the data are publicly available.)

4. Process the collected 30 s observations in two ways:

   (a) Use all SVs in view without data editing in an autonomous pseudorange solution to generate 30 s position residuals at all sites.

   (b) Use a receiver autonomous integrity monitoring (RAIM) algorithm (another PRSOLVE option) to remove outlier pseudorange measurements from which a "clean" set of 30 s position residuals is generated at all sites. The RAIM algorithm used by PRSOLVE is dependent on several parameters. The two most important parameters are the RMS limit on the post-fit residuals (default: 3.0 m) and the number of SVs that can be eliminated in the RAIM process (default: unlimited). This analysis was conducted using the default values.

5. Compute statistics on each set of data independently.

C.6 Plane/Slot Methodology

As discussed in Section B.3, Appendix A.7.4 of the SPSPS20 defines a slot as being occupied when the footprint of a satellite (or combined footprint of a pair of satellites, for expanded slots) on the surface of the Earth overlaps at least 95% of the nominal slot's footprint, averaged over an orbit revolution. An approximation for this requirement is given in terms of offsets in Right Ascension of the Ascending Node (RAAN) and Argument of Latitude (ArgLat), computed as satellite value minus nominal slot value, as

$$\frac{1}{4}(\Delta\text{RAAN})^2 + (\Delta\text{ArgLat} + 0.5736 \times \Delta\text{RAAN})^2 \leq (0.0333 \text{ semi-circles})^2,$$

defining an ellipse within which a satellite occupies the slot. Appendix A.2.4 of the SPSPS20 defines how to propagate the nominal slot centers provided in Section 3.2 of the SPSPS20.

To determine plane/slot assignments, satellite position and velocity data are obtained from NGA PE at an hourly cadence, which are then converted to Keplerian orbital elements. At each epoch, the Keplerian orbital elements of the nominal slot locations are propagated forward in time. The plane each satellite resides in is determined using the computed RAAN values, and the slot occupancy condition is then checked for each slot in the occupied plane. The slot occupancy results are then averaged every 12 hours (roughly the orbital period of 11 hours and 56 minutes) to determine which slots, if any, a satellite occupied during its orbit. This yields two sets of slot assignments per day for each satellite, which are consolidated into a single slot assignment per satellite per day. Lastly, any potential instances of satellite pairs in "equivalent-or-better" non-standard configurations, as described in Appendix A.7.2.4 and Appendix A.7.2.5 of the SPSPS20, are checked, updating the slot assignment data as necessary. These plane-slot assignments are then used when computing metrics such as availability and continuity.

Appendix D

Acronyms and Abbreviations

Table D.1: List of Acronyms and Abbreviations

2 SOPS	2nd Space Operations Squadron
AMCS	Alternate Master Control Station
AOD	Age of Data
AODO	Age of Data Offset
ARL:UT	Applied Research Laboratories, The University of Texas at Austin
BCP	Broadcast Clock and Position
CEI	Clock, Ephemeris, and Integrity
CMPS	Civil Monitoring Performance Specification
DCB	Differential Code Bias
DECOM	Decommission (NANU Type)
DF	Dual Frequency
DLR	Deutsches Zentrum für Luft- und Raumfahrt (German Aerospace Center)
DOP	Dilution of Precision
ECEF	Earth-Centered, Earth-Fixed
FAA	Federal Aviation Administration
FCSTDV	Forecast Delta-V (NANU Type)
FCSTEXTD	Forecast Extension (NANU Type)
FCSTMX	Forecast Maintenance (NANU Type)
FCSTRESCD	Forecast Rescheduled (NANU Type)

FCSTUUFN	Forecast Unusable Until Further Notice (NANU Type)
GDOP	Geometric Dilution of Precision
GEC	Groundtrack Equatorial Crossing
GLAN	Geographic Longitude of the Ascending Node
GNSS	Global Navigation Satellite System
GNSSTk	GNSS Toolkit
GPS	Global Positioning System
GPSTk	GPS Toolkit
HDOP	Horizontal Dilution Of Precision
ICD	Interface Control Document
IGS	International GNSS Service
IODC	Issue of Data, Clock
IODE	Issue of Data, Ephemeris
IS	Interface Specification
ISB	Inter-signal Bias
ISC	Inter-signal Correction
LNAV	Legacy Navigation Message
LSB	Least Significant Bit
MCS	Master Control Station
MSB	Most Significant Bit
MSI	Misleading Signal Information
MSN	Monitor Station Network
NANU	Notice Advisory to Navstar Users
NAV	Navigation Message
NAVSEA	U.S. Navy Naval Sea Systems Command
NGA	National Geospatial-Intelligence Agency
NMCT	Navigation Message Correction Table
NTE	Not to Exceed

OA	Operational Advisory
ORD	Observed Range Deviation
PCO	Antenna Phase Center Offset Corrections
PDOP	Position Dilution of Precision
PE	Precise Ephemeris
PEO	Program Executive Office
PNT	Positioning, Navigation, and Timing
PPS	Precise Positioning Service
PPS PS (PPSPS07)	2007 Precise Positioning Service Performance Standard
PRN	Pseudo-Random Noise
PVT	Position, Velocity, and Time
RAIM	Receiver Autonomous Integrity Monitoring
RINEX	Receiver Independent Exchange Format
RMS	Root Mean Square
RSS	Root Sum Square
SF	Single Frequency
SINEX	Station Independent Exchange Format
SIS	Signal-in-Space
SSC	Space Systems Command
SNR	Signal-to-Noise Ratio
SP3	Standard Product 3
SPS	Standard Positioning Service
SPS PS (SPSPS20)	2020 Standard Positioning Service Performance Standard
SV	Space Vehicle
SVN	Space Vehicle Number
TCP	Truth Clock and Position
TDOP	Time Dilution of Precision
TF	Triple Frequency

T_{GD}	Group Delay Differential
UERAE	User-Equivalent Range Acceleration Error
UERE	User-Equivalent Range Error
UERRE	User-Equivalent Range Rate Error
UNUNOREF	Unusable with No Reference (NANU Type)
UNUSUFN	Unusable Until Further Notice (NANU Type)
URA	User Range Accuracy
URAE	User Range Acceleration Error
URE	User Range Error
URRE	User Range Rate Error
USCG	U.S. Coast Guard
USNO	U.S. Naval Observatory
USSF	U.S. Space Force
UTC	Coordinated Universal Time
UTCOE	UTC Offset Error
UUTCE	User UTC(USNO) Error
VDOP	Vertical Dilution of Precision
WGS 84	World Geodetic System 1984
ZAOD	Zero Age of Data

Bibliography

[1] U.S. Department of Defense. Standard Positioning Service Performance Standard, 5th Edition. https://www.gps.gov/technical/ps/2020-SPS-performance-standard.pdf, 2020.

[2] U.S. Department of Defense. Navstar GPS Space Segment/Navigation User Interfaces, IS-GPS-200, Revision N. https://www.gps.gov/technical/icwg/IS-GPS-200N.pdf, August 2022.

[3] U.S. Department of Defense. Navstar GPS Space Segment/Navigation User Interfaces, IS-GPS-705, Revision J. https://www.gps.gov/technical/icwg/IS-GPS-705J.pdf, August 2022.

[4] J. M. Dow, R. E. Neilan, and C. Rizos. The International GNSS Service in a changing landscape of Global Navigation Satellite Systems. *Journal of Geodesy*, 2009.

[5] B. Renfro, D. Munton, R. Mach, and R. Taylor. Around the World for 26 Years - A Brief History of the NGA Monitor Station Network. In *Proceedings of the Institute of Navigation International Technical Meeting*, Newport Beach, CA, 2012.

[6] U.S. Coast Guard. GPS Constellation Status. https://www.navcen.uscg.gov/gps-constellation.

[7] W. Gurtner and L. Estey. RINEX: The Receiver Independent Exchange Format Version 2.11, 2006.

[8] U.S. Department of Defense. Navstar GPS Control Segment to User Support Community Interfaces, ICD-GPS-240, Revision D. https://www.gps.gov/technical/icwg/ICD-GPS-240D.pdf, May 2021.

[9] U.S. Department of Transportation. Global Positioning System (GPS) Civil Monitoring Performance Specification, DOT-VNTSC-FAA-20-08. https://www.gps.gov/technical/ps/2020-civil-monitoring-performance-specification.pdf, August 2020.

[10] P. Misra and P. Enge. *Global Positioning System: Signals, Measurements, and Performance*. Ganga-Jamuna Press, revised second edition, 2012.

[11] National Geospatial-Intelligence Agency. Department of Defense World Geodetic System 1984, Its Definition and Relationships With Local Geodetic Systems, Version 1.0.0, NGA.STND.0036_1.0.0_WGS84, July 2014.

[12] National Geospatial-Intelligence Agency. NGA Antenna Phase Center Precise Ephemeris products. `https://earth-info.nga.mil/index.php?dir=gnss&action=gnss`.

[13] O. Montenbruck and A. Hauschild and P. Steigenberger. Differential Code Bias Estimation using Multi-GNSS Observations and Global Ionosphere Maps. *Navigation Journal of the ION*, 61(3):191–201, 2014.

[14] International Global Navigation Satellite System Service. Upcoming convention regarding PCO and biases. `https://lists.igs.org/pipermail/igsmail/2021/008109.html`.

[15] International Global Navigation Satellite System Service. A new keyword in Bias-SINEX for antenna phase center corrections on geometry-free biases. `https://lists.igs.org/pipermail/igsmail/2022/008275.html`.

[16] O. Montenbruck et al. Multi-GNSS signal-in-space range error assessment - Methodology and results. *Advances in Space Research*, 61(12):3020–3038, 2018.

[17] B. Renfro, J. Drotar, A. Finn, M. Stein, E. Reed, and E. Villalba. An analytical derivation of the signal-in-space root-mean-square user range error. *NAVIGATION: Journal of the Institute of Navigation*, 71(1), 2024.

[18] B. Tolman et al. The GPS Toolkit - Open Source GPS Software. In *Proceedings of the 17th International Technical Meeting of the Satellite Division of the Institute of Navigation (ION GNSS 2004)*, Long Beach, CA, 2004.